ISSN 0021-9673

VOL. 467 NO. 2 APRIL 28, 1989

THIS ISSUE COMPLETES VOL. 467

JOURNAL OF CHROMATOGRAPHY

INTERNATIONAL JOURNAL ON CHROMATOGRAPHY, ELECTROPHORESIS AND RELATED METHODS

ELSEVIER

JOURNAL OF CHROMATOGRAPHY

Scope. The *Journal of Chromatography* publishes papers on all aspects of chromatography, electrophoresis and related methods. Contributions consist mainly of research papers dealing with chromatographic theory, instrumental development and their applications. The section *Biomedical Applications*, which is under separate editorship, deals with the following aspects: developments in and applications of chromatographic and electrophoretic techniques related to clinical diagnosis or alterations during medical treatment; screening and profiling of body fluids or tissues with special reference to metabolic disorders; results from basic medical research with direct consequences in clinical practice; drug level monitoring and pharmacokinetic studies; clinical toxicology; analytical studies in occupational medicine.

Submission of Papers. Papers in English, French and German may be submitted, in three copies. Manuscripts should be submitted to: The Editor of *Journal of Chromatography*, P.O. Box 681, 1000 AR Amsterdam, The Netherlands, or to: The Editor of *Journal of Chromatography, Biomedical Applications*, P.O. Box 681, 1000 AR Amsterdam, The Netherlands. Review articles are invited or proposed by letter to the Editors. An outline of the proposed review should first be forwarded to the Editors for preliminary discussion prior to preparation. Submission of an article is understood to imply that the article is original and unpublished and is not being considered for publication elsewhere. For copyright regulations, see below.

Subscription Orders. Subscription orders should be sent to: Elsevier Science Publishers B.V., P.O. Box 211, 1000 AE Amsterdam, The Netherlands, Tel. 5803 911, Telex 18582 ESPA NL. The *Journal of Chromatography* and the *Biomedical Applications* section can be subscribed to separately.

Publication. The *Journal of Chromatography* (incl. *Biomedical Applications*) has 37 volumes in 1989. The subscription prices for 1989 are:

J. Chromatogr. + *Biomed. Appl.* (Vols. 461–497):
Dfl. 6475.00 plus Dfl. 999.00 (p.p.h.) (total *ca.* US$ 3737.00)

J. Chromatogr. only (Vols. 461–486):
Dfl. 5200.00 plus Dfl. 702.00 (p.p.h.) (total *ca.* US$ 2951.00)

Biomed. Appl. only (Vols. 487–497):
Dfl. 2200.00 plus Dfl. 297.00 (p.p.h.) (total *ca.* US$ 1248.50).

Our p.p.h. (postage, package and handling) charge includes surface delivery of all issues, except to subscribers in Argentina, Australia, Brasil, Canada, China, Hong Kong, India, Israel, Malaysia, Mexico, New Zealand, Pakistan, Singapore, South Africa, South Korea, Taiwan, Thailand and the U.S.A. who receive all issues by air delivery (S.A.L. — Surface Air Lifted) at no extra cost. For Japan, air delivery requires 50% additional charge; for all other countries airmail and S.A.L. charges are available upon request. Back volumes of the *Journal of Chromatography* (Vols. 1–460)are available at Dfl. 195.00 (plus postage). Claims for missing issues will be honoured, free of charge, within three months after publication of the issue. Customers in the U.S.A. and Canada wishing information on this and other Elsevier journals, please contact Journal Information Center, Elsevier Science Publishing Co. Inc., 655 Avenue of the Americas, New York, NY 10010. Tel. (212) 633-3750.

Abstracts/Contents Lists published in Analytical Abstracts, ASCA, Biochemical Abstracts, Biological Abstracts, Chemical Abstracts, Chemical Titles, Chromatography Abstracts, Current Contents/Physical, Chemical & Earth Sciences, Current Contents/Life Sciences, Deep-Sea Research/Part B: Oceanographic Literature Review, Excerpta Medica, Index Medicus, Mass Spectrometry Bulletin, PASCAL-CNRS, Referativnyi Zhurnal and Science Citation Index.

See inside back cover for Publication Schedule, Information for Authors and information on Advertisements.

0021-9673/89/$03.50

This issue is printed on acid-free paper.

Printed in The Netherlands

CONTENTS

(Abstracts/Contents Lists published in Analytical Abstracts, ASCA, Biochemical Abstracts, Biological Abstracts, Chemical Abstracts, Chemical Titles, Chromatography Abstracts, Current Contents/Physical, Chemical & Earth Sciences, Current Contents/Life Sciences, Deep-Sea Research/Part B: Oceanographic Literature Review, Excerpta Medica, Index Medicus, Mass Spectrometry Bulletin, PASCAL-CNRS, Referativnyi Zhurnal and Science Citation Index)

High-speed size characterization of chromatographic silica by flow/hyperlayer field-flow fractionation
by S. K. Ratanathanawongs and J. C. Giddings (Salt Lake City, UT, U.S.A.) (Received December 6th, 1988) 341

Resolution of π-acid racemates on π-acid chiral stationary phases in normal-phase liquid and subcritical fluid chromatographic modes. A unique reversal of elution order on changing the nature of the achiral modifier
by P. Macaudière, M. Lienne, M. Caude and R. Rosset (Paris, France) and A. Tambuté (Vert-le-Petit, France) (Received January 10th, 1989) 357

Gas chromatographic detection of selected organochlorine species using an alternating current plasma detector
by R. B. Costanzo and E. F. Barry (Lowell, MA, U.S.A.) (Received January 16th, 1989) . 373

On-line flame photometric detection in micro-column liquid chromatography
by Ch. E. Kientz, A. Verweij and H. L. Boter (Rijswijk, The Netherlands) and A. Poppema, R. W. Frei, G. J. de Jong and U. A. Th. Brinkman (Amsterdam, The Netherlands) (Received September 15th, 1988) 385

Reversed-phase high-performance liquid chromatographic method for the quantification of 5-hydroxymethylfurfural as the major degradation product of glucose in infusion fluids
by A. P. Cook, T. M. Macleod and J. D. Appleton (Dundee, U.K.) and A. F. Fell (Bradford, U.K.) (Received January 6th, 1989) 395

Notes

Gas–liquid chromatographic resolution of some racemic synthons for lamtidine analogous histamine H_2-receptor antagonists via diastereomeric amides of (1*S*)-(−)-camphanic acid
by N. Büyüktimkin (Istanbul, Turkey) and F. Keller and W. Schunack (Berlin, F.R.G.) (Received January 13th, 1989) 402

Direct enantiomeric separation of anticholinergic drugs derived from (±)-cyclohexyl(3-thienyl)glycolic acid on a novel α_1-acid glycoprotein-bonded chiral stationary phase (Chiral-AGP)
by M. Lienne, M. Caude and R. Rosset (Paris, France) and A. Tambuté (Vert-le-Petit, France) (Received January 17th, 1989) 406

Normal-phase and reversed-phase liquid chromatographic techniques for the determination of dithranol and its degradation products
by I. C. L. Cheah, B. R. Sitaram, A. Pappas, N. L. Thi, B. C. Finnin and B. L. Reed (Parkville, Australia) (Received February 6th, 1989) 414

Packed-column supercritical fluid chromatographic separation of highly explosive compounds
by W. H. Griest, C. Guzman and M. Dekker (Oak Ridge, TN, U.S.A.) (Received December 12th, 1988) 423

High-performance liquid chromatography as an alternative to microbiological measurements in the assay of tetracyclines
by A. Ray and R. Harris (Potters Bar, U.K.) (Received January 30th, 1989) 430

Separation of intravenous IgG containing albumin by high-performance size-exclusion chromatography on TSKgel G3000SWXL
by Y. Yamasaki and Y. Kato (Yamaguchi, Japan) (Received December 19th, 1988) . . . 436

Analysis of phenols from lignin depolymerization by capillary gas chromatography
by R. W. Thring and E. Chornet (Sherbrooke, Canada) and R. P. Overend (Ottawa, Canada)
(Received February 6th, 1989) 441

Book Review

Chromatographie mit überkritischen verdichteten Gasen zur Trennung von Oligomeren und Polymeren (by F. P. Schmitz), reviewed by M. Lederer 447

Author Index 448

Erratum 452

In articles with more than one author, the name of the author to whom correspondence should be addressed is indicated in the article heading by a 6-pointed asterisk (*)

Journal of Chromatography, 467 (1989) 341–356
Elsevier Science Publishers B.V., Amsterdam — Printed in The Netherlands

CHROM. 21 318

HIGH-SPEED SIZE CHARACTERIZATION OF CHROMATOGRAPHIC SILICA BY FLOW/HYPERLAYER FIELD-FLOW FRACTIONATION

S. KIM RATANATHANAWONGS and J. CALVIN GIDDINGS*
Department of Chemistry, Henry Eyring Building, University of Utah, Salt Lake City, UT 84112 (U.S.A.)
(Received December 6th, 1988)

SUMMARY

Flow/hyperlayer field-flow fractionation (FFF) has been successfully applied to the rapid size-based fractionation and characterization of various 3-μm and 5-μm commercial high-performance liquid chromatography silica supports. Because high-resolution information on both average particle diameter and size distribution was obtained in less than 3 min by using a relatively simple apparatus, the method is attractive for the routine characterization of chromatographic packing material. Flow/hyperlayer FFF is not only faster than most sedimentation methods, it is ideally suited for the characterization of porous particles since separation is based solely on diameter and is independent of density.

INTRODUCTION

The column is often referred to as the heart of the chromatographic system. However, the physical characteristics of the packing material on which the chromatographic activity of the column is based are often not well defined. The uncertainties that exist involve differences between nominal and actual mean particle diameters, the breadth of size distributions, batch-to-batch size variations, and the presence of fines and particle agglomerates, to name a few[1–5]. These factors result in inconsistent column-to-column performance and in some cases high back pressures. The inaccuracy in the reported characteristics of column packings could present a problem in the correlation of experimental results from different columns. In particular, these inaccuracies could interfere with the correlation of column performance according to reduced plate height/reduced flow velocity parameters, as first proposed by one of the authors[6]. Thus, it is of importance to gain as much accurate information as possible concerning the physical properties of the column packing material.

Many of the methods that have been used for the size-based separation and for the determination of mean particle diameters and size distributions of chromatographic supports are based on sedimentation. McMurtrey and DesLauriers[7], for example, employed sedimentation under gravity for the preparative-scale fractionation of thin-layer chromatography silica. The resulting material gave a comparable performance to commercial high-performance liquid chromatography (HPLC) pack-

0021-9673/89/$03.50

ing materials. However, the sedimentation process was time consuming, requiring up to 12 h for 5-μm particles. Unger and Gimpel[8] reported an analysis time of only 30 min for the size determination of 10-μm silica using photosedimentation. However, this analysis time did not include the time needed for measurement of the specific pore volume and the apparent density of the porous silica particles, parameters used in the subsequent calculation of the Stokes diameter. The diameters obtained by photosedimentation differed from those of scanning electron microscopy by up to 12%. Large discrepancies were observed for particles with big pores (*e.g.*, 400 nm). In a related work, Hanggi and Carr[9] monitored the turbidity of a settling silica suspension at a specific observation plane. Particle size distributions and mean particle diameters were derived from the resulting absorbance *versus* time curve using an assumed density for solvent-filled silica. Analysis times were of the order of 2 h for 5-μm silica.

Another process utilizing gravitational sedimentation forces, but in this case falling in the field-flow fractionation (FFF) category, was described by Giddings *et al.*[10]. These authors used sedimentation/steric FFF to examine a number of different chromatographic supports with regard to their size characteristics. Analysis times were under 30 min for silica particles of diameters between 5 and 20 μm. More recently, using a centrifuge in place of gravity, run times were reduced to 3–4 min[11], but this modified FFF technique has not been applied to chromatographic supports. A comparison of the system used in this work, flow/hyperlayer FFF, and all the techniques using sedimentation will be made in a later section.

Other methods that have been used for the determination of the particle size distribution of porous silicas include microscopy[1,8] and electrozone sensing[2,12,13]. Column permeability has also been used as a means by which the average particle diameter of the column packing can be approximated[2,14]. For a general discussion on porous silica sizing methods, see ref. 15.

FFF was first proposed and implemented in the latter half of the 1960s. Since then it has evolved into a versatile family of methods with many subtechniques, each applicable to a different class of macromolecules and particulate materials. These subtechniques are categorized by the type of field employed and the mode of operation. A discussion of the nomenclature and a description of the various subtechniques is given by Giddings *et al.*[16].

Generally, FFF utilizes laminar flow in a channel formed between two closely spaced parallel plates across which a driving force is applied. The FFF process can be carried out in many ways and applied to many materials. Of the subtechniques available, both sedimentation/steric and flow/hyperlayer FFF are applicable to large (>1 μm diameter) particles. In both cases, sample is injected into the FFF channel followed by a stopflow period during which the driving force remains operational. The particles are positively displaced by the driving force to form a thin layer near the so-called accumulation wall. When the channel flow is restarted, particles of different diameters are transported downstream at different rates depending on the degree of their protrusion into the parabolic flow profile. In both methods the centers of mass of the larger particles occupy faster streamlines; thus, they elute more quickly than the smaller particles.

In the steric mode of operation, particles migrate very close to the accumulation wall. Discrepancies between the predicted and experimental retention ratios that have

been observed[10,17] are due to hydrodynamic lift forces which tend to drive the particles away from the accumulation wall. With sufficiently strong lift forces, the particles form a narrow band, or hyperlayer, at some distance above the accumulation wall. This gives us hyperlayer FFF[18].

Because the particles in hyperlayer FFF occupy faster flowing streamlines than they would near the wall, they elute more quickly than predicted by the steric model. The position of the compressed particle cloud within the channel corresponds to the point at which the two opposing forces, the primary driving force (in the present case caused by crossflow) and the lift force, are balanced. Retention in flow/hyperlayer FFF is thus based on the relationship between the crossflow driving force and the lift force. The latter force is a complex function of channel flow velocity, particle diameter, and distance from the wall. The lift force, which becomes increasingly significant at high flow-rates and for large particles, is currently being investigated[19].

THEORY

The parabolic flow profile in an FFF channel is described by the equation

$$v = 6\langle v\rangle \left[\frac{x}{w} - \left(\frac{x}{w}\right)^2\right] \tag{1}$$

where v is the local fluid velocity, $\langle v\rangle$ is the mean flow velocity, x is the distance from the accumulation wall, and w is the channel thickness. As previously noted, the balance between two opposing forces establishes an equilibrium position, $x = x_{eq}$, for each particle band in the channel. A band at position x_{eq} is carried along at a velocity v defined by the above parabolic equation.

The retention ratio R is defined as $v/\langle v\rangle$. From eqn. 1 we obtain the following expression for R[18]

$$R = \frac{v}{\langle v\rangle} = 6\left[\frac{x_{eq}}{w} - \left(\frac{x_{eq}}{w}\right)^2\right] \tag{2}$$

Because x_{eq} depends in part on imperfectly characterized lift forces, the positions of the particle bands in the channel cannot be accurately predicted. Hence the particle velocities v and retention ratios R are not presently calculable from first principles. This inability to predict retention ratios in this size range necessitates the use of calibration curves from which the diameter of different fractions can be obtained. Fortunately, in the size range of chromatographic supports, excellent latex particle standards of precisely known diameters are available for calibration.

The calibration process is best understood in relationship to selectivity. The diameter-based selectivity, which represents the intrinsic resolving power of the system with respect to particle diameter d, is defined as[20]

$$S_d = \left|\frac{\mathrm{d}\log t_r}{\mathrm{d}\log d}\right| \tag{3}$$

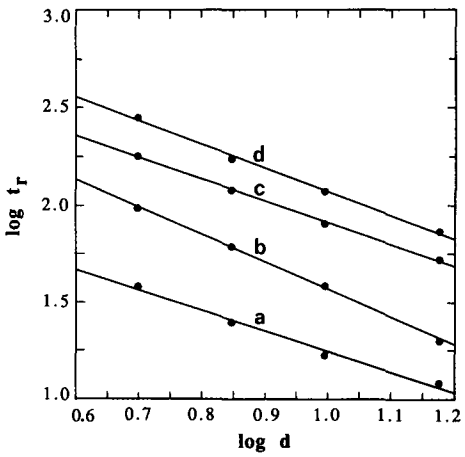

Fig. 1. Calibration curves of log retention time *versus* log diameter under different separation conditions. (a) Channel flow-rate, $\dot{V} = 7.55$ ml/min, crossflow flow-rate, $\dot{V}_c = 1.70$ ml/min; (b) $\dot{V} = 6.34$ ml/min, $\dot{V}_c = 2.09$ ml/min; (c) $\dot{V} = 3.64$ ml/min, $\dot{V}_c = 2.04$ ml/min; and (d) $\dot{V} = 3.93$ ml/min, $\dot{V}_c = 3.33$ ml/min. The latex particle standards used to establish the calibration curves have nominal diameters of 15.00, 9.87, 7.0 and 5.002 μm. The slope of the calibration curves yields the S_d value needed in polydispersity calculations.

where t_r is the particle retention time. Both theoretical and empirical evidence suggests that S_d is nearly constant over a substantial range of diameters for most FFF systems[21,22]. Thus a plot of log d *versus* log t_r generally yields a straight line. By injecting latex standards of different diameters and plotting log t_r against log d, a value for S_d may be obtained from the slope of the line. Such plots can be used for calibration purposes. Fig. 1 shows a series of selectivity plots or calibration curves for different diameter latex particle standards fractionated using various separation conditions. These graphs can be used to obtain particle diameters from the measured elution times of the samples. The different positions of the calibration lines in Fig. 1 reflect the complex interplay between lift forces and crossflow and channel flow-rates.

As in chromatography, peak broadening in FFF is measured by plate height H. For large particles, where axial diffusion can be assumed to be negligible, H can be written as the sum of a system contribution H_s and a sample polydispersity contribution H_p

$$H = H_s + H_p \tag{4}$$

Most particulate samples, including chromatographic supports, have considerable size variation (> 50% between size extremes). Because of the high selectivity ($S_d > 1$) of the system as displayed by Fig. 1, the different particle sizes are well spread out along the retention time axis t_r (see later), yielding a large effective plate height H_p. Generally we can assume $H_p \gg H_s$; the observed plate height H can thus be approximated as

$$H \cong H_p \tag{5}$$

The polydispersity of particulate samples is often expressed in terms of the

coefficient of variation (C.V.), equal to the standard deviation in particle diameter σ_d divided by the mean diameter d. The following expression, yielding C.V. in terms of experimentally observed elution profiles, is based on a previous derivation[23] that leads to

$$H_p = LS_d^2\left(\frac{\sigma_d}{d}\right)^2 = LS_d^2(\text{C.V.})^2 \tag{6}$$

which shows H_p to be dependent on the channel length L, the selectivity S_d, and the coefficient of variation (C.V.). Assuming that the polydispersity is the only significant contributor to the plate height (see eqn. 5) and expressing the number N of theoretical plates as L/H, we get

$$N = \frac{L}{H_p} = \frac{1}{S_d^2(\text{C.V.})^2} \tag{7}$$

Eqn. 7 can be rearranged in the following manner

$$\text{C.V.} = \frac{1}{S_d\sqrt{N}} \tag{8}$$

to yield C.V. in terms of measured plate numbers. Alternatively, if we express N as

$$N = \left(\frac{t_r}{\sigma_t}\right)^2 \tag{9}$$

where σ_t is the peak standard deviation in units of time, we obtain

$$\text{C.V.} = \frac{\sigma_t}{S_d t_r} \tag{10}$$

which relates C.V. directly to the experimental quantities σ_t and t_r. The variables in the above equation for C.V. are measured from the fractograms.

EXPERIMENTAL

Equipment

The modules that comprise the flow FFF system used here for hyperlayer operation are shown in Fig. 2. A standard HPLC pump, Kontron 410 (Kontron Electrolab, London, U.K.) is used to provide the axial channel flow while a syringe pump (designed in-lab) delivers a continuous and pulseless flow of carrier liquid across the channel. The Spectroflow 757 UV–visible detector (Applied Biosystems, Ramsey, NJ, U.S.A.) was set at 254 nm and in most cases 0.02 a.u.f.s. Short time constants (0.1–1 s) were used so as not to bias the shape of the response, particularly for high-speed runs. Coiled lengths of 0.01 in. (254 μm) internal diameter stainless-steel tubing were used to balance the flow-rates of the crossflow and channel flow. Pressure

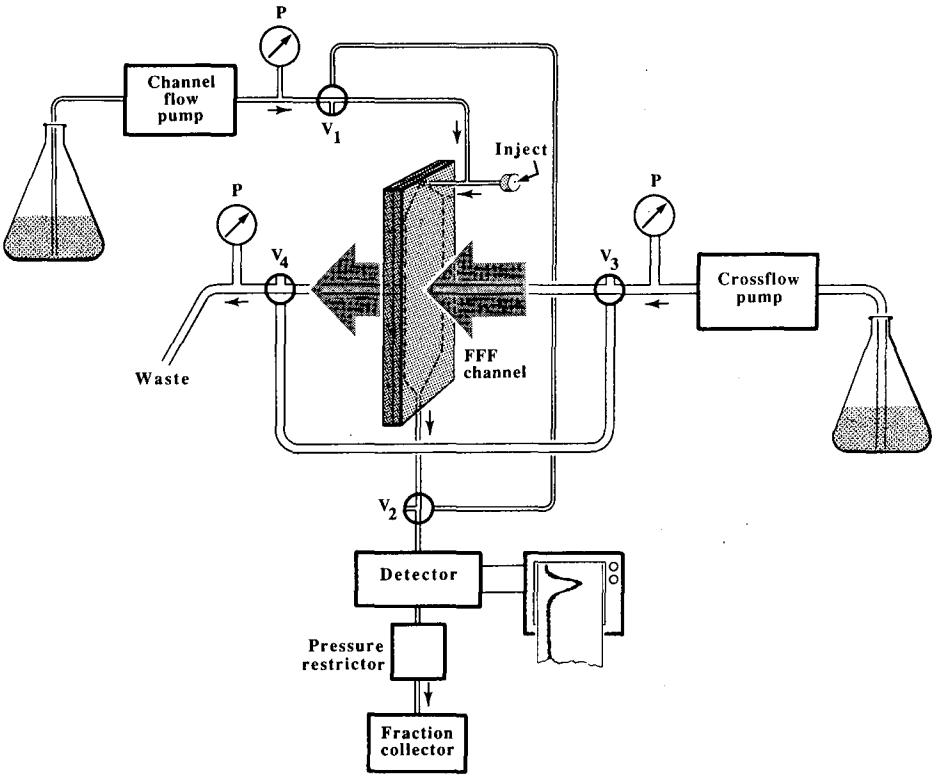

Fig. 2. Schematic diagram of a flow FFF apparatus. Flow paths are denoted by lines, the three-way valves are represented by V_1 ... V_4, and the pressure gauges are shown as P.

gauges were situated at the points indicated in Fig. 2 to monitor changes in pressure that could be indicative of obstructed flow paths.

FFF channel

The FFF channel consists of two Lucite blocks, each inset with a ceramic frit with 5-μm pores. Sandwiched between these two blocks are a Mylar spacer from which the channel volume has been cut and a 10000 molecular weight cutoff membrane (Amicon YM10, Amicon, Danvers, MA, U.S.A.). This membrane is stretched over one of the frit surfaces and serves as the accumulation wall. The opposing (depletion) wall is defined by the frit of the second block. The dimensions of the channel are 27.2 cm in tip-to-tip length, 2 cm in breadth, and 0.0254 cm in thickness. The channel was placed in a vertical position so as to avoid gravitational contributions to the crossflow field[24].

Experimental procedure

After sample is injected into the system, the channel flow is halted during the relaxation period, equal to the time that it takes to displace one channel volume through the system by the crossflow. This stopflow procedure is implemented by using

two three-way valves, V_1 and V_2, to reroute the channel flow along an external pathway. At the end of the stopflow period, V_1 and V_2 are returned to their original positions. A flow-control modification that is often used involves the addition of a crossflow loop. By connecting the inlet of the crossflow pump to the outlet of the crossflow stream (emerging from the Lucite block), the syringe pump acts as an "unpump" to withdraw a volume of liquid from the channel equal to that being pumped in. This configuration alleviates problems of flow control associated with the frequent change in lengths of tubing used as pressure restrictors on the channel flow or crossflow streams. This crossflow loop is not used at all times because of the possible contamination of the recirculated carrier due to permeation through the membrane of unknown substances present in the sample. An alternative would be to use a separate pump to withdraw the crossflow.

Reagents and samples

The carrier liquid is doubly distilled and deionized water containing 0.1% of the surfactant Fl-70 (Fisher Scientific, Fairlawn, NJ, U.S.A.) and 0.02% NaN_3, a baeteriocide. Polystyrene latex particle standards (Duke Scientific, Palo Alto, CA, U.S.A.) with nominal diameters of 19.58, 15.00, 9.87, 7.0 and 5.002 μm (hereafter 20, 15, 10, 7, and 5 μm) were used to determine the calibration parameters for the system. The identity and characteristics of the HPLC-grade silicas that were surveyed are summarized in Table I. Sample volumes of 20 μl of 5-mg/ml silica suspensions were injected directly onto the channel using a 25-μl syringe (Hamilton, Reno, NV, U.S.A.).

Electron microscopy

Electron micrographs of various fractograms were obtained using a Hitachi S-450 scanning electron microscope (Hitachi Scientific Instruments, Nissei Sangyo America, Mountain View, CA, U.S.A.). The specimens of the unfractionated samples

TABLE I

IDENTITY AND CHARACTERISTICS OF HPLC SILICA SUPPORTS SURVEYED

	Type	*Supplier*	*Batch number*	*Pore size (Å)*	*Pore volume (ml/g)*	*Surface area (m^2/g)*
Nominal 5-μm spherical silica						
a	Spherex	Phenomenex	N6052	100		180
b	Hypersil	Shandon	5-148R	120	0.61	175
c	IB-Sil	Phenomenex	5-272	110		160
d	Nucleosil	Machery-Nagel	5121	120	0.7	
e	W-Porex	Phenomenex	PR12187	100		370
f	Spherisorb	Phase Separations		80		190
Nominal 3-μm spherical silica						
g	Hypersil	Shandon	3-51	120	0.63	185
Nominal 5-μm irregular silica						
h	Maxsil	Phenomenex	7081	65		520
i	Partisil	Whatman	101801	85		350
j	LiChrosorb	EM Science	702F424488	100		420

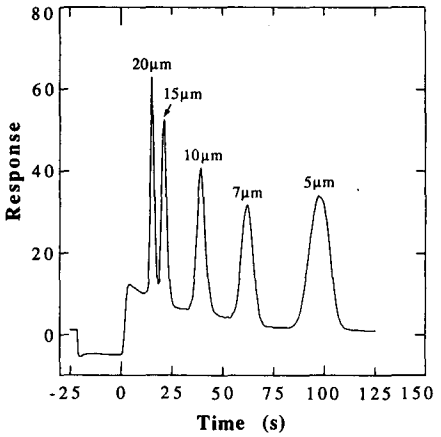

Fig. 3. Fractogram of nominal 19.58 (20)-, 15.00 (15)-, 9.87 (10)-, 7.0 (7)-, and 5.002 (5)-μm polystyrene standards. The experimental conditions were stopflow time t_{sf} = 60 s, channel flow-rate $\dot{V}$ = 6.34 ml/min, and crossflow flow-rate $\dot{V}_c$ = 2.09 ml/min. The detector was set at 254 nm and 0.02 a.u.f.s.

were prepared by filtering 0.5 ml of a 0.15-mg/ml silica suspension through a Swinney filter holder (Gelman Sciences, Ann Arbor, MI, U.S.A.). Particles were collected on a 13-mm Nuclepore membrane filter (Pleasanton, CA, U.S.A.) with 0.1-μm pores. This membrane filter was mounted on a steel stub and the filter surface was coated with gold and palladium. Typical microscope settings were 15 kV acceleration voltage with 1000 × magnification. Measurement of particle sizes could be made to within 0.05 μm with the help of a magnifier. The electron microscope was calibrated using an NBS (now National Institute of Standards and Technology) 9.89-μm polystyrene standard (SRM 1960).

RESULTS AND DISCUSSION

Preliminary experiments were carried out to determine a suitable sample concentration, specifically, one that gave a good detector response without overloading the system[25]. This was done by injecting samples of varying particle concentrations and noting changes in peak shapes and elution times. Concentrations of *ca.* 5 mg/ml of silica injected in 20-μl volumes (totaling *ca.* 100 μg of silica) gave satisfactory results and were used throughout these experiments.

The high degree of selectivity and the speed of separation attainable by flow/hyperlayer FFF is demonstrated in Fig. 3, which shows a fractogram of five polystyrene latex standards ranging from 5 to 20 μm in diameter. Baseline (or higher) resolution of all particle populations is obtained within 2 min of the start of flow (following a stopflow period of 1 min). This separation time can be significantly shortened by employing a higher axial flow-rate and/or a lower field strength. As demonstrated previously[16], the partial separtion of 49, 30, and 29-μm latex beads can be accomplished in 6 s. However, there is a loss of resolution with increasing analysis speed. Fig. 3 also confirms that the selectivity of flow/hyperlayer FFF is greater than unity. This is demonstrated by the fact that the retention time for the 5-μm latex particle is more than twice that of the 10-μm latex.

The series of fractograms shown in Fig. 4a and b were obtained for spherically and irregularly shaped HPLC silicas, respectively. Each specific packing material yields a characteristic peak shape and maximum, indicating differences in size distributions and in most cases in mean particle diameters. The size variation or polydispersity of the samples is reflected in the peak width in accordance with our earlier theoretical discussion.

In order to obtain quantitative information on particle size characteristics, a moments analysis was carried out for all the fractograms shown in Fig. 4. The first moment was used to identify the center of gravity of the peak. The retention time of the center of gravity can be converted into a mean particle diameter by means of the diameter scale shown on the upper horizontal axis of the figures. The diameter scale was obtained from the latex calibration procedure noted earlier using calibration line a from Fig. 1. The second moment was used to calculate the polydispersity or C.V. of

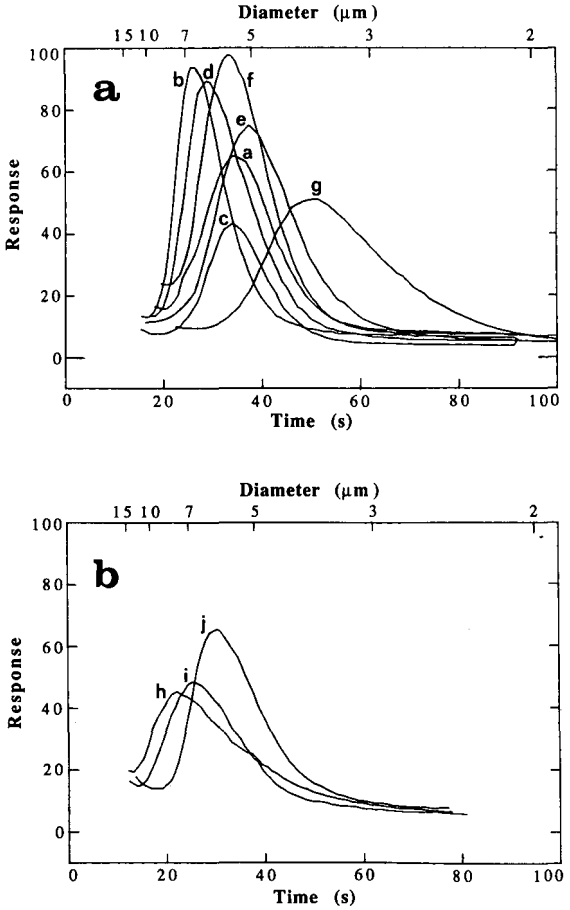

Fig. 4. Fractograms of HPLC silicas. Conditions were t_{sf} = 70 s, $\dot{V}$ = 7.55 ml/min, and $\dot{V}_c$ = 1.70 ml/min, (a) for spherical 5- and 3-μm silica and (b) for irregular 5-μm silica. The lettered fractograms correspond to silica packings from various manufacturers as listed in Table I. The diameter scale on the upper x-axis was determined using polystyrene standards.

TABLE II

SUMMARY OF THE MEAN RETENTION TIMES (t_r), DIAMETERS, AND POLYDISPERSITIES (C.V.) OF VARIOUS CHROMATOGRAPHIC SILICAS

		t_r (s)	Diameter (μm)		% C.V.
			FFF[a]	SEM	FFF[b]
Nominal 5-μm spherical particles					
a	Spherex	38.0	4.78	4.72	17.2
b	Hypersil	30.2	5.97	6.11	16.6
c	Nucleosil	36.3	5.00	5.15	15.3
d	IB-Sil	32.9	5.42	5.54	18.4
e	W-Porex	42.3	4.31	4.26	20.0
f	Spherisorb	36.9	4.87	4.94	15.1
Nominal 3-μm spherical particles					
g	Hypersil	59.0	3.19	3.29	20.5
Nominal 5-μm irregularly shaped particles					
h	Maxsil	29.7	6.21	–	22.4
i	Partisil	30.7	5.97	–	21.3
j	LiChrosorb	35.9	5.10	–	19.4

[a] Diameter calculated using the first moment of the FFF particle peak.
[b] % C.V. = $\sigma_t/(S_d t_r)$ where S_d = 1.05.

the sample by means of eqn. 10. Values of the mean diameter and the C.V. of all the samples are presented in Table II.

We note that the sample peaks shown in Fig. 4 are obtained by means of a conventional HPLC UV detector. When applied to particles, the signal from such a detector is largely generated by light scattering. The intensity of the scattered light is a complex function of particle diameter. Thus the curves in Fig. 4 cannot be precisely identified with either number distributions or mass distributions. However, the light scattering distortions for large particles are relatively small, making it likely that the peaks in Fig. 4 represent an intermediate distribution between number and mass distributions. Because the peaks are relatively narrow, the differences are less substantial than for broader distributions. The validity of this procedure for determining mean particle diameters is verified by a comparison with the results of scanning electron microscopy (SEM), also shown in Table II.

Each of the SEM diameters listed in Table II represents an average of at least 200 diameter measurements. From these measurements, the number average diameter was calculated. The maximum difference between the mean diameters obtained by FFF and SEM is 3%. Note that no SEM values are reported for the irregular particles because of the difficulty of specifying a unique diameter. The FFF diameters reported for the irregular particles in Table II are an equivalent spherical diameter.

All experiments were initially carried out with sample introduction at the top of the channel (followed by downward flow). A second series of experiments was conducted with samples injected from the bottom (followed by upward flow) to verify the results already obtained. A difference of approximately 5% was observed between the two elution time values. This discrepancy, which is not observed for polystyrene

particles, is due to gravitational effects which become more pronounced with higher density samples. The ideal (gravity-free) elution time lies between the values obtained by injection from the top and from the bottom of the channel; thus, the average of these two retention times was used to obtain the t_r in Table II.

With the exception of the small gravitational effect that is found in comparing upward and downward flow, gravity has no effect on the outcome of flow/hyperlayer FFF experiments. Thus density has no substantial role in the acquisition of particle size data. In this respect, flow/hyperlayer FFF has a definite advantage over all sedimentation-based techniques where both size and density play a role in characterization. In the latter case, particle-to-particle differences in density would lead to apparent size differences. It is possible that density as well as size variations could be examined by combining flow/hyperlayer and sedimentation/steric FFF as a multidimensional technique. However, for size data alone, unless there is some assurance of density uniformity, flow/hyperlayer FFF is advantageous.

Table II shows that the average diameters obtained for the nominal 5-μm spherical silica particles by the FFF technique range from 4.3 to almost 6.0 μm. These results are confirmed by the electron microscopy data in the table. The different support sizes reflected by these numbers will cause measurable differences in back pressure, column efficiency, and reduced plate height.

The size variations within the HPLC silicas from different suppliers, as measured by the % C.V. values, lie between 15 and 23%. The % C.V. value for 5–10-μm silica is commonly reported to be between 10 and 20%[15].

The reproducibility of the data obtained by flow/hyperlayer FFF is demonstrated in Table III. This table reports the standard deviation (S.D.) and percentage relative standard deviation (% R.S.D.) in the mean retention time t_r and in the peak

TABLE III

REPRODUCIBILITY OF THE FLOW/HYPERLAYER FFF RESULTS

	Retention time (s)			*Peak width (s)*		
	t_r[a]	*S.D.*	*% R.S.D.*	σ_t	*S.D.*	*% R.S.D.*
Nominal 5-μm spherical particles						
Spherex	37.0	0.153	0.414	6.68	0.106	1.59
Hypersil	29.4	0.577	1.96	5.12	0.187	3.65
Nucleosil	35.4	0.945	2.67	5.68	0.416	7.32
IB-Sil	32.0	0.503	1.57	6.18	0.265	4.29
W-Porex	41.2	0.153	0.371	8.66	0.254	2.93
Spherisorb	35.9	0.954	2.66	5.71	0.178	3.12
Nominal 3-μm spherical particles						
Hypersil	57.5	0.651	1.13	12.4	0.352	2.84
Nominal 5-μm irregularly shaped particles						
Maxsil	28.9	–	–	7.97	–	–
Partisil	29.9	1.58	5.28	6.69	0.361	5.40
LiChrosorb	35.0	0.543	2.86	7.13	0.135	1.89

[a] Injection from the top of the channel.

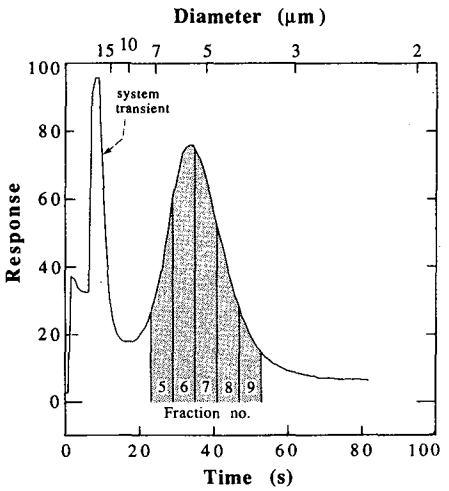

Fig. 5. Spherex 5-μm silica was characterized using the same conditions as listed in Fig. 4. Fractions of 0.76 ml were collected every 6 s starting at the time that channel flow is resumed after stopflow. The labelled fractions were examined by SEM. The observed system transients are due to pressure fluctuations in the system as the channel flow is recommenced.

width expressed as σ_t for 3–5 measurements on each sample of t_r and σ_t. The % R.S.D. in t_r and σ_t average only about 2 and 4%, respectively. The % R.S.D. in mean particle diameter and C.V. are comparable to these values.

The ability of FFF to differentiate a continuous distribution of particle sizes is demonstrated when fractions of the eluting sample are collected for further study. Silica (Spherex) was injected and the fractions collected at 6-s intervals as shown in Fig. 5. Micrographs for the original sample along with fractions 5, 7 and 9 are shown in Fig. 6. A distinct size difference can be observed among the various fractions. The results of diameter measurements made from the micrographs are summarized in Table IV. Based on the time that the cut was made, it was possible to calculate the expected diameter range of the particular fraction. The average diameters obtained from SEM measurements (based on approximately 60 particles for each sample) fall within this range for fractions 5, 6, and 7 and are only slightly higher for fractions 8 and 9. The observed trend is for smaller SEM diameters than predicted with the fractions collected on the rising slope of the peak and larger average diameters for those collected on the decreasing slope. This is as expected since there is a continuous gradient in the particle population from one edge of the cut to the other. The average particle diameter in each fraction will then be biased toward the center of the peak[23]. The C.V. of the fractions as obtained from SEM measurements for each fraction is considerably lower than that of the original sample (5–7% with the exception of fraction 5). The C.V. is, nonetheless, relatively large due to the finite volume of each cut.

It is possible to utilize the present FFF method to identify the presence of unusual and undesirable particle sizes or particle aggregates in a sample. A fractogram of a commercially available 3-μm silica packing is shown in Fig. 7. The first two peaks

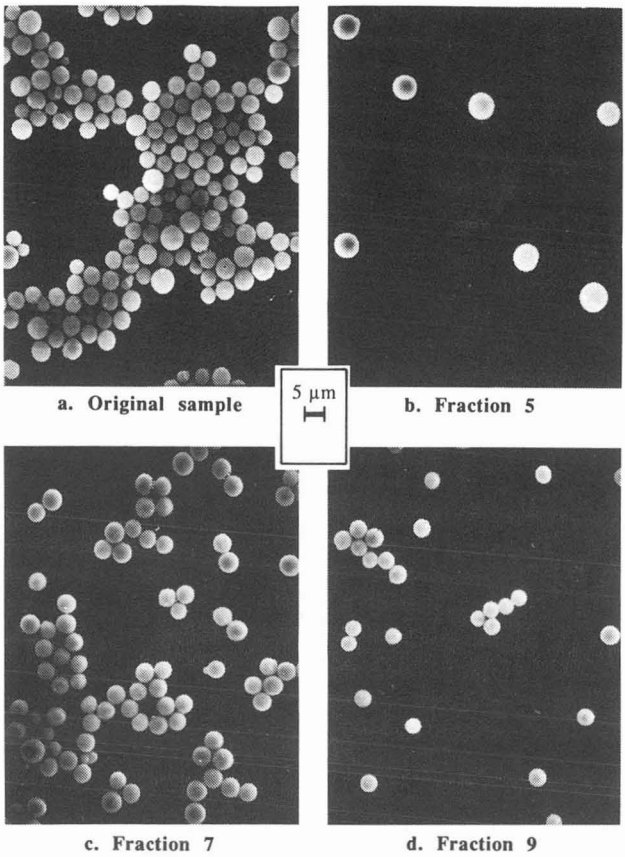

Fig. 6. Micrographs corresponding to (a) original sample, (b) fraction 5, (c) fraction 7, and (d) fraction 9 of the Spherex silica. The cut positions are depicted in Fig. 5. The micrographs were taken at 1000× magnification and at an acceleration voltage of 15 kV.

are system transients that are caused by slight changes in pressure when the channel flow is resumed at the end of the relaxation period. The presence of two sample peaks, at 13 and 56 s, suggests a bimodal size distribution. The second peak of the two

TABLE IV

COMPARISON OF EXPECTED AND ACTUAL DIAMETERS OF FRACTIONS COLLECTED FOLLOWING FRACTIONATION OF SPHEREX SILICA

Fraction number	*Time of cut (s)*	*Diameter based on time of cut (μm)*	*Diameter based on SEM (μm)*
5	24–30	7.43–6.01	6.21 ± 0.68
6	30–36	6.01–5.05	5.49 ± 0.40
7	36–42	5.05–4.36	4.86 ± 0.28
8	42–48	4.36–3.84	4.58 ± 0.29
9	48–54	3.84–3.43	4.18 ± 0.28

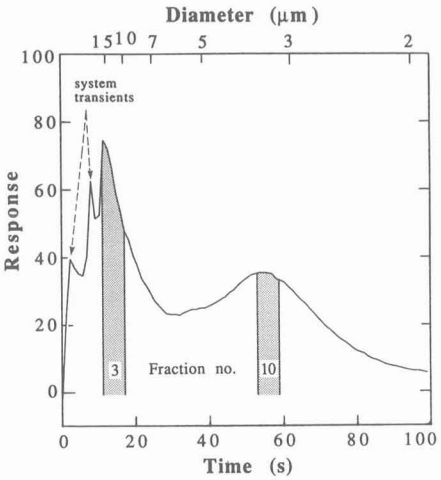

Fig. 7. Fractogram of a 3-μm commercial HPLC silica indicating the presence of anomalous large diameter components. Conditions are identical to those listed in Fig. 4.

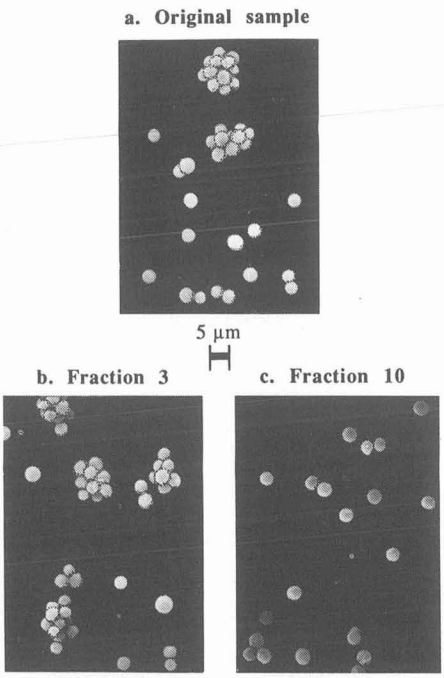

Fig. 8. Electron micrographs of the 3-μm silica whose fractogram is shown in Fig. 7. (a) Original sample, (b) fraction 3, and (c) fraction 10. SEM conditions are 15 kV acceleration voltage and 1000 × magnification.

corresponds to a particle diameter of just over 3 μm as expected for this material. The first peak corresponds to a diameter of approximately 13 μm, indicating the presence of particles that obviously do not belong in the support material. These two peaks can be explained by the micrographs of Fig. 8. Fraction 3, taken from the first peak (see Fig. 7), contains aggregates whereas fraction 10, from the second peak, consists of uniform silica monomers. The micrograph of the original sample, Fig. 8a, shows a collection of aggregates and monomers of various sizes. Micrographs of the original samples taken after 20 min of sonication still showed the presence of these aggregates.

CONCLUSION

Flow/hyperlayer FFF is a rapid and reproducible technique for particle characterization. The high speed of analysis makes this technique well suited for quality control. Adjustments for any day-to-day fluctuations in the systems are easily achieved using polystyrene latex beads as internal standards. Other attractive features include the operational and instrumental simplicity of the system and the straightforward calculations of particle size and polydispersity. Flow/hyperlayer FFF has also been demonstrated as a potential tool in the preparation of small quantities of samples having narrow size distributions.

ACKNOWLEDGEMENTS

The authors would like to thank Phenomenex for contributing most of the silica packings used in this work and Shandon and Machery-Nagel for donations of samples manufactured by their respective companies. This work was supported by National Science Foundation Grant CHE-8800675.

REFERENCES

1 M. Verzele, J. Lammens and M. Van Roelenbosch, *J. Chromatogr.*, 186 (1979) 435.
2 R. Ohmacht and I. Halasz, *Chromatographia*, 14 (1981) 155.
3 R. Ohmacht and I. Halasz, *Chromatographia*, 14 (1981) 216.
4 C. Gonnet, C. Bory and G. Lachatre, *Chromatographia*, 16 (1982) 242.
5 H. Engelhardt and G. Ahr, *Chromatographia*, 14 (1981) 227.
6 J. C. Giddings, *J. Chromatogr.*, 13 (1964) 301.
7 K. D. McMurtrey and P. J. DesLauriers, *Anal. Chem.*, 55 (1983) 396.
8 K. K. Unger and M. G. Gimpel, *J. Chromatogr.*, 180 (1979) 93.
9 D. A. Hanggi and P. W. Carr, *J. Liq. Chromatogr.*, 7 (1984) 2323.
10 J. C. Giddings, M. N. Myers, K. D. Caldwell and J. W. Pav, *J. Chromatogr.*, 185 (1979) 261.
11 T. Koch and J. C. Giddings, *Anal. Chem.*, 58 (1986) 994.
12 R. Karuhn, R. D. Wood and S. D. Wyatt, *LC · GC Mag. Liq. Gas Chromatogr.*, 4 (1986) 1072.
13 B. Monaghan, Shandon Southern Products Limited, Cheshire, personal communication.
14 R. Endele, I. Halász and K. Unger, *J. Chromatogr.*, 99 (1974) 377.
15 K. K. Unger, *Porous Silica. Its Properties and Use as Support in Column Liquid Chromatography* (*J. Chromatogr. Libr.*, Vol. 16), Elsevier, Amsterdam, 1979.
16 J. C. Giddings, X. Chen, K.-G. Wahlund and M. N. Myers, *Anal. Chem.*, 59 (1987) 1957.
17 K. D. Caldwell, T. T. Nguyen, M. N. Myers and J. C. Giddings, *Sep. Sci. Technol.*, 14 (1979) 935.
18 J. C. Giddings, *Sep. Sci. Technol.*, 18 (1983) 765.
19 P. S. Williams, T. Koch and J. C. Giddings, in preparation.
20 M. N. Myers and J. Calvin Giddings, *Anal. Chem.*, 54 (1982) 2284.

21 Y. S. Gao, K. D. Caldwell, M. N. Myers and J. C. Giddings, *Macromolecules*, 18 (1985) 1272.
22 S. Lee, M. N. Myers, R. Beckett and J. C. Giddings, *Anal. Chem.*, 60 (1988) 1129.
23 J. C. Giddings and F.-S. Yang, *J. Colloid Interface Sci.*, 105 (1985) 55.
24 X. Chen, K.-G. Wahlund and J. C. Giddings, *Anal. Chem.*, 60 (1988) 362.
25 M. E. Hansen, J. C. Giddings and R. Beckett, *J. Colloid Interface Sci.*, in press.

Journal of Chromatography, 467 (1989) 357–372
Elsevier Science Publishers B.V., Amsterdam — Printed in The Netherlands

CHROM. 21 263

RESOLUTION OF π-ACID RACEMATES ON π-ACID CHIRAL STATIONARY PHASES IN NORMAL-PHASE LIQUID AND SUBCRITICAL FLUID CHROMATOGRAPHIC MODES

A UNIQUE REVERSAL OF ELUTION ORDER ON CHANGING THE NATURE OF THE ACHIRAL MODIFIER

P. MACAUDIÈRE, M. LIENNE, M. CAUDE* and R. ROSSET
Laboratoire de Chimie Analytique de l'Ecole Supérieure de Physique et Chimie Industrielles de Paris, 10 Rue Vauquelin, 75231 Paris Cedex 05 (France)
and
A. TAMBUTÉ
Direction des Recherches et Etudes Techniques, Centre d'Etudes du Bouchet, BP No. 3, Le Bouchet, 91710 Vert-le-Petit (France)
(First received October 6th, 1988; revised manuscript received January 10th, 1989)

SUMMARY

The enantiomeric separation of a series of π-acid N-(3,5-dinitrobenzoyl) (DNB) derivatives of α-amino esters, α-aminoamides and α-amino alcohols was investigated in the normal-phase mode on several π-acid chiral stationary phases (CSPs) derived from (*S*)-DNB-tyrosine, (*R*)-DNB-phenylglycine and (*R*)-DNB-*p*-hydroxyphenylglycine (chiral selectors, CSs). CSs were covalently grafted on to either γ-mercaptopropylsilica gel (type-1 CSPs) or γ-aminopropylsilica gel (type-2 CSPs). A comparison of the selectivities obtained under liquid (LC) and subcritical fluid chromatographic (SubFC) modes indicated important differences in the stereoselectivity of the separation of α-aminoamide test solutes. Studies of the relationship between the nature of the achiral mobile phase (in LC) and enantioselectivity showed a unique reversal of elution order on changing from hexane–ethanol to hexane–chloroform (or hexane–methylene chloride) mobile phases. Finally, chiral recognition models are discussed. Difficulties in correlating chromatographic data (selectivity, elution order) with the proposed mechanisms are outlined. This study emphasizes the importance of the part played by the mobile phase during the separation process; the mobile phase can induce major changes in the conformation of the molecules, thus leading to different chiral recognition processes.

INTRODUCTION

In previous papers[1,2], the syntheses and evaluations of new chiral stationary phases (CSPs) derived from tyrosine were presented. Various families of enantiomers could be resolved both in liquid chromatographic (LC) and subcritical fluid chroma-

0021-9673/89/$03.50

tographic (SubFC) modes. These CSPs were compared with closely related CSPs derived from phenylglycine, *p*-hydroxyphenylglycine and phenylalanine[2]. The choice of two methods of grafting on to silica gel (type 1 and 2 CSPs, Fig. 1) demonstrated considerable discrepancies in the chiral recognition ability of the corresponding CSPs. The relationship between enantioselectivity and solute and CSP structures was extensively studied in previous work[2]. It can be expressed by three simple rules: (a) solutes containing three or more attractive sites of interaction (SI) (amide dipole or π-donor groups) can be resolved on CSPs containing only two SI; if the CSP also contains numerous SI, it must then be sterically hindered; (b) solutes possessing few SI can be resolved on CSPs with multiple SI or on CSPs with a limited number of SI but of low steric hindrance; and (c) conformationally rigid and/or sterically hindered solutes can be resolved on CSPs containing various SI but with a conformation flexible enough to fit the solute structure.

The 3,5-dinitrobenzoyl (DNB) group confers a π-acid character to these CSPs. However, their ability to separate π-acid enantiomers was demonstrated with the resolution of a series of DNB α-amino esters[2]. To our knowledge, very few examples of such separations have been described in literature; Wainer and Doyle[3] resolved a DNB derivative of 1-phenyl 2-aminopropane on (*R*)-DNBPG CSP with a very low selectivity ($\alpha = 1.03$) and Kip *et al.*[4] separated chiral selectors of π-acid CSPs on these ones. In this study we focused our investigations on this particular point. The scope of application was extended to DNB derivatives of α-aminoamides, α-amino alcohols and amines. The elution orders were not always consistent with the absolute configuration of the CSPs. Moreover, in contrast to common observations on the resolution of π-basic solutes[5], important differences in selectivity values were found between LC and SubFC depending on the solute or the CSP structures. These intriguing results led us to study in detail the influence of the nature and composition of the mobile phase on both selectivity and elution order in normal-phase liquid chromatography. A unique enantiomeric reversal of elution order occurred on changing the polar modifier from ethanol to chloroform (or methylene chloride). This is the first example of a reversal of elution order owing to achiral mobile phase modifiers (such an inversion has already been observed by Pirkle *et al.*[6] but between normal- and reversed-phase modes). We attempted to connect these results with the dominant character of the polar modifier (proton donor, proton acceptor or strong dipole) as defined by Snyder[7] according to the Rohrschneider solubility data[8]. Finally, several chiral recognition models are discussed.

EXPERIMENTAL

Apparatus

For LC, a modular liquid chromatograph (Gilson, Villiers-le-Bel, France) was used. The standard operating conditions were flow-rate 2 ml/min and temperature 25°C.

For SubFC, carbon dioxide, kept in a container with an eductor tube, was passed into a Model 303 pump (Gilson) through an ethanol cooling bath. The pump head (10 SC) was cooled in order to improve the pump efficiency. The inlet adaptor and cooling jacket were laboratory made. Polar modifiers were added by use of a second Gilson pump and mixed with carbon dioxide through a Gilson mixer (Model

802). A constant-temperature water-bath provided temperature control for the column. A Polychrom 9060 diode-array detector (Varian, Palo Alto, CA, U.S.A.) was used without modification. The pressure was monitored by a back-pressure regulator (TESCOM, Model 26-1700, GEC Composants, Asnières, France) connected in-line after the detector and maintained at 45°C by a water-bath. All results were recorded with a Shimadzu CR 3A integrator (Touzart et Matignon, Vitry-sur-Seine, France). The standard operating conditions were average column pressure 200 bar, temperature 25°C and average carbon dioxide flow-rate, 4.5 ml/min at 0°C.

Chiral stationary phases

All the CSP structures are shown in Fig. 1. General procedures for the synthesis of the stationary phases derived from (*S*)-tyrosine [CSPs 1a (thio-DNBTyr-E), 1c (thio-DNBTyr-A) and 2a (DNBTyr)] were given in a previous paper[1]. The other CSPs were synthesized according to the experimental procedure for the corresponding tyrosine CSPs: CSP 1b (thio-DNBPG-E) was obtained like CSP 1a, starting from

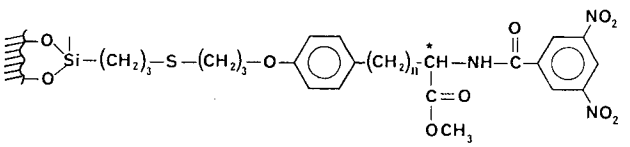

n=1 (S)-CSP 1a (*thio*-DNBTyr-E)

n=0 (R)-CSP 1b (*thio*-DNBPG-E)

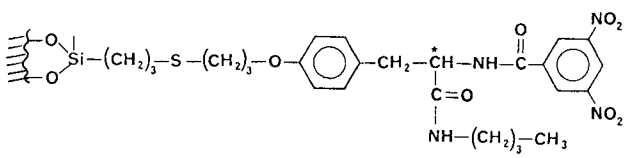

(S)-CSP 1c (*thio*-DNBTyr-A)

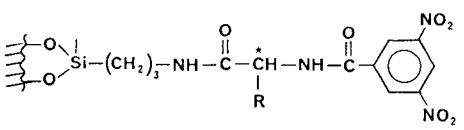

(S)-CSP 2a : R = 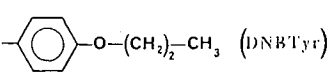 (DNBTyr)

(R)-CSP 2b : R =  (DNBPG)

Fig. 1. Structure of the CSPs derived from (*S*)-tyrosine (CSPs 1a, 1c and 2a), (*R*)-*p*-hydroxyphenylglycine (CSP 1b) and (*R*)-phenylglycine (CSP 2b). Type 1 CSPs: grafting on to a γ-mercaptopropylsilica gel. Type 2 CSPs: grafting on to a γ-aminopropylsilica gel.

p-hydroxyphenylglycine, and CSPs 2b (DNBPG) were obtained like CSP 2a, starting from phenylglycine[9]. Grafting rates were calculated according to the elemental analyses for each CSP (Service Central de Microanalyse du CNRS, France): CSP 1a (0.18 mmol of chiral selector per gram of CSP), CSP 1b (0.22 mmol/g), CSP 1c (0.20 mmol/g), CSP 2a (0.32 mmol/g) and CSP 2b (0.28 mmol/g).

The CSPs were obtained starting from either γ-aminopropylsilica gel (LiChrosorb-NH_2 Si 60, 5 μm, type 2 CSPs) or LiChrosorb Si 60 (5 μm) modified with γ-mercaptopropyltrimethoxysilane (type 1 CSPs). Silica gels were purchased from Merck (Darmstadt, F.R.G.). If not indicated in the captions of figures, the analytical column size was 15 cm × 4.6 mm I.D.

Elution orders were determined by successive injections of racemic and enriched mixtures (in the *S* form) of test solutes.

Mobile phase

Carbon dioxide was N 45-grade (99.995% pure, Air Liquide, Alphagaz, Paris, France). Ethanol and *n*-hexane were of LiChrosolv grade, purchased from Merck. Chloroform [stabilized with 0.6% (w/w) of ethanol] and methylene chloride [stabilized with 0.1% (w/w) of ethanol] of analytical-reagent grade were purchased from Prolabo (Paris, France).

RESULTS AND DISCUSSION

The structures of DNB racemates are shown in Fig. 2. A comparison of LC and SubFC stereoselectivities obtained on the different DNB CSPs is presented in Table I for some typical test solutes. A π–π interaction as a driving force can hardly be advocated during the formation of the transient diastereomeric complexes; the main attractive interactions involved are then dipole–dipole or hydrogen bonding. The lack of a directional π–π interaction gives the solutes various possibilities to approach the CSP; a noticeable influence of the steric hindrance in the vicinity of chiral centres on stereoselectivity can be expected.

Moreover, let us mention again[2] that the resolution of such π-acid compounds could not be achieved on the π-basic CSP designed by replacing the DNB group of CSP 1a by a 1-naphthoyl moiety [except for tyrosine derivative **2a** ($\alpha = 1.08$) and phenylglycinol **4b** ($\alpha = 1.10$)].

Several discrepancies between LC and SubFC are observed for α-aminoamides **2a** and **3** and phenylglycinol **4b** on CSPs 1a, 2a and 2b. A regular increase in selectivity is observed on CSP 2b in the SubFC mode whereas a significant decrease occurs on CSPs 1c and 2a for tyrosine **2a** and leucine **3** derivatives. For α-amino alcohols (**4**), an improvement in selectivity occurs on CSPs 1c and 2b.

Elution order of enantiomers

To complete the data in Table I, a study of the elution order of enantiomers was carried out (Table II). In Table II, the orders always refer to an (*S*)-CSP and to a hexane–ethanol mobile phase. Several comments can be made as follows: (a) for α-amino esters (**1**), inverted elution orders occur between CSPs derived from tyrosine and phenylglycine, whatever the grafting mode; (b) a surprising inversion is observed for α-aminoamides (**2**) and **3** between CSPs 1b and 2b [both derived from (*R*)-phenyl-

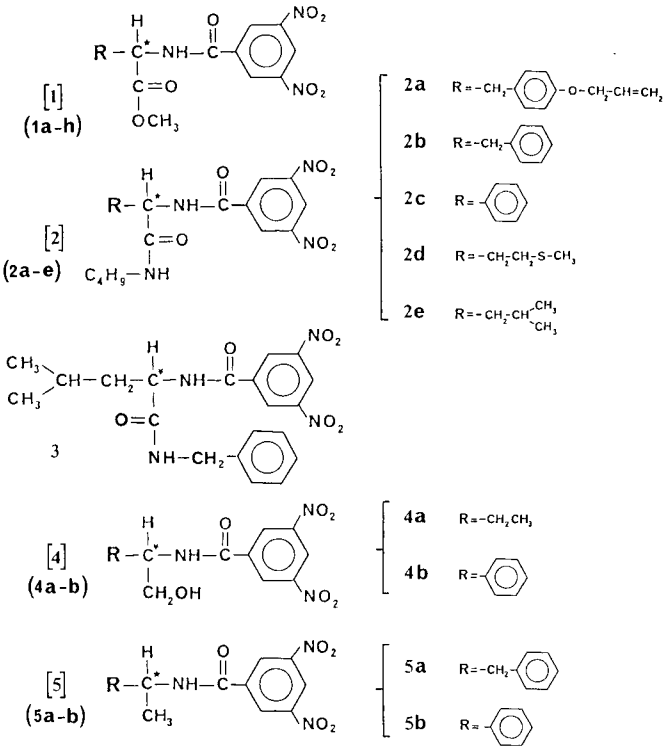

Fig. 2. Structures of 3,5-dinitrobenzoyl (DNB) derivatives of α-amino esters (**1**) (solutes **1a–h**; for R, see Fig. 3), α-aminoamides (**2**) and **3**, α-amino alcohols (**4**) and amines (**5**) investigated.

TABLE I

COMPARISON OF THE SELECTIVITY VALUES, α, OBTAINED UNDER LC OR SUBFC CONDITIONS FOR SOME TYPICAL DNB DERIVATIVES

LC mode: mobile phase, hexane–ethanol (85:15, v/v) with CSPs 1c and 2b, (90:10, v/v) with CSPs 1a and 1b and (92.5:7.5, v/v) with CSP 2a; flow-rate, 2 ml/min; temperature, 25°C; UV detection at 254 nm . SubFC mode: mobile phase, carbon dioxide–ethanol (93:7, w/w); flow-rate, 4.5 ml/min at 0°C; average column pressure, 200 bar; temperature, 25°C; UV detection at 254 nm. Values in italics indicate puzzling discrepancies between LC and SubFC results.

Solute	*CSP*									
	(S)-CSP 1a		*(R)-CSP 1b*		*(S)-CSP 1c*		*(S)-CSP 2a*		*(R)-CSP 2b*	
	α_{LC}	α_{SubFC}	α_{LC}	α_{SubFC}	α_{LC}	α_{SubFC}	α_{LC}	α_{SubFC}	α_{LC}	α_{SubFC}
Leucine **1c**	1.05	1.07	1.07	1.10	1.31	1.25	1.12	1.11	1.06	1.16
Leucine **3**	1.49	1.46	1.09	nr[a]	*1.48*	*1.05*	*1.36*	*1.09*	*1.26*	*1.91*
Tyrosine **1h**	nr	1.04	nr	nr	1.26	1.23	1.09	1.08	1.05	1.15
Tyrosine **2a**	1.52	1.45	1.17	1.12	*1.23*	*nr*	*1.28*	*1.05*	*1.26*	*1.84*
Phenylglycine **1f**	1.05	1.04	1.04	1.05	1.18	1.12	1.09	1.07	nr	nr
2-Aminobutanol **4a**	1.06	1.04	nr	nr	1.04	1.18	nr	nr	*1.18*	*1.54*
Phenylglycinol **4b**	1.11	1.14	1.18	1.18	*1.28*	*1.51*	1.25	1.28	*1.43*	*2.40*

[a] No resolution.

TABLE II

ELUTION ORDERS OF DNB α-AMINO ESTER, α-AMINOAMIDE AND α-AMINO ALCOHOL DERIVATIVES

The elution orders are given with regard to an *S* configuration of each CSP and for hexane–ethanol mobile phase.

Solute as DNB derivative	*(S)-CSP chiral selector*				
	CSP 1a DNB-tyrosine	*CSP 1c DNB-tyrosine*	*CSP 2a DNB-tyrosine*	*CSP 1b DNB-p-hydroxy-phenylglycine*	*CSP 2b DNB-phenyl-glycine*
α-Amino esters (**1**)	(*R*,*S*)	(*R*,*S*)	(*R*,*S*)	(*S*,*R*)	(*S*,*R*)
α-Aminoamides (**2**, **3**)	(*R*,*S*)	(*R*,*S*)	(*R*,*S*)	(*R*,*S*)	(*S*,*R*)
α-Amino alcohols (**4**)	(*S*,*R*)	(*S*,*R*)	(*S*,*R*)	(*S*,*R*)	(*S*,*R*)

glycine]; (c) only α-amino alcohols (**4**) display a regular elution order, whatever the CSP; and (d) the elution order of α-amino alcohols (**4**) is inverted compared with that of α-amino esters (**1**) or α-aminoamides (**2**) and **3** on CSPs derived from tyrosine.

Comparison of resolution of a series of α-N-(3,5-dinitrobenzoyl)amino esters

Selectivity values were plotted against the characterizing side-group, R, of various α-amino esters (**1**) on the five CSPs (Fig. 3). For these solutes, the sites of interaction are limited to the dinitrobenzamide dipole and the ester carbonyl group. As previously argued[2], the selectivity will be enhanced on a CSP with two easily accessible amide dipoles (CSP 1c). Steric hindrance due to the silica matrix on the aliphatic amide dipole (CSP 2a) slightly decreases the selectivity. Comparing now phenylglycine- and tyrosine-derived CSPs, the higher steric hindrance resulting from the presence of a phenyl instead of a benzyl group may account for the loss in selectivity and for the inversion of elution order observed from CSP 1a (or 2a) to CSP 1b (or 2b) (Table II); in fact, the accessibility to the chiral centre for phenylglycine CSPs is limited to one side only. Moreover, on tyrosine-derived CSPs, the occurrence of a weak π–π overlapping between benzyl and dinitrobenzoyl moieties cannot be entirely disregarded; with a phenyl group directly attached to the asymmetric centre (CSPs 1b and 2b), good overlapping is not possible. Such a π–π interaction can also be considered for solutes derived from tyrosine and phenylalanine, whatever the CSP.

Finally, on CSPs 1a, 1b, 2a and 2b, the structure of the R group has a minor effect on stereoselectivity, unlike previous observations on π-basic CSPs derived from tertiary phosphine oxides[10,11]. However, as CSP 1c combines the presence of multiple sites of interaction and a reduced steric hindrance, it is expected to be sensitive to the solute steric bulkiness. We indeed observed more significant variations in selectivity on this CSP in the amino ester series (**1**).

Influence of the nature of the mobile phase

Chromatographic data. Hitherto, selectivities were always similar in LC and SubFC on Pirkle-type CSPs[5,12], but the studies concerned the resolution of π-basic solutes on π-acid CSPs. In this work, dealing with the resolution of π-acid solutes on π-acid CSPs, the nature of the mobile phase appears to play a decisive part in the

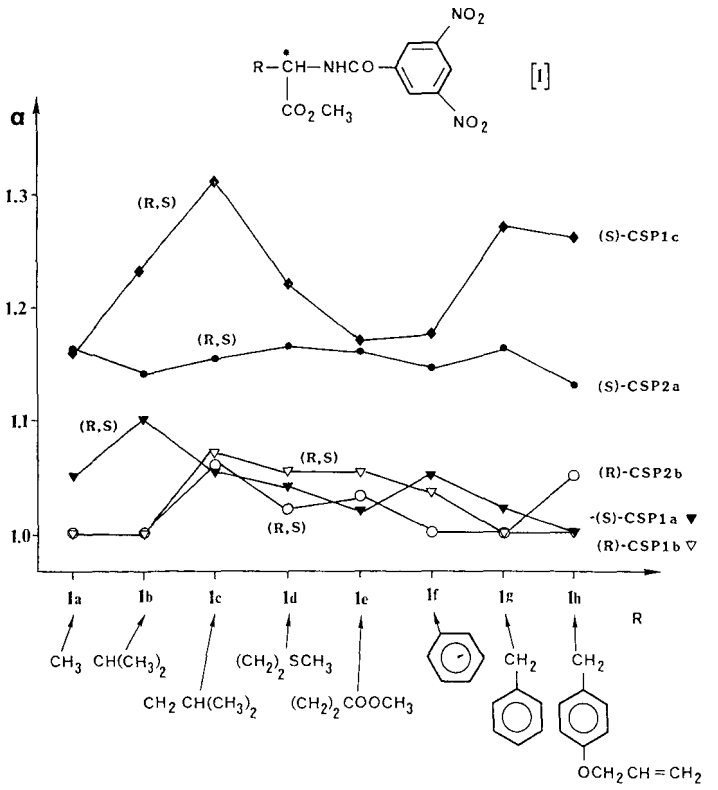

Fig. 3. LC resolution of DNB α-amino esters (**1**). Influence of the nature of the R substituent group on the selectivity α. Mobile phase, hexane–ethanol (85:15, v/v) with CSPs 1a, 1c and 2b (90:10, v/v) with CSP 1b and (92.5:7.5, v/v) with CSP 2a (the ethanol content was set to give a similar capacity factor, k'_2, for the last eluted enantiomer of a racemate on the five CSPs); flow-rate, 2 ml/min; temperature, 25°C; UV detection at 254 nm.

chiral recognition, as shown by the aforementioned discrepancies observed for aminoamides **2a** and **3** and amino alcohol **4b**. We therefore studied the influence in LC of the nature of the polar modifier on the stereoselectivity. The separation of four typical racemates derived from leucine ester **1c**, tyrosine ester **1h**, tyrosine amide **2a** and phenylglycinol **4b** was investigated.

TABLE III

SELECTIVITY PARAMETERS, AS DEFINED AND CALCULATED BY SNYDER[4] FROM SOLUBILITY DATA REPORTED BY ROHRSCHNEIDER

Values in italics indicate the dominant character of the solvent: χ_e (proton acceptor), χ_d (proton donor) and χ_n (strong dipole).

Polar solvent	χ_e	χ_d	χ_n
Ethanol	*0.52*	0.19	0.29
Chloroform	0.25	*0.41*	0.33
Methylene chloride	0.29	0.18	*0.53*

TABLE IV

INFLUENCE OF THE NATURE OF THE MOBILE PHASE ON THE RESOLUTION OF COMPOUNDS **1c, 1h, 2a** AND **4b** ON TYPE 1 CSPs (CSPs 1a, 1b AND 1c)

Values in italics indicate an inversion of elution order with regard to the hexane–ethanol mobile phase. Values between parentheses indicate the polar solvent content in hexane.

Solute	*(S)-CSP 1a*				*(S)-CSP 1c*				*(R)-CSP 1b*		
	C_2H_5OH (15%)	*$CHCl_3$ (%)*	*CH_2Cl_2 (%)*	*SubFC*[a]	*C_2H_5OH (15%)*	*$CHCl_3$ (%)*	*CH_2Cl_2 (%)*	*SubFC*[a]	*C_2H_5OH (10%)*	*$CHCl_3$ (%)*	*SubFC*[a]
Leucine **1c**	1.04	1.45 (45)	1.46 (40)	1.07	1.31	1.86 (50)	2.01 (40)	1.25	1.07	1.12 (40)	1.10
Tyrosine **1h**	nr	1.25 (40)	1.26 (35)	1.04	1.26	1.61 (35)	1.71 (40)	1.23	nr	nr (55)	nr
Tyrosine **2a**	1.45	1.87 (55)	1.53 (60)	1.45	1.23	*1.51* (65)	*1.52* (90)	nr	1.17	nr (55)	1.12
Phenylglycinol **4b**	1.10	1.08 (70)	nr (75)	1.14	1.28	1.57 (85)	1.36 (90)	1.51	1.18	1.12 (70)	1.18

[a] SubFC conditions as in Table I.

Ethanol, chloroform and methylene chloride were chosen according to their dominant character with regard to the selectivity parameters χ_e, χ_d and χ_n (Table III)[7]. These parameters reflect the relative ability of a solvent to act as a proton acceptor (χ_e), a proton donor (χ_d) or a strong dipole (χ_n). Ethanol can be mainly considered as a proton acceptor, chloroform as a proton donor and methylene chloride as a dipole.

Stereoselectivities, α, observed with binary hexane–polar modifier mixtures are gathered in Table IV (type 1 CSPs) and Table V (type 2 CSPs). SubFC results are given again to allow easy comparison with LC. For each solute, the mobile phase composition was adjusted in order to maintain a similar capacity factor, k'_2, of the last eluted enantiomer on a given CSP (isoeluotropic mobile phases).

Two major observations can be made from these data on changing the polar modifier from ethanol to chloroform (or methylene chloride): (a) a unique reversal of elution order of enantiomers for tyrosine amide derivative **2a** on CSPs 1c and 2a; and (b) a systematic and noticeable increase in selectivity for ester derivatives **1c** and **1h**.

The chromatograms in Fig. 4a and c show the reversal of the elution order for tyrosine amide **2a** on CSP 1c. It is noteworthy that a complete loss of resolution is observed with the subcritical carbon dioxide–ethanol mobile phase (Fig. 4b). Regarding the stereoselectivity of this separation, SubFC can be considered as intermediate between the two LC binary mixtures, hexane–ethanol and hexane–chloroform (or methylene chloride). This intermediate behaviour is also observed for the resolution of phenylglycinol derivative **4b** (Fig. 5): $\alpha_{SubFC} = 2.40$ while $\alpha_{LC,C_2H_5OH} = 1.45$ and $\alpha_{LC,CHCl_3} = 3.37$. In LC, the increase in α has to be attributed to a strengthening of the stability of the (*R*)-CSP 2b–(*S*)-solute **4b** transient diastereomeric complex; a 190% increase in k'_2 is observed for only a 10% increase in k'_1 on changing from ethanol (15% in hexane) to chloroform (90% in hexane).

TABLE V

INFLUENCE OF THE NATURE OF THE MOBILE PHASE ON THE RESOLUTION OF COMPOUNDS **1c**, **1h**, **2a** AND **4b** ON TYPE 2 CSPs (CSPs 2a AND 2b)

Values in italics indicate an inversion of elution order with regard to the hexane–ethanol mobile phase. Values between parentheses indicate the polar solvent content in hexane.

Solute	*(S)-CSP 2a*				*(R)-CSP 2b*			
	C_2H_5OH (7.5%)	*$CHCl_3$ (%)*	*CH_2Cl_2 (%)*	*SubFC[a]*	*C_2H_5OH (15%)*	*$CHCl_3$ (%)*	*CH_2Cl_2 (%)*	*SubFC[a]*
Leucine **1c**	1.12	1.50 (50)	1.46 (50)	1.11	1.06	1.18 (40)	1.21 (50)	1.16
Tyrosine **1h**	1.09	1.34 (50)	1.32 (50)	1.08	1.05	1.16 (40)	1.17 (50)	1.15
Tyrosine **2a**	1.28	*1.14* (55)	*1.05* (65)	1.05	1.26	2.00 (60)	2.07 (65)	1.84
Phenylglycinol **4b**	1.25	1.23 (95)	1.23 (100)	1.28	1.43	3.37 (90)	2.88 (95)	2.40

[a] SubFC conditions as in Table I.

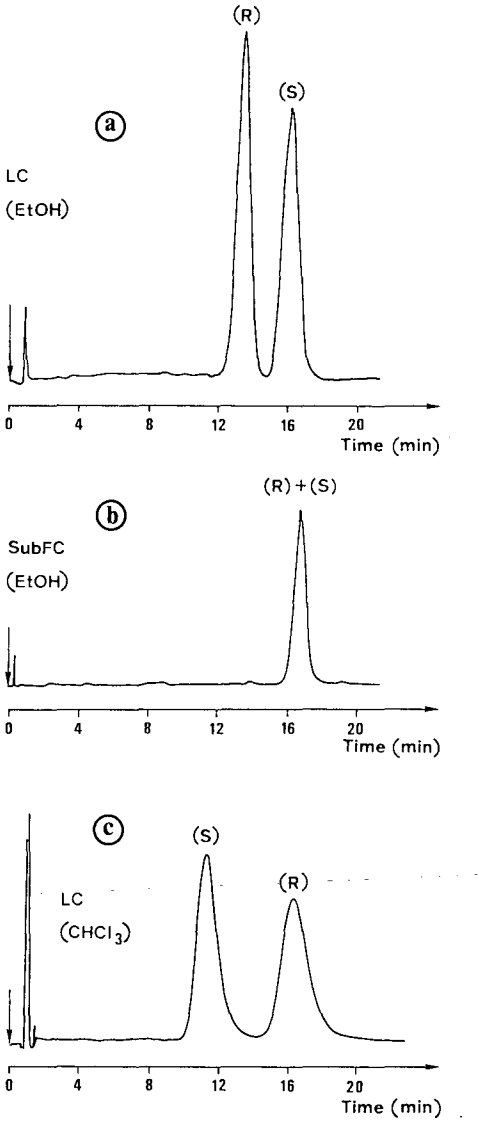

Fig. 4. Influence of the nature of the achiral mobile phase on resolution and elution order of tyrosine derivative **2a** enantiomers on (*S*)-CSP 1c. LC conditions: mobile phase, (a) hexane–ethanol (85:15, v/v) or (c) hexane–chloroform (35:65, v/v); flow-rate, 2 ml/min; temperature, 25°C; UV detection at 254 nm. SubFC conditions: mobile phase, (b) carbon dioxide–ethanol (93:7, w/w); flow-rate, 4.5 ml/min at 0°C; average column pressure, 200 bar; temperature, 25°C; UV detection at 254 nm. EtOH = Ethanol.

The inversion of the elution order with hexane–chloroform mobile phase was demonstrated for other aminoamides on CSP 1c, except for the phenylglycine derivative **2c** (Table VI). This last result is in good agreement with the regular elution order of tyrosine derivative **2a** observed on the phenylglycine-derived CSP 2b (Table V), whatever the mobile phase (reciprocality concept[13]).

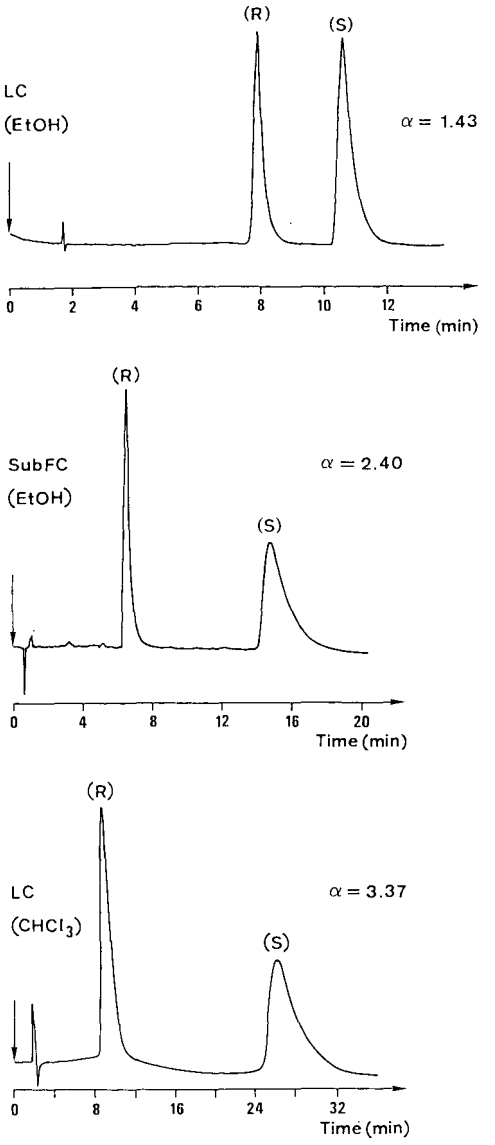

Fig. 5. Influence of the nature of the mobile phase on the resolution of phenylglycinol derivative **4b** on (*R*)-CSP 2b. LC conditions: mobile phase, hexane–ethanol (85:15, v/v) [$k'_{(R)}$ = 3.9, $k'_{(S)}$ = 5.6] or hexane–chloroform (10:90, v/v) [$k'_{(R)}$ = 4.3, $k'_{(S)}$ = 16.3]; flow-rate, 2 ml/min; temperature, 25°C; UV detection at 254 nm. SubFC conditions: mobile phase, carbon dioxide–ethanol (93:7, w/w); flow-rate, 4.5 ml/min at 0°C; average column pressure, 200 bar; temperature, 25 °C; UV detection at 254 nm.

*Relationship between elution order of α-aminoamides (**2**) and selectivity parameters of solvents.* The reversal of elution order was also checked using ternary mixtures, as shown in Fig. 6 (hexane–ethanol–chloroform) and Fig. 7 (hexane–ethanol–methylene chloride). The considerable decrease in the capacity factors, k'_1 and k'_2, has already been reported on CSP 2b with hexane–alcohol–chloroform mixtures for the resolu-

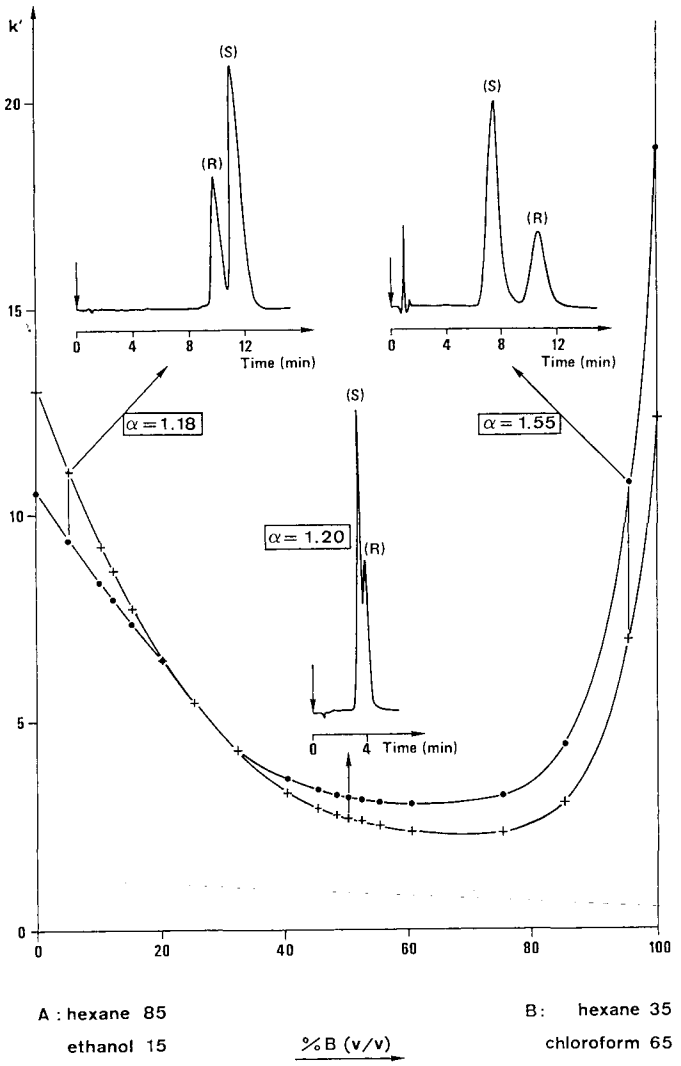

Fig. 6. Reversal elution order of **2a** enantiomers on (*S*)-CSP 1c on changing from hexane–ethanol (85:15, v/v) (solvent A) to hexane–chloroform (35:65, v/v) (solvent B) mobile phase. The capacity factors, k', of (*S*)-**2a** (+) and (*R*)-**2a** (●) are plotted *versus* the content of binary mixture B in the ternary mixture A–B. The elution order was established using an enriched mixture of **2a** in the *S* form. Flow-rate, 2 ml/min; temperature, 25°C; UV detection at 254 nm.

tion of phosphine oxide enantiomers[14]. However, for the latter solutes, no inversion of elution order was observed.

Chloroform and methylene chloride display two different dominant characters (χ_d and χ_n, respectively), although reversal of elution order was observed with both solvents. This leads us to attribute this phenomenon to the loss of the prevailing χ_e character in the mobile phase on changing from solvent A to B, to the benefit of either the χ_d or χ_n character. This is corroborated by the fact that, in the inversion region

TABLE VI

COMPARISON OF SELECTIVITY AND ELUTION ORDERS FOR AMINOAMIDES (**2**) AND **3** ON CSP 1c (*S*)-THIO-DNBTyr-A WITH HEXANE–ETHANOL (85:15, v/v) AND HEXANE–CHLOROFORM (35:65, v/v)

Solute	*Hexane–ethanol (85:15, v/v)*				*Hexane–chloroform (35:65, v/v)*			
	k'_1	k'_2	α	*Elution order*	k'_1	k'_2	α	*Elution order*
(4-Propyloxy)tyrosine **2a**	12.94	15.86	1.23	(*R*,*S*)	10.67	16.11	1.51	(*S*,*R*)
Phenylalanine **2b**	7.42	9.02	1.40	(*R*,*S*)	11.03	13.42	1.22	(*S*,*R*)
Phenylglycine **2c**	7.00	9.74	1.39	(*S*,*R*)	5.38	18.44	3.43	(*S*,*R*)
Methionine **2d**	6.61	8.96	1.35	(*R*,*S*)	10.85	12.86	1.19	(*S*,*R*)
Leucine **2e**	3.18	4.79	1.51	(*R*,*S*)	11.63	12.75	1.10	(*S*,*R*)
Leucine **3**	6.75	9.42	1.39	(*R*,*S*)	15.66	20.30	1.30	(*S*,*R*)

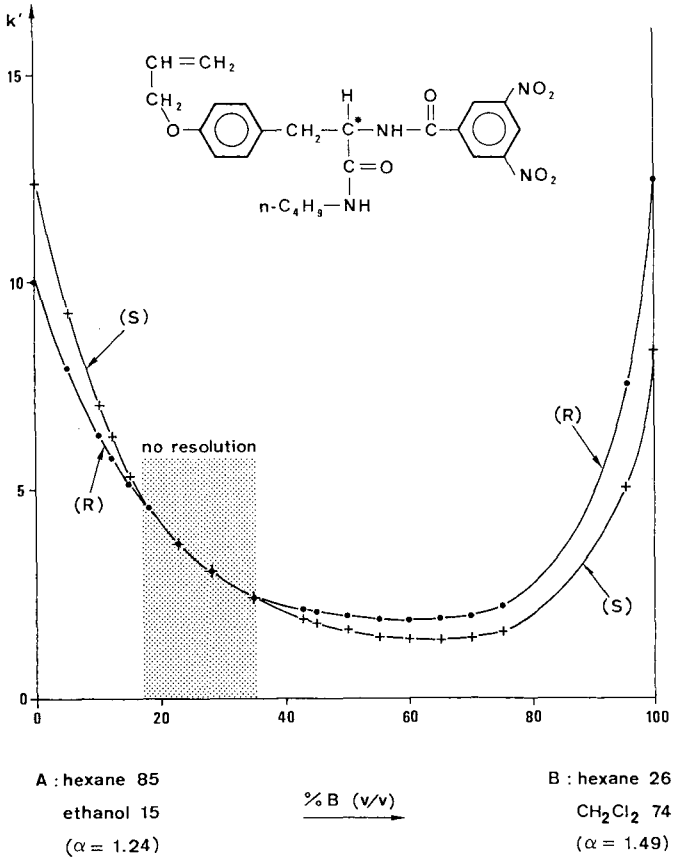

Fig. 7. Reversal of elution order of **2a** enantiomers on (*S*)-CSP 1c on changing from hexane–ethanol (85:15, v/v) (solvent A) to hexane–methylene chloride (26:74, v/v) (solvent B) mobile phase. The capacity factors, k', of (*S*)-**2a** (+) and (*R*)-**2a** (●) are plotted *versus* the content of binary mixture B in the ternary mixture A–B. Analytical conditions as in Fig. 6.

TABLE VII

CALCULATION OF THE RELATIVE CONTRIBUTIONS χ_e, χ_d AND χ_n FOR THE MOBILE PHASE COMPOSITION CORRESPONDING TO THE LIMITS OF THE INVERSION REGION WITH HEXANE–ETHANOL–CHLOROFORM OR HEXANE–ETHANOL–METHYLENE CHLORIDE TERNARY MIXTURES

Values in italics indicate the dominant character.

Mobile phase composition	χ_e	χ_d	χ_n
Hexane–ethanol–chloroform:			
18% B (76:12.3:11.7, v/v/v)	*0.39*	0.30	0.31
35% B (67.5:9.8:22.7, v/v/v)	0.33	*0.35*	0.32
Hexane–ethanol–methylene chloride:			
18% B (74.4:12.3:13.3, v/v/v)	*0.37*	0.24	*0.39*
35% B (64.3:9.8:25.9, v/v/v)	0.36	0.18	*0.46*

where no resolution is observed (18–35% of solvent B in the mobile phase, Figs. 6 and 7), at least two of the three contributions are of same order of magnitude (Table VII). Moreover, we can expect (from calculations in Table VII) that the balance point (α = 1.00) will arise for a content of solvent B close to 35% for chloroform (χ_e = 0.33 and χ_d = 0.35) and close to 18% for methylene chloride (χ_e = 0.37 and χ_n = 0.39). This assumption cannot be precisely confirmed owing to peak broadening on adding chloroform or methylene chloride to the mobile phase; the resulting decrease in efficiency contributes to the lack of resolution in the inversion region (*e.g.*, when $\alpha \leqslant 1.10$).

Chiral recognition models. The inversion region corresponds to the occurrence of two chiral recognition mechanisms working in opposite stereochemical senses and with similar contributions to the overall process[6]. Either solvation or conformation of both the solute and CSP are affected by the change in the nature of the polar modifier. This may in turn alter the type of interaction involved during the chiral recognition process.

At this stage of investigation, it is impossible to ascribe a given mechanism to the resolution of a given solute on a given chromatographic system (CSP, mobile phase). Too many different factors are involved during the separation process and we failed to correlate the experimental data with observations inferred from the examination of CPK models[a]. Moreover, many of the results appeared to be contradictory from one CSP (or solute) to another. This has to be attributed to the lack of a clear driving force such as a strong π–π overlapping which orientates the molecules inside the diastereomeric complex and is conformationally restrictive. However, general comments can be made as follows:

(a) The reversal of elution order was observed only for amide derivatives (**2**) (which contain two amide dipoles) on tyrosine-derived CSPs 1c and 2a (bearing also two amide dipoles); the multiplicity of possible sites of interaction may then favour the occurrence of competitive opposite-sense chiral recognition mechanisms, depend-

[a] CPK precision molecular models are improved versions of the Corey–Pauling models designed at the California Institute of Technology in the late 1940s, with new connectors by Dr. W. Koltun.

ing on the nature of the mobile phase. Alteration of the conformation of solutes and CSPs may play an important part in the inversion (intramolecular hydrogen bonding, solvation, etc.).

(b) The abnormal behaviour of phenylglycine amide **2c** and CSP 2b (derived from phenylglycine) remains unclear; we can assume that the phenyl group limits the access of the chiral centre to one side only, thus reducing the number of possible chiral recognition mechanisms.

(c) For phenylglycinol derivative **4b**, the existence of a prevailing hydrogen bonding interaction involving the hydroxyl group can explain the regular elution order on all the CSPs (Table II). Differences in α values according to the nature of the CSP or mobile phase are not yet explained.

(d) The influence of the nature of the polar modifier is not elucidated. It was not possible to connect the dominant character of a modifier with its ability to favour dipole–dipole or hydrogen bonding interactions. We can note, however, that alcohols will interact preferentially with NH moieties whereas chloroform, as a proton donor, will act with carbonyl groups. The resulting alteration of the conformations of the solute and CSP may induce changes in the dominant chiral recognition mechanism, leading eventually to inversion of the elution order of enantiomers.

CONCLUSION

We have demonstrated the ability of π-acid DNB CSPs to resolve π-acid DNB racemates. However, the lack of π–π interactions as the driving force during the diastereomeric complex formation renders more difficult the understanding of chiral recognition mechanisms. Moreover, we found a reversal of elution order for a series of DNB aminoamide derivatives on just changing the polar modifier from ethanol to chloroform (or methylene chloride). This indicates the importance of a knowledge of the conformational state of both the solute and CSP during the chromatographic separation. We think that[15], together with chromatographic data, NMR studies of bimolecular solute–CSP complexes[16] would be useful means of elucidating chiral recognition processes, as they would also take into account the solvent contribution (even if the evaluation of the intrinsic role of the silica matrix still remains a problem).

REFERENCES

1 A. Tambuté, A. Begos, M. Lienne, P. Macaudière, M. Caude and R. Rosset, *New J. Chem.*, (1988) in press.
2 M. Lienne, P. Macaudière, M. Caude, R. Rosset and A. Tambuté, *Chirality*, 1 (1989).
3 I. W. Wainer and T. D. Doyle, *J. Chromatogr.*, 259 (1983) 465.
4 J. Kip, P. Van Haperen and J. C. Kraak, *J. Chromatogr.*, 356 (1986) 423.
5 P. Macaudière, M. Caude, R. Rosset, A. Tambuté, M. C. Alembik and I. W. Wainer, *J. Chromatogr.*, 371 (1986) 177.
6 W. H. Pirkle, M. H. Hyun and B. Bank, *J. Chromatogr.*, 316 (1984) 585.
7 L. R. Snyder, *J. Chromatogr. Sci.*, 16 (1978) 223.
8 R. Rohrschneider, *Anal. Chem.*, 45 (1973) 1241.
9 W. H. Pirkle, A. Tsipouras and T. J. Sowin, *J. Chromatogr.*, 319 (1985) 392.
10 A. Tambuté, A. Begos, M. Lienne, M. Caude and R. Rosset, *J. Chromatogr.*, 396 (1987) 65.
11 M. Lienne, M. Caude, R. Rosset, A. Tambuté and A. Begos, paper presented at the *International Symposium on Chiral Separations, Guilford, U.K., September 3–4, 1987.*

12 P. Macaudière, M. Caude, R. Rosset and A. Tambuté, *J. Chromatogr. Sci.*, in press.
13 W. H. Pirkle, D. W. House and J. M. Finn, *J. Chromatogr.*, 192 (1980) 143.
14 P. Pescher, M. Caude, R. Rosset and A. Tambuté, *J. Chromatogr.*, 371 (1986) 159.
15 P. Macaudière, M. Lienne, A. Tambuté and M. Claude, in A. M. Krstulovic (Editor), *Chiral Separation by HPLC: Application to Compounds of Pharmaceutical Interest*, Ellis Horwood, Chichester, 1989, pp. 399–445.
16 W. H. Pirkle, T. C. Pochapsky, G. S. Mahler, D. E. Corey, D. S. Reno and D. M. Alessi, *J. Org. Chem.*, 51 (1986) 4991.

Journal of Chromatography, 467 (1989) 373–384
Elsevier Science Publishers B.V., Amsterdam — Printed in The Netherlands

CHROM. 21 320

GAS CHROMATOGRAPHIC DETECTION OF SELECTED ORGANOCHLORINE SPECIES USING AN ALTERNATING CURRENT PLASMA DETECTOR

ROBERT B. COSTANZO and EUGENE F. BARRY*
Department of Chemistry, University of Lowell, 1 University Avenue, Lowell, MA 01854 (U.S.A.)
(First received October 11th, 1988; revised manuscript received January 16th, 1989)

SUMMARY

The alternating current plasma detector for gas chromatography is shown to be a useful detector for selective organochlorine detection. The detector incorporates a simple design and a power source that produces a stable discharge which does not extinguish under high solvent concentration conditions. The plasma discharge produces diatomic emission of CCl species, with few atomic chlorine emission lines. Detection limits for various organochlorine compounds are approximately 1.0 ng/s. The detector exhibits a complex response dependent on molecular structure and environment. Detector selectivity towards CCl *versus* C_2 emission is presented, along with various selective chlorine detection applications in complex matrices.

INTRODUCTION

Many different kinds of organochlorine compounds are introduced into the environment each year through human activities. Analysis of many chlorinated organics is commonly done by packed or high-resolution capillary column gas chromatography (GC) equipped with a halogen-selective detector[1], the most common of which are the Hall electrolytic conductivity detector (HECD) and the electron-capture detector (ECD)[2–5]. Both detectors provide pg/s detection limits and high selectivity for halogens. However, these detectors are prone to contamination by interfering impurities in the chromatographic system or sample, such as water, by detector overload of halogenated compounds and by septum and column bleed[6,7].

Microwave-induced plasma (MIP) detection incorporating the Beenakker cavity TM_{010}[8] is finding continued success due to its ability to selectively distinguish between types of halogens, limits of detection in the pg/s range and ability to do multi-element determination[9–12]. The MIP also has a uniform relative response to most organochlorines per unit mass. Therefore, molecular structure does not influence the detector response, allowing empirical formula determination[13,14].

The direct current plasma detector (DCPD) for GC, sustained in a helium or argon atmosphere, is also a sensitive and selective detector in many applications[15–17]. Both two- and three-electrode configurations are used for selective detection of metallic and non-metallic elements at detection limits between the nanogram to

0021-9673/89/$03.50

picogram range. The incorporation of GC–inductively-coupled plasma (ICP) as an element selective detector continues to show little use compared to GC–MIP; although, detection limits for the metallic and non-metallic elements vary from the microgram to nanogram range and selectivity ratios are high[18,19]. Improvements in the GC interface problems encountered in this technique may help to widen the range of applications and performance enjoyed currently. The helium afterglow detector for GC shows great potential as an element selective detector, since detection limits and selectivities rival values found for GC–MIP[20,21].

Recently, our laboratory developed an alternating current plasma detector (ACPD) for selective capillary GC detection[22,23]. The ACPD is similar to a d.c. microarc plasma source[24] and can tolerate high mass flow-rates of solvent without extinguishing and, therefore, requires no venting valve. This leads to a less complex interface design and minimizes band broadening. The plasma is self-seeding and reignites itself every half cycle, which is 120 times per second for a 60-Hz power supply. As a result, a tesla coil is not required to initiate the plasma as long as the a.c. voltage supply is above the breakdown voltage. This communication describes the detection of a number of chlorinated species, polychlorinated biphenyls (PCBs) and pesticides by capillary GC–ACPD. Linearity, detection limits, selectivity and applications are discussed.

EXPERIMENTAL

Materials

The organochlorine compound standard solutions were prepared in spectra-grade *n*-pentane (Fisher Scientific, Fair Lawn, New Jersey, U.S.A.). The organochlorines used in the study were as follows: tetrachloroethylene, *n*-dodecane, *n*-nonane, *o*-chlorotoluene (Aldrich, Milwaukee, WI, U.S.A.); *p*-dichlorobenzene, 1,5-dichloropentane, Aroclor 1254 (Chem Service, West Chester, PA, U.S.A.); 1,10-dichlorodecane, carbon tetrachloride (Eastman Kodak, Rochester, NJ, U.S.A.); 1,2-dichloroethane (Fisher Scientific, Fair Lawn, NJ, U.S.A.); lindane (Polyscience Corp., Niles, IL, U.S.A.); number 2 fuel oil; regular gasoline (Texaco, White Plains, NY, U.S.A.). The carrier and make-up helium gas were filtered with moisture, oxygen and hydrocarbon traps (Supelco, Bellefonte, PA, U.S.A.).

Instrumentation

The GC–ACPD system arrangement, described in detail elsewhere[22], is shown in Fig. 1 and includes a Hewlett-Packard model 5890A gas chromatograph (Hewlett-Packard, Palo Alto, CA, U.S.A.), a single-beam McPherson grating monochromator EU700 (McPherson, Acton, MA, U.S.A.), an optical bench equipped with an adjustable optical mount and 75-mm biconvex quartz lens (Oreil, Stratford, CT, U.S.A.), a R212 PMT (Hamamatsu, Middlesex, NJ, U.S.A.) coupled to a McPherson Model 7640 voltage supply and a Hewlett-Packard 3392A integrator. The two fused-silica capillary megabore columns employed in this study were a 30 m × 530 μm I.D. column with a 1.5-μm film thickness of DB-1 (J & W Scientific, Cordova, CA, U.S.A.) and a 10 m × 530 μm I.D. column with a 4.8-μm film thickness of CP SIL-8 CB (Chrompack, Bridgewater, NJ, U.S.A.). Table I lists general operating conditions for the GC and ACPD employed throughout the studies. The GC–ACPD interface has

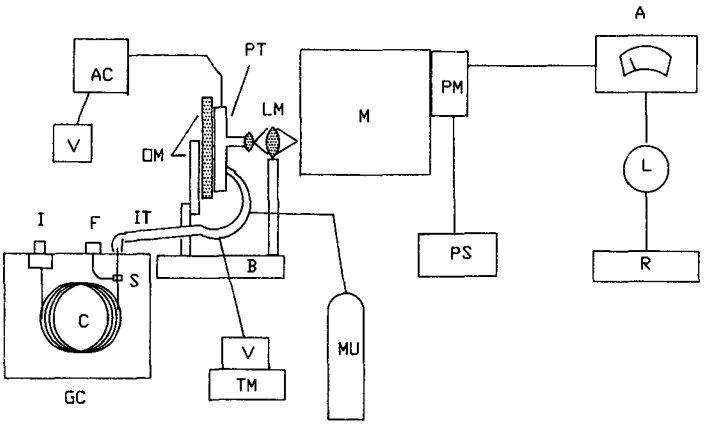

Fig. 1. Schematic diagram of the GC–ACPD experimental arrangement. (GC) gas chromatograph; (C) megabore capillary column; (I) injection port; (F) FID; (S) column oven tee split; (IT) detector interface tube; (V) variac; (AC) a.c. power supply; (OM) optical plasma mount; (PT) plasma discharge tube; (LM) lens and mount; (MU) helium make-up gas; (B) optical bench; (TM) thermocouple thermometer; (M) monochromator; (PM) photomultiplier tube; (PS) PMT power supply; (A) picoammeter; (L) low-pass filter; (R) recorder integrator.

also been described in detail by the authors[23] and includes a PTFE union adaptor that created an electrical barrier between the flexible metal interface capillary column jacket and the 1/8 in. O.D. × 8 in. copper electrode tube. The megabore column is inserted through the interface tube/electrode and a series of rubber septa for electrical insulation. The column is inserted through the middle of the bottom electrode so that 1 mm of the column extends beyond the tip of the electrode. The interface unit is then attached to a Pyrex discharge tube with a 1/4 in. O.D.[23] and mounted onto the optical bench.

Procedure

The optimal operating parameters for the ACPD were previously determined[23] and were employed in the present study, listed in Table I. The optimal helium make-up gas flow-rate was established at 1 ml/min for this study. The low make-up flow-rate

TABLE I

GENERAL GC–ACPD OPERATING CONDITIONS USED IN THE STUDY

Parameter	*Condition*
Injector temperature	230°C
Interface temperature	210°C
Column flow-rate	20 ml/min
Helium make-up flow rate	1 ml/min
a.c. power output	11 000 V a.c.
PMT voltage	1000 V d.c.
Slit width	1500 μm
Low-pass filter time constant	0.11 s
Analytical emission band for the C–Cl species	278.84 nm

results from the fact that since the column flow-rate is rapid (20 ml/min), a 1 ml/min flow serves only to minimize turbulance and create an outside flow pattern. As a result, this flow pattern serves as a sheath and directs the sample vapor plugs into the center of the plasma plume and minimizes the solute skirting the plume. The window arm of the discharge tube was directed to the monochromator and the plasma emission was focused for a maximum signal at a copper wavelength by adjusting the optical mount. The chlorine lines and C–Cl diatomic species bands were obtained by purging a helium stream saturated with chloroform vapor through the plasma and scanning the appropriate wavelength regions. The region scanned was 270.0–800.0 nm at 0.5 nm/s. A smaller region was examined more closely between 230 nm and 330 nm and yielded a few intense diatomic C–Cl analytical emission bands as well as C_2 emission bands. The diatomic species, C–Cl, produced the most intense emission band, which was employed as the analytical emission band in the study.

Standard solutions of 1,10-dichlorodecane (DCD), *p*-dichlorobenzene (DCB), tetrachloroethylene (TCE) and *n*-butylchloride (NBC) were chromatographed at oven temperatures of 150, 80, 50 and 85°C, respectively, on the DB-1 megabore column. The appropriate injection volumes and split ratios were established for each compound in order to introduce the desired amounts into the ACPD. Calibration curves were then constructed from the response data and the detection limits were determined. The selectivity was established by examining a response mixture containing 164 ng C–Cl as DCD and 541 ng C_2 as dodecane in a 0.5-μl injection on the DB-1 megabore column at a split ratio of 16.5 to 1. The separation was achieved at a column temperature of 40°C (0.5 min) to 185°C (10 min) at 7 °C/min, 20.5 ml/min, slit width of 1000 μm with a 1-mm slit height and the output voltage of the detector is governed by a picoammeter setting of 0.3 mA full scale.

The relative response study was performed by recording the response of the ACPD per unit mass of C–Cl for select organochlorine substances that included saturated and unsaturated moieties and contained only one C–Cl per molecule. The GC column used was the CP SIL-8 CB megabore capillary column at a temperature of 32°C (0.5 min) to 150°C at 10°C/min. Applications were done at GC conditions listed in the corresponding figure captions. First, a mixture of volatile organochlorine compounds, each in the amount of 1000 ng, was made in 1 ml of *n*-pentane. A 10-μl injection of the head vapor was introduced onto the CP SIL-8 CB megabore capillary column, described previously. Next, a gasoline sample was spiked with a known amount of lindane and a known aliquot was injected with subsequent detection by FID and ACPD. The detection of Aroclor1254 in diesel gas was done by spiking a 10-ml aliquot of number 2 fuel oil with 10 mg of Aroclor 1254 and injecting 1 μl onto the CP SIL-8 CB megabore column.

RESULTS AND DISCUSSION

Analytical emission bands

The emission profile associated with the plasma emission within the range of 230 nm to 300 nm is depicted in Fig. 2. There are numerous molecular emission bands associated with C_2, CN, CH and C–Cl diatomic emission between 250 nm and 280 nm. Between the two C–Cl bands displayed in Fig. 2 centered at 277.83 nm and 278.84 nm (peaks a and b in Fig. 2), respectively, there is an intense C_2 band (c) which also

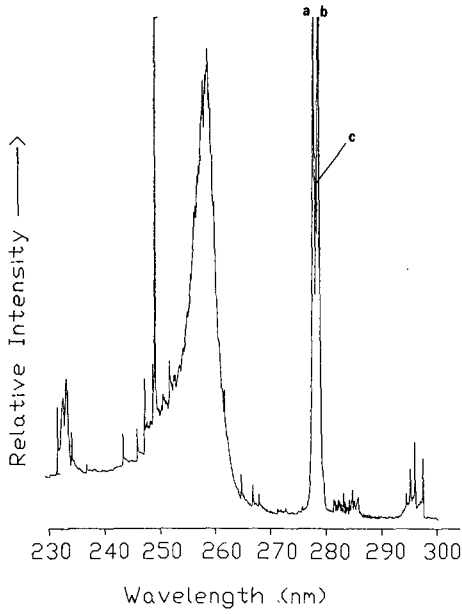

Fig. 2. Wavelength scan of helium saturated with chloroform vapor by the ACPD. Scan rate was 0.5 nm/s with a chart speed of 1 cm/min. (a) CCl 277.83 nm; (b) CCl 278.84 nm; (c) C_2 interference emission band *ca.* 277.0 nm to 278.9 nm.

overlaps with peaks a and b. Peak a is less intense than band b; therefore, the analytical C–Cl emission band used in the entire study was the 278.84 nm band for selective chlorine detection. Dagnall *et al.*[25] and McCormack *et al.*[26] also employed this C–Cl emission band for selective chlorine determination for GC–MIP applications. Most chlorine detection by GC–MIP utilizes the 479.5 nm lines characteristic of atomic chlorine emission, which is an atomic chlorine line. However, helium-MIP is typically a more intense emission source than a.c.-arc techniques, which leads to predominately atomic emission lines. The emission spectra of chloroform generated in this study, which was from 210 nm to 800 nm, showed no chlorine atomic emission that was sufficiently intense for analytical use and showed only a few intense diatomic C–Cl emission bands existed for potential use. However, many of these C–Cl bands are overlapped by very intense C_2 bands, rendering them useless.

A slit width of 50 μm (bandpass of 0.09 nm) yielded sufficient resolution to determine atomic and molecular emission. However, intense molecular emission throughout the spectral region may have masked potential atomic chlorine emission, particularly in the region between 320 nm and 450 nm where many atomic chlorine lines lie[27]. The percentage of C_2 at 278.63 nm (peak c in Fig. 2) which overlaps with the C–Cl emission at 278.84 nm (peak b in Fig. 2) was determined by calculating the percent overlap of peak area of the emission profile. The emission intensity of the C–Cl band actually consists of only 3.1% of C_2 emission and this overlap was not studied in great detail. Within the concentration region studied, the C_2 overlap did not seriously vary from the 3.1% value determined; therefore, linearity was assumed for the region. The linear response of the ACPD can be attributed to C–Cl emission. However, the

overlap is significant enough to affect the detector selectivity towards C–Cl *versus* carbon. The C–Cl emission bands in other regions of the spectra, including the less intense band at 277.83 nm, yielded poorer S/N than the analytical band; C_2 overlap for these peaks were usually worse than 10% of the actual C–Cl emission intensity.

Detection limits

All ACPD parameters were set to their previously determined optima[23]. Calibration curves for DCD, TCE, DCB and NBC were constructed. In general, the linearity extended over 3 orders of magnitude. Some linearity was lost due to self-absorption at high concentrations and excessive background molecular emission interference at low concentrations. The correlation coefficients ranged from 0.995 to 0.999 for the compounds examined in the study, as listed in Table II. Detector reproducibility was determined by the long term relative standard deviation, over a three-week period. Typically, the reproducibility was 10% week to week. The detection limit is defined as the minimum mass that produces a response (peak area) that is twice that of the noise (peak area) at the retention time of the compound[10,28,29]. The mass in this case is represented by the C–Cl diatomic species. The detection limits and correlation coefficient values are listed in Table II.

Some experimental limitations did affect our detection limits and selectivity. First, although the light gathering power of the McPherson monochromator employed is quite high (f/7), the band emission of the C–Cl band is weak compared to atomic emission. The predominance of diatomic emission may be due to the fact that a.c.-arc plasma temperatures are comparatively lower than most other plasma temperatures[30]. Therefore, complete fragmentation is not achieved, even with the more energetic helium plasma. Finally, no attempt was made to reduce the background spectral interference caused by molecular emission. Techniques, such as lock-in amplifying, oscillating quartz plates incorporated within a monochromator and pulsed power sources, have previously been suggested and often lead to enhanced S/N and selectivity[31–33].

Selectivity and relative response

The maximum S/N for the C–Cl signal was obtained with a slit width of 1500 μm (bandpass 0.3 nm), as noted by the authors previously[23]. However, to reduce the inclusion of adjacent C_2 swan bands as part of the C–Cl response, the slit was reduced to 500 μm (bandpass 0.1 nm). The background that directly overlapped with the 278.84 nm C–Cl band could not be eliminated without seriously affecting the detector sensitivity due to a large decrease in energy throughput. The selectivity was established

TABLE II

DETECTION LIMITS FOR ORGANOCHLORINES STUDIED

Compound	*Detection limit (ng/s)*	*Correlation coefficient (r)*
Tetrachloroethylene	1.59	0.995
n-Butylchloride	1.12	0.998
p-Dichlorobenzene	1.53	0.999
1,10-Dichlorodecane	0.706	0.999

TABLE III

RELATIVE RESPONSE FACTORS (RRFs) FOR VARIOUS ALKYLCHLORIDES AND PHENYLCHLORIDES

Compound	*Number of carbon in backbone*	*No. of CCL moieties*	*RRF*
1-Chloropropane	3	1	1.21
n-Butylchloride	4	1	1.00
n-Pentylchloride	5	1	1.87
n-Hexylchloride	6	1	2.05
3-Chloromethylhexane	7	1	2.23
o-Chlorotoluene	7	1	2.56
p-Dichlorobenzene	6	2	3.73
1,6-Dichlorohexane	6	2	2.33
1,2,3-Trichloropropane	3	3	5.61
Tetrachloroethylene	2	4	3.55
1,10-Dichlorodecane	10	2	2.82

at 500 μm by injecting a 0.5-μl solution of DCD and dodecane at known concentrations. A known mass of C–Cl (representing DCD) and C_2 (representing dodecane) was introduced into the detector by adjusting the split ratio to 16.5/1 at a fixed flow-rate.

The selectivity is defined as the ratio of the peak area response of the ACPD towards C–Cl at 278.84 nm per gram of C–Cl to the peak area response of the ACPD towards C_2 originating from *n*-dodecane per gram of C_2[9]. In the presence of molecular background emission, the selectivity towards C–Cl was 24 under the GC/ACPD conditions employed, which agrees favorably with the selectivity values obtained with GC–MIP by McCormack *et al.*[26]. The selectivity of the ACPD towards C–Cl *versus* other molecular species, such as C–Br, CN and OH were then studied for potential interference. The values were calculated from the response towards standards of *p*-bromobenzene[11], dipropylamine[17] and *n*-octanol[15], representing C–Br, CN and

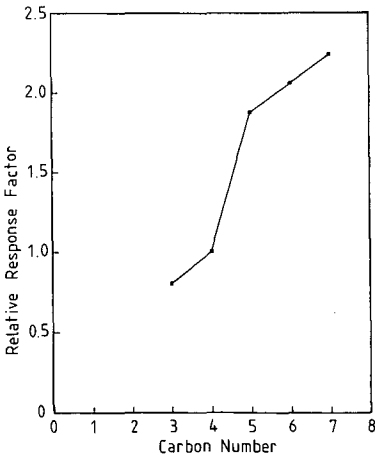

Fig. 3. Dependence of relative response factors on carbon number for chloro compounds containing one CCl per molecule.

OH, respectively. However, since the technique of GC–ACPD is a speciating technique, spectral interferences from these moieties are unlikely to be serious.

In order to study the effect of the molecular structure on the C–Cl response, a standard solution containing compounds of varying aromatic and aliphatic character were examined at known masses of C–Cl. Table III lists the relative response factors (RRFs) of the ACPD towards different organochlorine compounds, with *n*-butylchloride (NBC) being the internal standard. The relative response factor is defined as the mass of C–Cl in the sample compound per mass of C–Cl in NBC times the peak area of NBC to the peak area of the sample compound[34].

As seen in Table III, there is a complex trend that emerges with respect to the RRFs. Fig. 3 illustrates the overall increase in RRF with an increase of carbon number for *n*-alkylchlorides that produce one C–Cl entity per molecule of sample compound. This nonlinear increase is due to the enhancement in C_2 background emission with increasing carbon backbone. This phenomenon has been reported earlier in flame photometric detectors[35] and MIP[26] techniques. Examination of Table III reflects that in the case of *o*-chlorotoluene *versus* 3-chloromethylhexane counterpart with respect to carbon number and DCB *versus* its aliphatic counterpart 1,6-dichlorohexane, the aromatic ring introduces a larger contribution to the RRF than the alkane, probably because of the greater number of C_2 molecules produced per aromatic compound. Furthermore, TCE was expected to have a larger RRF than 1,2,3-trichloropropane (TCP). Since TCE contains only two carbons per molecule, only two C–Cl species can be formed per molecule compared to the three C–Cl that TCP can produce, thus TCP emission is greater than that of TCE emission.

Analytical applications

Several applications were performed in order to demonstrate the selectivity and stability that the ACPD exhibits to organochlorine compounds in complex matrices. First, a head space analysis was performed on a 1-ml mixture containing 1000 ng of the following organochlorine components in pentane: methylene chloride, chloroform, 1,2-dichloroethane, 1,3-dichloropropane, tetrachloroethylene, *p*-dichlorobenzene and 1,2,3-trichloropropane. Eluates of low k' values appear as sharp, well resolved peaks, as seen in Fig. 4. The chromatogram demonstrates that the ACPD introduces no detrimental effects on the separation, such as band broadening and memory effects as it compares favorably with a typical FID chromatographic profile of the same sample generated under similar conditions and with similar instrumentation. The slight decrease in base line is due to either self-absorption by a certain fragment present or the rapid decrease in the concentration of electrons caused by a species of high electron affinity. The latter would cause a decrease in plasma temperature and, therefore, a decrease in emission intensity[30].

A separation of a 1-μl aliquot of a 10-ml gasoline sample spiked with 10.72 mg of lindane was performed and is displayed in Fig. 5. The parallel chromatograms of the gasoline sample detected by both FID (A) and ACPD (B) under the same conditions clearly demonstrate the selectivity of the ACPD in a complex matrix. The high concentrations cause temperature fluctuations and self-absorption within the plasma, which leads to a lower background emission intensity and negative base line in certain regions. It should be noted that the hydrocarbons in the gasoline did not cause the plasma to extinguish. In fact, the base line became quite stable after, and in some cases

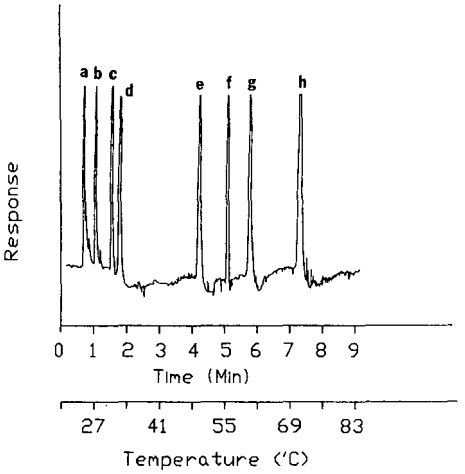

Fig. 4. Chromatogram of volatile organochlorine head space. GC conditions: column temperature 27°C (1 min) to 83°C at 7°C/min, 10 μl of vapor injected, injector split 5/l; column used was the DB-1 megabore column. (a) *n*-pentane; (b) methylene chloride; (c) chloroform; (d) 1,2-dichloroethane; (e) 1,3-dichloropropane; (f) tetrachloroethylene; (g) *p*-dichlorobenzene; (h) 1,2,3-trichloropropane.

during, the initial plasma cooling effect caused by these components.

Finally, a 10-ml aliquot of number 2 fuel oil was spiked with 10 mg of Aroclor 1254 and the parallel FID and ACPD chromatograms are displayed in Fig. 6a–c. Fig. 6a is the FID chromatogram of Aroclor 1254, which was run under the same conditions as the ACPD chromatogram of Aroclor 1254 in fuel oil (Fig. 6b). The ACPD chromatogram in Fig. 6b has more noise associated with it compared to Fig. 6a because diesel oil is also present, which leads to an increase in background emission. However, Fig. 6b demonstrates that the ACPD greatly simplifies the complex chromatogram of fuel oil and Aroclor 1254, shown in Fig. 6c, in addition to providing valuable qualitative information.

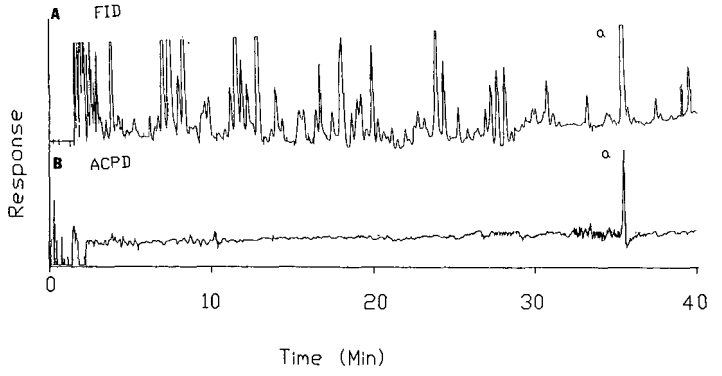

Fig. 5. (A) lindane (a) in gasoline detected by FID; GC conditions: 35°C (5 min) to 100°C at 4°C/min then to 230°C at 5°C/min on DB-1 megabore column. (B) lindane (a) in gasoline detected by ACPD, same GC conditions as above.

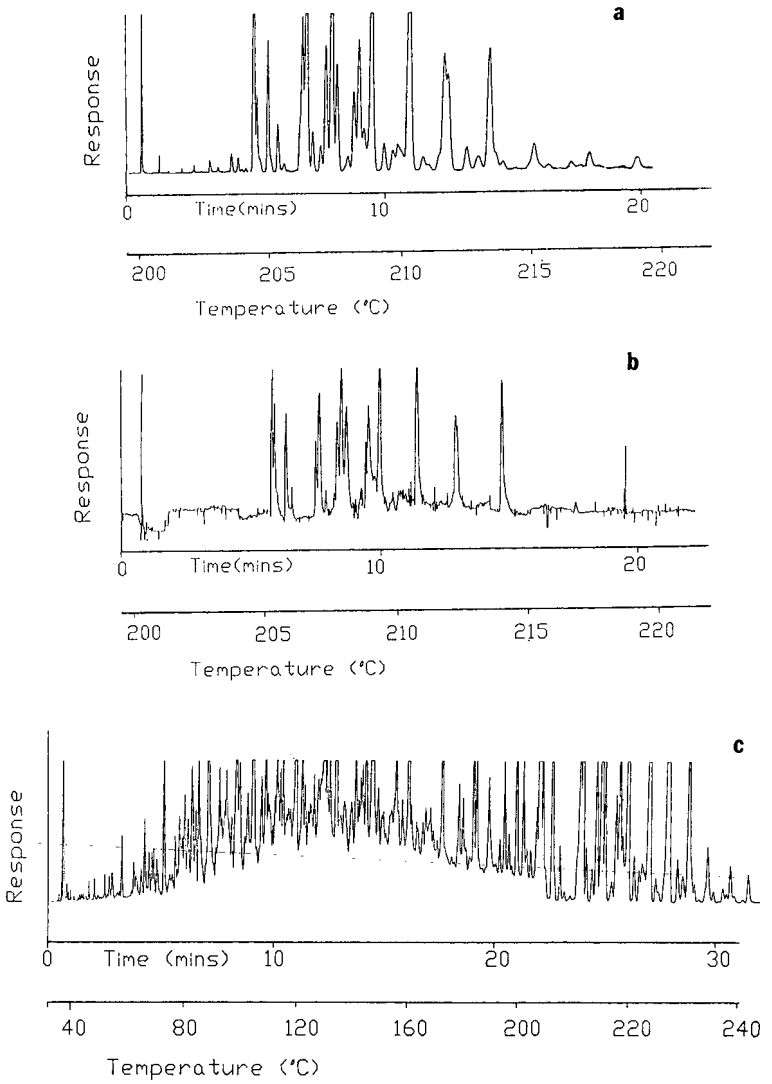

Fig. 6. (a) Aroclor 1254 detected by FID on the CP SIL-8 CB megabore column; GC conditions: 200°C (0.5 min) to 225°C at 1°C/min, 1 μl injection, injector split 5/1. (b) Aroclor 1254 in diesel gas detected by ACPD; same conditions as above. (c) Aroclor 1254 in diesel gas detected by FID; GC conditions: 40°C (1 min) to 200°C at 8°C/min then to 240°C at 4°C/min.

CONCLUSION

The alternating current plasma detector for capillary GC presented here offers considerable potential as a selective detector for organochlorine compounds, although detector sensitivity and selectivity are lower than those associated with GC–MIP techniques due to the experimental limitations. The RRFs show a complicated trend and a complete series of organochlorine compounds would have to be examined in

order to completely understand the complicated response dependency. However, it can be seen that two factors, aromatic character and carbon number, clearly contribute to the response of the detector.

In addition, the ACPD shows great potential in many applications of selective chlorine detection. The ACPD is a relatively inexpensive and simple detector to construct and operate. It circumvents many of the disadvantages assciated with MIP detection, such as solvent extinguishment and complicated interface venting devices. Detector selectivity for the diatomic C–Cl species did provide less complex chromatograms of a complex sample. Background correction devices and further filtering techniques will only improve the ACPD performance enough to be as popular as GC–MIP, with a simpler design. These modifications are currently being investigated and will be the subject of a future communication.

ACKNOWLEDGEMENTS

The authors wish to acknowledge the Graduate School of the University of Lowell for a research fellowship (R.B.C.) and Professor Harry Rubinstein for glass blowing assistance for the discharge tube used in this study.

REFERENCES

1 J. Sherma, *Anal. Chem.*, 59 (1987) 20R.
2 K. Grob and A. Habich, *J. High Resolut. Chromatogr. Chromatogr. Commun.*, 6 (1983) 11.
3 C. Nulton, C. Haile and D. Redford, *Anal. Chem.*, 56 (1984) 598.
4 D. Miller and E. Grimsrud, *Anal. Chem.*, 51 (1979) 851.
5 J. Dressler, *Selective Gas Chromatographic Detectors* (*J. Chromatogr. Library Series*, Vol. 36), Elsevier, New York, NY, 1986, p. 248.
6 J. A. Perry, *Introduction to Gas Chromatography: History, Principles and Practice*, Marcel Dekker, New York, NY, 1981, p. 165.
7 R. Anderson and R. Hall, *Am. Lab. (Fairfield, Conn.)*, 2 (1980) 110.
8 C. Beenakker, *Spectrochim. Acta, Part B*, 32B (1977) 173.
9 B. Quimby, P. Uden and R. Barnes, *Anal. Chem.*, 50 (1978) 2112.
10 M. Eckhoff, T. Ridgeway and J. Caruso, *Anal. Chem.*, 55 (1983) 1004.
11 K. Slatkavitz, P. Uden, L. Hoey and R. M. Barnes, *J. Chromatogr.*, 302 (1984) 277.
12 A. Mohamad, M. Zerezghi and J. Caruso, *Anal. Chem.*, 58 (1986) 469.
13 D. Hagen, J. Marhevka and L. Haddad, *Spectrochim. Acta, Part B*, 40B (1985) 335.
14 W. McClean, D. Stanton and E. Penketh, *Analyst (London)*, 98 (1973) 432.
15 C. Feldman and D. Batistoni, *Anal. Chem.*, 49 (1977) 2215.
16 R. Lloyd, R. Barnes, P. Uden and W. Elliot, *Anal. Chem.*, 50 (1978) 2025.
17 K. Panaro, D. Erickson and I. Krull, *Analyst (London)*, 112 (1987) 1097.
18 G. Rice, A. D'Silva and V. Fassel, *Anal. Chim. Acta*, 166 (1984) 27.
19 G. Rice, A. D'Silva and V. Fassel, *Spectrochim. Acta, Part B*, 40B (1985) 1573.
20 D. Windsor and M. B. Denton, *J. Chromatogr. Sci.*, 17 (1979) 492.
21 D. Windsor and M. B. Denton, *Anal. Chem.*, 51 (1979) 1116.
22 R. Costanzo and E. Barry, *Anal. Chem.*, 60 (1988) 826.
23 R. Costanzo and E. Barry, *Appl. Spectrosc.*, 42 (1988) 1387.
24 R. Green and R. Williams, *Anal. Chim. Acta*, 187 (1986) 301–305.
25 R. Dagnall, T. West and P. Whitehead, *Anal. Chim. Acta*, 60 (1972) 31.
26 A. McCormack, S. Tong and W. Cooke, *Anal. Chem.*, 37 (1965) 1470.
27 J. Reader and C. Corliss, *Wavelengths and Transition Probabilities for Atoms and Atomic Ions*, Part I, Nat. Bur. Stand., U.S. Government Printing Office, Washington, DC, 1980, pp. 29–31.

28 J. Sevick and J. Lipps, *Chromatographia*, 12 (1979) 701.
29 L. Ettre, *J. Chromatogr.*, 165 (1979) 235.
30 J. Mika and T. Torok, *Analytical Emission Spectroscopy*, Crane, Russak and Co., New York, NY, 1974, pp. 51–96.
31 L. Lendero, K. Cammann and K. Ballschmiter, *Mikrochim. Acta*, 1 (1984) 110.
32 C. Feldman and D. Batistoni, *Anal. Chem.*, 49 (1977) 2217.
33 D. Hass and J. Caruso, *Anal. Chem.*, 57 (1985) 847.
34 D. David, *Gas Chromatography Detectors*, Wiley, New York, NY, 1974, p. 104.
35 Y.-Z. Tang and W. A. Aue, *J. Chromatogr.*, 408 (1987) 69.
36 M. Muller and H. R. Buser, *Environ. Sci. Technol.*, 20 (1986) 1151.

Journal of Chromatography, 467 (1989) 385–394
Elsevier Science Publishers B.V., Amsterdam — Printed in The Netherlands

CHROM. 21 085

ON-LINE FLAME PHOTOMETRIC DETECTION IN MICRO-COLUMN LIQUID CHROMATOGRAPHY

Ch. E. KIENTZ*, A. VERWEIJ and H. L. BOTER
Prins Maurits Laboratory TNO, P.O. Box 45, 2280 AA Rijswijk (The Netherlands)
and
A. POPPEMA, R. W. FREI[a], G. J. DE JONG and U. A. Th. BRINKMAN
Section of Environmental Chemistry, Free University, De Boelelaan 1083, 1081 HV Amsterdam (The Netherlands)
(First received July 8th, 1988; revised manuscript received September 15th, 1988)[b]

SUMMARY

An improved interface coupled to a commercially available flame photometric detector designed for gas chromatography has been investigated for its applicability in micro-column (0.32 mm I.D.) liquid chromatography. The column effluent is directly introduced into the flame via a 0.1 mm I.D. fused-silica capillary. The influence on the detector performance of parameters such as the position of the effluent introduction into the flame, the composition and flow-rates of the gases and the quenching by the eluent is discussed. With a series of organophosphorus acids as model compounds, plots of peak area *vs.* amount injected are linear ($r > 0.998$) in the range 0.5–200 ng investigated. The repeatability is better than 6% ($n = 148$). The system shows a detection limit of 20 pg of phosphorus per second (0.5–2 ng of analyte) when using an aqueous ammonium acetate or nitric acid solution as the eluent. The addition of methanol or acetonitrile to the eluent quenches the detector response. A mass flux of 1.2 mg/s of oxidizable carbon causes a 20% loss in detector signal.

INTRODUCTION

In recent years, the use of miniaturized liquid chromatography (LC) with 0.2–1 mm I.D. columns has increased considerably. One major advantage is the possibility to couple LC directly to several types of flame-based gas chromatographic (GC) detectors, such as, *e.g.*, phosphorus-selective detectors. Initial research in this field was carried out by Novotny and co-workers[1–4] who used packed micro-columns (0.2–0.3 mm I.D.) and a nebulization interface to introduce the effluent into a dual-flame thermionic detector. A different approach was used by Brinkman and co-workers[5–7] who applied narrow-bore columns (0.7–1 mm I.D.) and an interface designed to vaporize the LC effluent before it enters the thermionic detector. For a series of

[a] Author deceased.
[b] Publication delayed at the authors' request.

organophosphorus pesticides the authors reported detection limits varying from 0.2 to 0.5 pg/s of phosphorus[7]. The use of a flame photometric detector in micro-column LC has been described by McGuffin and Novotny[8], who were able to detect 2 ng of phosphorus by means of the direct introduction of the column effluent into the flame. The mass flux at the peak maximum was 71 pg/s of phosphorus when using the relatively volatile trimethyl phosphate as a test compound. Karnicky *et al.*[9] have reported on an ultrasonic micro nebulizer-flame photometric detector as an LC detector using both dual-flame and dual-wavelength operation to improve signal-to-noise ratios and to eliminate baseline shifts. With this relatively sophisticated interface, the authors were able to detect sugar phosphates and phospholipids in water down to 50 pg/s of phosphorus. Unfortunately, no further work using this approach has been published.

Our group is interested in the trace-level determination of polar, acidic and other non-volatile phosphorus-containing compounds. Generally, LC with UV detection and GC analysis are unsuitable for such compounds without prior derivatization. Therefore, the direct coupling of packed capillary fused-silica LC columns to a commercially available flame photometric detector is being investigated in our laboratories. Preliminary experiments[10] showed that such a system allows the detection of volatile organophosphorus compounds. However, non-volatile analytes such as organophosphorus acids or high-molecular-weight compounds were not detected. In the present study the interface has been further improved to obtain a suitable introduction of non-volatile organophosphorus compounds into the flame.

EXPERIMENTAL

Materials

All solvents were of HPLC-grade quality (Merck, Darmstadt, F.R.G.). LiChrosorb RP-18, particle size 10 μm (Merck), and PRP-1 styrene–divinylbenzene copolymer, particle size 10 μm, from Hamilton (Reno, NE, U.S.A.) were used as column packing materials. Phosphoric acid (PA) was supplied by Merck, methylphosphonic acid (MPA), ethyl methylphosphonic acid (EMPA), isopropyl methylphosphonic acid (IMPA), dimethyl phosphoric acid (DMP) and diethyl phosphoric acid (DEP) were synthesized at the Prins Maurits Laboratory TNO.

Apparatus

The system was assembled from an LC-5A pump (Shimadzu, Kyoto, Japan) a Valco sample injection valve (VICI, Schenkon, Switzerland) with a 60-nl internal volume and a flame photometric detector Model 380 (Carlo Erba, Milan, Italy). The different fused-silica connective tubings (0.02–0.3 mm I.D.) were supplied by Chrompack (Middelburg, The Netherlands). The fused-silica capillaries (0.3 mm I.D.) were packed with LiChrosorb RP-18 or PRP-1 according to the procedure of Gluckman *et al.*[11].The column performance was tested using a laboratory-made 40-nl micro-flow UV cell[12]. In the experimental set-up a second Valco valve was inserted between the micro-column and the detector interface. The micro-column was connected to both Valco valves using finger-tightened PTFE ferrules and nuts (Hibar, Merck), its packing being held by porous PTFE frits (Alltech, Eke, Belgium) inserted into both valves. This experimental set-up allows easy inspection or replacement of the fused-silica capillary outlet (see Fig. 1) without the need to disconnect or depressurize the micro-LC column.

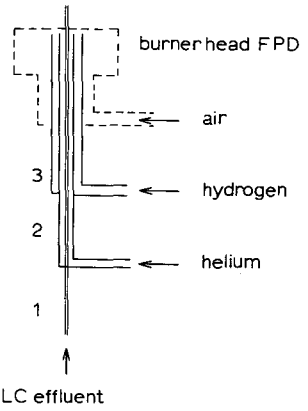

Fig. 1. Schematic interface design. 1 = Fused-silica capillary (0.10 mm I.D.); 2 = fused-silica capillary (0.32 mm I.D.); 3 = stainless-steel tube (0.50 mm I.D., 1.6 mm O.D.); 4 = burner head. For further details, see text.

Data acquisition was performed on a personal computer (Type PC 350; Digital Equipment Corporation, Maynard, MA, U.S.A.) via a Minichrom interface and the appropriate software (VG Laboratory Systems, Altrincham, U.K.). Additional calculations were carried out on a VAX 8200 computer (Digital Equipment Corporation). To evaluate the external peak broadening of the system a computer program was written to calculate the second moment, M_2, of the chromatographic peaks with the statistical method, using the algorithm described by Yau[13] and with the Foley and Dorsey[14] equations. The program was validated using the exponentially modified gaussian (EMG) peak generation method[15]. The M_2 value was obtained with an accuracy of 0.6% as derived from generated M_2 values in the range of 0.05–1.8 μl^2 at a peak asymmetry ratio of 0.1–3 τ/σ as defined according to ref. 15.

RESULTS AND DISCUSSION

Liquid chromatography–flame photometric detection (FPD)

The interface previously constructed and used for micro-column LC–FPD studies[10], was based on the principle of evaporation of the liquid eluent before its introduction into the flame. When using this interface it was found that organophosphorus acids were not detected. These experiences were similar to those published in another paper on the utilization of an evaporation interface for LC with thermionic detection (TID)[6]. In that study a variety of phosphorus-containing compounds including polar pesticides was measured. All non-volatile or high-molecular-weigth compounds were found to be difficult to detect. This may well indicate the limitation of interfaces based on the principle of simple evaporation. In order to determine non-volatile organophosphorus acids with LC–FPD, the effect of several modifications to the interface mentioned before was examined.

In the final set-up (see Fig. 1) the LC effluent is introduced into the detector by means of a fused-silica capillary (no. 1), while an helium purge flows through the wider coaxial fused-silica capillary (no. 2). In the previous design a nitrogen flow was

added. The stability of the system was found to improve upon replacing nitrogen by helium. The hydrogen flows through a stainless-steel tube (no. 3) into the burner just below the tips of the two fused-silica capillaries. The hydrogen flow-rate, the air flow-rate and the helium purge flow-rate are set at 650, 350 and 40 ml/min, respectively, as deduced from experiments discussed below.

The position of the tip of the fused-silica capillary which introduces the column effluent into the flame (Fig. 1, no. 1) was varied as well as the internal diameter of this capillary. The best results were obtained by introducing the liquid effluent into the relatively cold centre of the hydrogen flame. Finally, the position of the tip of the fused-silica capillary was fixed 1.4 mm above the outlet of the hydrogen flow (Fig. 1, no. 3) to obtain maximum stability of the detector response. Comparing the performance of fused-silica outlet capillaries with internal diameters of 25, 50 and 100 μm, the best stability and reproducibility of the detector response were found using the 100-μm capillary.

The flame photometric detector used contains a burner head configuration as originally presented by Brody and Chaney[16]. The flame burns in a hollow metal tip of the burner head which shields the blue flame envelope from direct view by the photomultiplier. In this way interferences from flame emission are eliminated whereas, if phosphorus or sulphur atoms are present, the emission of the excited POH an S_2 fragments appears above the shield[16]. In order to maintain this situation the hydrogen outlet and, thus, the position of the stainless-steel tube (Fig. 1, no. 3) should be at its original position, *i.e.*, at the bottom of the burner head. However, considerable heat transfer will then take place towards the lower part of the burner, causing clogging of the 100-μm fused-silica capillary when non-volatile solutes are present. From these experiments it was concluded that a cooler burner base must be used. This was obtained by lifting the entire interface (Fig. 1, nos. 1–3) to the same level as the top of the burner head.

The helium flow was added close below the LC column outlet (Fig. 1, no. 2) which probably provides an additional cooling effect.

Detector gas flows

In the present system, hydrogen may have a two-fold function, *viz.*, as a fuel and as an LC effluent transporting gas. Consequently, the flow-rate affects the shape and, more importantly, the position of the diffusion flame. In all experiments, the flow was set at 650 ml/min which is relatively high in comparison with conditions in GC, where a flow of 50–200 ml/min is conventionally used[17]. A decrease of the present flow-rate causes a lower flame position, that is, too high a position of the fused-silica tip via which the LC effluent is introduced into the flame. On removing the photomultiplier tube, bad positioning of this fused-silica capillary in the flame was seen: when decreasing the hydrogen flow-rate the tip of the capillary started to glow. Under such conditions non-volatile compounds will block the fused-silica capillary.

The dependence of the response or, rather, the signal-to-noise ratio, for the test compounds on the air flow-rate is shown in Fig. 2. As is seen, there is a distinct optimum air flow-rate at about 375 ml/min for all three compounds. At this optimum the hydrogen-to-oxygen ratio amounts to approximately 5, which corresponds nicely with the ratio of 4 to 7 generally reported in the literature for GC–FPD applications

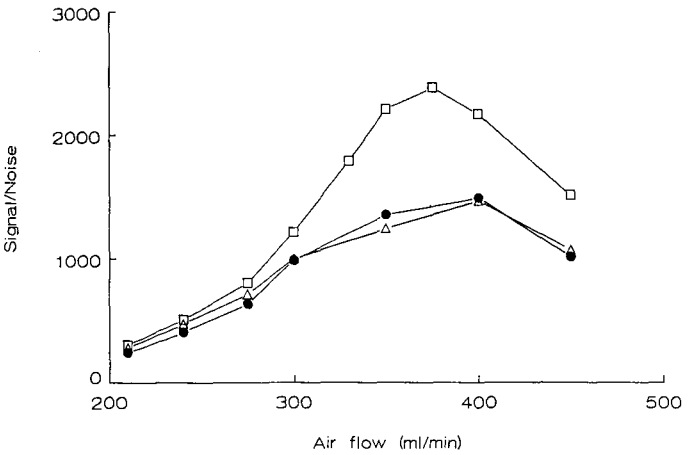

Fig. 2. Influence of air flow-rate on signal-to-noise ratio. □, Methylphosphonic acid; ●, ethyl methylphosphonic acid; △, isopropyl methylphosphonic acid. Hydrogen flow-rate 650 ml/min and helium flow-rate 40 ml/min.

with similar, inverted air-hyperventilated flames as introduced by Burgett and Green[18]. The flow-rate of helium was varied between 0 and 100 ml/min. Flow-rates up to 50 ml/min did not affect either the detector response or the noise level. However, higher flow-rates resulted in an irregular and spiking baseline, whereas the absence of a helium flow caused system instability. Therefore, the helium flow was set at 40 ml/min.

Performance of the micro-column LC–FPD system

Chromatography. The performance of the micro-column LC–FPD system was studied by investigating the separation and detection of a number of organophosphorus acids. The evaluation of the chromatographic conditions has been previously reported[19]. Fig. 3 presents a characteristic chromatogram for the separation of meth-

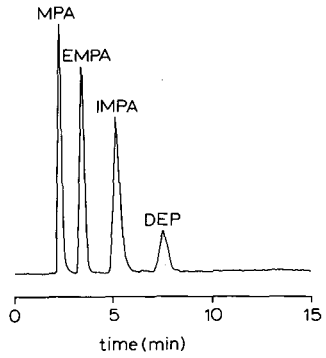

Fig. 3. Chromatogram of a number of organophosphorus acids, using FPD. Eluent: 0.05 *M* ammonium acetate, pH 5; flow-rate 8 μl/min. Column: 300 mm × 0.32 mm I.D. fused-silica capillary packed with 10-μm LiChrosorb RP-18. Injection volume: 60 nl. MPA = Methylphosphonic acid; EMPA = ethyl methylphosphonic acid; IMPA = isopropyl methylphosphonic acid; DEP = diethyl phosphoric acid.

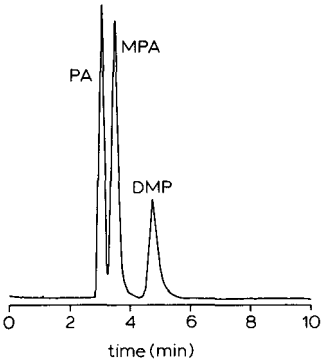

Fig. 4. Chromatogram of three phosphorus-containing acids, using FPD. Eluent: 0.1 *M* nitric acid; flow-rate, 6 μl/min. Column: 300 mm × 0.32 mm I.D. fused-silica capillary packed with 10-μm PRP-1. Injection volume: 60 nl. PA = Phosphoric acid; MPA = methylphosphonic acid; DMP = dimethyl phosphoric acid.

ylphosphonic acid, ethyl methylphosphonic acid, isopropyl methylphosphonic acid and diethyl phosphoric acid under ion-pair LC conditions. Closely related compounds such as phosphoric acid, methylphosphonic acid and dimethyl phosphoric acid are difficult to separate under these conditions. For these analytes, separation was achieved using a micro-LC column packed with the styrene–divinylbenzene copolymer PRP-1, and working under ion-suppression conditions at pH 1 (Fig. 4).

The repeatability of the system was determined by injecting 60 nl of a solution containing 3–250 ng of each compound. Peak height determination gave a relative standard deviation (S.D.) of 1.7–6.1%, derived from 31 series of measurements with a total of 148 injections. In the range 0.5–200 ng a good linear correlation of over 0.998 was obtained.

External peak broadening. The total peak broadening of the system was calculated as the initial M_2 values [k' (lim 0)] derived from the statistical moment method, the method of Yau and that of Foley and Dorsey using analytical data such as are shown in Fig. 3. The results obtained for 50-μm and 100-μm fused-silica capillary outlets of the interface are given in Table I; the average values are 0.28 and 0.50 μl^2, respectively.

From separate experiments with a micro-column LC–UV system[12], the peak broadening caused by the injector, column and connection tubes is known to be 0.22 μl^2. This indicates that the contribution of the flame photometric detector and the

TABLE I

TOTAL PEAK BROADENING, M_2, OF THE MICRO-COLUMN LC–FPD SYSTEM

Capillary I.D. (μm)	*M_2 (μl^2) according to* [a]		
	1	*2*	*3*
100	0.48	0.48	0.53
50	0.25	0.28	0.31

[a] 1 = Statistical moment method; 2 = method of Yau[13]; 3 = method of Foley and Dorsey[14].

TABLE II

DETECTION LIMITS OF ORGANOPHOSPHORUS ACIDS IN MICRO-COLUMN LC–FPD

Compound	*Detection limit of phosphorus*[a] *(pg/s)*
Phosphoric acid	34
Methylphosphonic acid	18
Ethyl methylphosphonic acid	22
Isopropyl methylphosphonic acid	20
Dimethyl phosphoric acid	20
Diethyl phosphoric acid	22

[a] Signal-to-noise ratio, 2:1; average mass flux.

interface amounts to 0.06 and 0.28 μl^2 for the 50- and 100-μm capillary outlets, respectively, at an effluent flow-rate of 8 μl/min. Although the 100-μm capillary is seen, contrary to the 50-μm capillary, to contribute significantly to the total peak broadening, it is still preferred because of the higher stability and reproducibility of the detector response.

Detection limits. Table II shows the detection limits calculated for the six organophosphorus acids measured in the present system, using various aqueous mobile phases. The average detection limit is about 20 pg/s of phosphorus as against about 1 pg/s of phosphorus in GC. This result, which corresponds with an injected amount of about 1 ng of analyte (injection volume 60 nl), is rather promising when one realizes that due to the necessity of (i) the position of the flame above the shield, and (ii) the relatively high hydrogen flow-rate, the photomultiplier probably is not in its optimum position relative to the flame and the POH emission.

Quenching effects. From the literature, the phenomenon of quenching of the POH emission intensity is well known[20] for a flame photometric detector used as a GC detector. The degree of quenching depends on various factors such as the type and concentration of the organic analyte, the oxygen-to-hydrogen ratio in the gas stream passing through the detector, the detector construction[21] and, finally, the temperature of the detector[22].

In the present study aqueous LC effluents were used containing 0.01–0.5 *M* ammonium formate or ammonium acetate and, occasionally, 0.05 *M* tetraethylammonium hydroxide (in order to achieve ion-pair chromatography), or 0.01–0.1 *M* nitric acid (in order to achieve ion suppression). Neither type of eluent affects the baseline stability or detector limit. The absence of quenching is in good agreement with results obtained in molecular emission spectroscopy experiments by Dagnall *et al.*[23] and Aldous *et al.*[24], who found no interference upon the addition of several acidic and ionic compounds which included nitric acid and acetates.

Table III shows the influence of the addition of methanol on the detection limit. As found previously, the quenching strongly depends on the flow-rate[10]. With increasing flow-rate, the increase of the detection limit in the absence of methanol is caused by an increased noise level, while the response remains constant. In the presence of methanol, the increase of the detection limit is chiefly due to a decrease of the

TABLE III

INFLUENCE OF THE METHANOL PERCENTAGE AND THE ELUENT FLOW-RATE ON THE DETECTION LIMIT OF METHYLPHOSPHONIC ACID (M) AND DIMETHYL PHOSPHORIC ACID (D) IN MICRO-COLUMN LC–FPD

–, Not detected due to early evaporation of the effluent.

Methanol in eluent (%)	*Detection limit (pg/s of P) at flow-rate (μl/min) of:*							
	2		*5*		*10*		*15*	
	M	*D*	*M*	*D*	*M*	*D*	*M*	*D*
0	18	25	24	30	44	60	61	78
5	19	27	30	40	97	67	125	158
10	24	30	29	43	83	120	200	290
20	–	–	80	110	288	440	1260	2160
30	–	–	100	160	850	1150	2520	4940

signal intensity. In order to limit the loss in detection performance in the case of water–methanol eluents, flow-rates of 5 μl/min or below are recommended. This is also advantageous, because the negative effect of methanol on the detection limit is less at lower flow-rates.

When using 10% acetonitrile in water as the eluent, at a flow-rate of 8 μl/min, detection limits of 44 and 77 pg/s of phosphorus were found for methylphosphonic acid and dimethyl phosphoric acid, respectively. This indicates that the quenching is of the same order of magnitude as when using 10% methanol in water as an eluent. The magnitude of the quenching effect is nicely illustrated in Fig. 5, where the dependence of the intensity ratio, Φ, as defined according to Sugiyama *et al.*[20]

$$\Phi = \frac{\text{FPD response (eluent with modifier)}}{\text{FPD response (eluent without modifier)}} \quad (1)$$

is plotted as a function of the mass flux of methanol. The data obtained with dimethyl phosphoric acid as a test compound indicate that a mass flux of 0.1 μmol of methanol

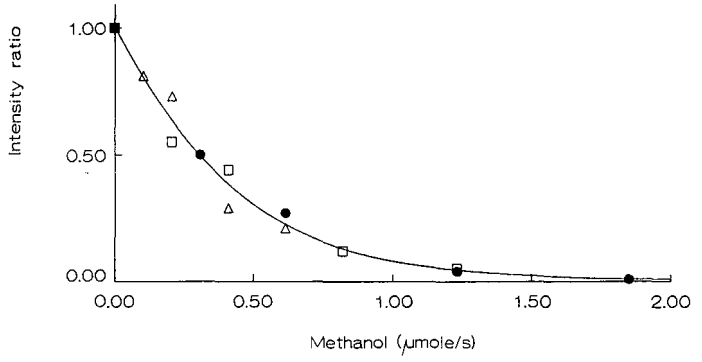

Fig. 5. Influence of mass flux (μmol/s) of methanol on intensity ratio (eqn. 1). Eluent flow-rate: ●, 15; □, 10; △, 5 μl/min. Test compound: dimethyl phosphoric acid.

or 1.2 μg of oxidizable carbon per second is permitted if one accepts a 20% loss in intensity ratio.

In GC using FPD in the sulphur mode, Dressler[22] found a 22% quenching effect at 4 ng/s of oxidizable carbon. However, using the same detector mode and quenching compound (cyclohexane), Fredriksson and Cedrgren[21] reported a quenching value of about 20% for as high a carbon flow-rate as 4 mg/s. They applied a hydrogen hyperventilated burner type as designed by Brody and Chaney[16], their results being obtained after optimization of the hydrogen-to-oxygen ratio as a function of the amount of carbon per second. Optimization of the hydrogen-to-oxygen ratio in the presence of a modifier and exchanging the positions of the hydrogen and air entrance to create an hydrogen hyperventilated flame, may therefore also be interesting when trying to extend the use of organic modifiers in microcolumn-LC–FPD.

CONCLUSIONS

The on-line coupling of microcolumn-LC to a commercially available flame photometric detector has been improved to permit the detection of non-volatile organophosphorus acids. As yet, these analytes cannot be handled by LC with on-line thermionic detection. The system has been succesfully applied to the separation of a series of these acids with a detection limit of 20 pg/s of phosphorus, a relative S.D. of less than 6% and a linear range of more than two orders of magnitude. The interface used is of simple design and may be suitable for other flame-based GC detectors as well. Preliminary experiments on coupling the microcolumn-LC interface to a thermionic detector are rather promising. Future research will deal with the utilization of the present microcolumn-LC–FPD system in the analysis of various types of samples. Besides, the potential and limitations of the use of several organic modifiers will be studied.

REFERENCES

1 V. L. McGuffin and M. Novotny, *J. Chromatogr.*, 218 (1981) 179.
2 V. L. McGuffin and M. Novotny, *Anal. Chem.*, 55 (1983) 2296.
3 J. C. Gluckman and M. Novotny, *J. Chromatogr.*, 314 (1984) 103.
4 J. C. Gluckman and M. Novotny, *J. Chromatogr.*, 333 (1985) 291.
5 F. A. Maris, R. J. van Delft, R. W. Frei, R. B. Geerdink and U. A. Th. Brinkman, *Anal. Chem.*, 58 (1986) 1634.
6 J. C. Gluckman. D. Barceló, G. J. de Jong, R. W. Frei, F. A. Maris and U. A. Th. Brinkman, *J. Chromatogr.*, 367 (1986) 35.
7 D. Barceló, F. A. Maris, R. W. Frei, G. J. de Jong and U. A. Th. Brinkman, *Int. J. Environ. Anal. Chem.*, 30 (1987) 65.
8 V. L. McGuffin and M. Novotny, *Anal. Chem.*, 53 (1981) 946.
9 J. F. Karnicky, L. T. Zitelli and Sj. van der Wal, *Anal. Chem.*, 59 (1987) 327.
10 Ch. E. Kientz and A. Verweij, *Int. J. Environ. Anal. Chem.*, 30 (1987) 255.
11 J. C. Gluckman, A. Hirose, V. L. McGuffin and M. Novotny, *Chromatographia*, 17 (1984) 303.
12 Ch. E. Kientz and A. Verweij, *J. High Resolut. Chromatogr. Commun.*, 3 (1988) 294.
13 W. W. Yau, *Anal. Chem.*, 49 (1977) 395.
14 J. P. Foley and J. G. Dorsey, *Anal. Chem.*, 55 (1983) 730.
15 E. Grushka, *Anal. Chem.*, 49 (1972) 1733.
16 S. S. Brody and J. E. Chaney, *J. Gas Chromatogr.*, 4 (1966) 42.
17 C. H. Burnett, D. F. Adams and S.O. Farrel, *J. Chromatogr. Sci.*, 16 (1978) 68.

18 C. A. Burgett and L. E. Green, *J. Chromatogr. Sci.*, 12 (1974) 356.
19 A. Verweij, Ch. E. Kientz and J. van den Berg, *Int. J. Environ. Anal. Chem.*, in press.
20 T. Sugiyama, Y. Suzuki and T. Takeuchi, *J. Chromatogr.*, 80 (1973) 61.
21 S. A. Fredriksson and A. Cedrgren, *Anal. Chem.*, 53 (1981) 614.
22 M. Dressler, *J. Chromatogr.*, 270 (1983) 145.
23 R. M. Dagnall, K. C. Thompson and T. S. West, *Analyst (London)*, 93 (1968) 72.
24 K. M. Aldous, R. M. Dagnall and T. S. West, *Analyst (London)*, 95 (1970) 417.

Journal of Chromatography, 467 (1989) 395–401
Elsevier Science Publishers B.V., Amsterdam — Printed in The Netherlands

CHROM. 21 314

REVERSED-PHASE HIGH-PERFORMANCE LIQUID CHROMATOGRAPHIC METHOD FOR THE QUANTIFICATION OF 5-HYDROXYMETHYLFURFURAL AS THE MAJOR DEGRADATION PRODUCT OF GLUCOSE IN INFUSION FLUIDS

AMANDA P. COOK*,[a] and T. M. MACLEOD
Area Pharmaceutical Laboratory, Ninewells Hospital, Dundee DD1 9SY (U.K.)
J.D. APPLETON
Tayside Health Board, "Vernonholme", Riverside Drive, Dundee DD1 9NL (U.K.)
and
A. F. FELL
Department of Pharmaceutical Chemistry, University of Bradford, Bradford BD7 1DP (U.K.)
(First received January 29th, 1988; revised manuscript received January 6th, 1989)

SUMMARY

Analysis of 5-hydroxymethylfurfural (5-HMF) is an important indicator of degradation in glucose infusion fluids. Current pharmacopoeial methods for analysis are insensitive and non-specific. A method is described here, incorporating an internal standard, to give a sensitive, accurate and precise method, suitable for use in the quality control of glucose infusion fluids, and with possible applications for the quantitative determination of 5-HMF in food and drink, bacterial cultures and hydrothermolysed wood.

INTRODUCTION

Sterilisation of infusion fluids by autoclaving is the recommended method, providing that the product can withstand high temperatures. There are, however, some products that are autoclaved although they are known to have some instability, and in these cases their degradation products are controlled by limit tests. The most notable example of this is glucose infusion fluid. The degradation of glucose on heating is known to yield 5-hydroxymethylfurfural (5-HMF) via the formation of unknown intermediates [1–6]. Some of the 5-HMF is then reported to break down to give two acids, 5-hydroxymethylfuroic acid and furan-2,5-dicarboxylic acid[1]. Quantification of the 5-HMF gives an important indication of the extent to which glucose may have been degraded, this being of clinical significance when administering in-

[a] Address for correspondence: Pharmacy Department, Peterborough District Hospital, Thorpe Road, Peterborough PE3 6DA, U.K.

0021-9673/89/$03.50

fusion fluids because of the association of high levels of 5-HMF with thrombophlebitis[7,8] and possible interactions of 5-HMF with heparin[9] and other drugs[10].

The current pharmacopoeial monograph for glucose injections includes a limit test for 5-HMF and related products using a spectrophotometric method based on the absorption of 5-HMF at 283 nm; this method has been reported to be insensitive and non-specific[3]. In the present work a sensitive, accurate and precise method is described, based on reversed-phase high-performance liquid chromatography (HPLC). An assay for 5-HMF will have applications in various fields of work; assays have been described for its determination in caramel solutions[11], in hydrothermolysed poplar wood[12], in bacterial cultures[13], as well as in infusion fluids[3]. Our assay has been applied to the analysis of heat-treated glucose samples, in a series of experiments where 5% (w/v) glucose solutions were heat-treated in a microprocessor-controlled autoclave to examine the effect of various combinations of temperature and time on the extent of degradation. The qualitative nature of the degradation process was examined by rapid-scanning photodiode array detection, a technique which will become of widespread use in the future[14].

EXPERIMENTAL

Materials and methods

The mobile phase was prepared as follows. Sodium dihydrogenphosphate (AnalaR Grade, BDH, Poole, U.K.) was made up at 0.05 *M* using glass-distilled water, the pH adjusted to 5.5 and the solution filtered through a 0.45-μm membrane. HPLC-grade methanol (Rathburn, Walkerburn, U.K.) was used as the organic modifier. The mobile phase was degassed under reduced pressure in an ultrasonic bath for 10 min. 5-HMF (Sigma, Poole, U.K.) was used as received. Benzophenone, benzaldehyde, vanillin and benzoic acid were obtained from BDH and used as received. The internal standard, 2-furaldehyde (2-FA) (Aldrich, Gillingham, U.K.) was prepared as a 0.05 *M* solution in distilled water and introduced into standards and samples. Glucose Monohydrate BP 5% (w/v) in water was prepared in the Sterile Production Unit an Ninewells Hospital (Dundee, U.K.) and distributed in 500-ml glass bottles of the Medical Research Council (MRC) type, fitted with rubber bungs and aluminium caps.

Equipment

The modular HPLC system consisted of a Gilson 302/802 pump, a Rheodyne 7125 injection valve equipped with a 20-μl loop and a Gilson Holochrome variable-wavelength detector (the detection wavelength being 283 nm at a sensitivity of 0.05 a.u.f.s.), connected to a Shimadzu C-R1B integrator–printer. The column was 125 mm × 4.6 mm I.D. stainless steel, slurry-packed under pressure with Hypersil ODS (5 μm) (Shandon Southern Instruments, Runcorn, U.K.). The flow-rate was 2 ml/min at a pressure of 2000 p.s.i. For diode array detection a Hewlett-Packard HP-1040A system was used, which consisted of a detector mainframe connected to an HP-85 laboratory microcomputer and an HP82901M dual 5.25-in. flexible disc drive; in addition a Hewlett-Packard Model 74700 plotter and Model 7222 print-plotter were used. The autoclave used in degradation work was a Drayton Castle bottled-fluids steriliser, adapted by CMI (Consolidated Medical Industries, Sunningdale, U.K.) and

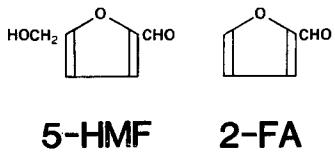

Fig. 1. Structures of 5-hydroxymethylfurfural (5-HMF) and 2-furaldehyde (2-FA).

with microprocessor control using the Apotec 2000 system from IMS (Instrumental and Microelectronic Systems, Rosyth, Fife, U.K.).

Quantitative procedures

Calibration was carried out according to one of two methods — external standardisation using the external standard mode on the Shimadzu integrator and internal standardisation. In the external standardisation mode, full 20-μl loop repetitive injections of a single-concentration 5-HMF standard solution were used for single-point calibration, based on the principle where test samples are "bracketted" by standards injected before and after the test. An internal standard method was also used for comparison. The ratio of the peak area of the 5-HMF to internal standard was used to construct a calibration graph. A number of possible internal standards were explored for 5-HMF quantification. The criteria applied in assessing a suitable candidate were: (1) UV absorption in the region of 283 nm; (2) solubility in the aqueous mobile phase; (3) chemical similarity to 5-HMF; (4) a phase capacity ratio (k') close to that of 5-HMF[15].

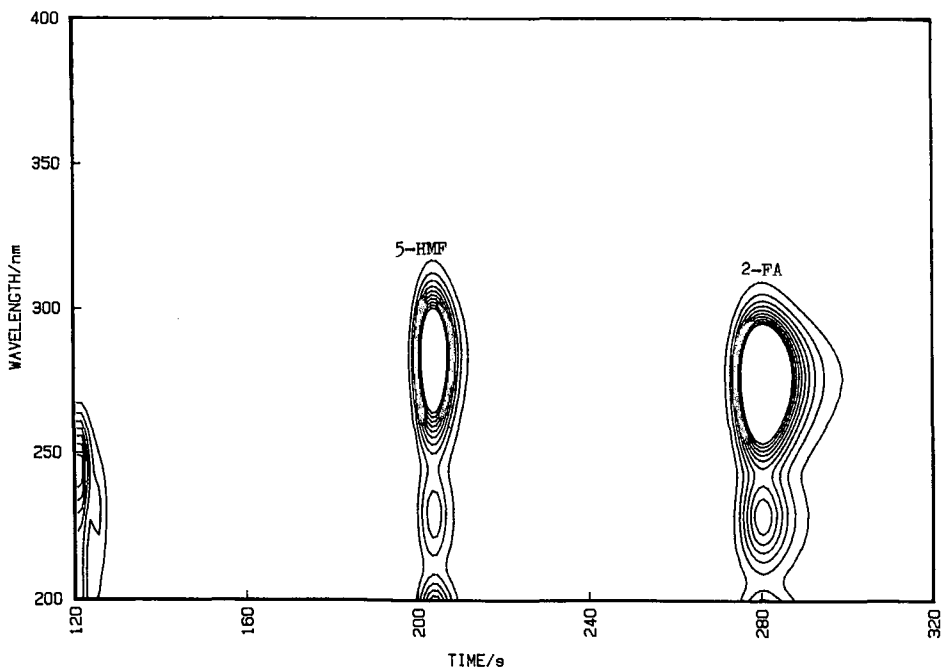

Fig. 2. Contour plot of a degraded glucose sample with internal standard.

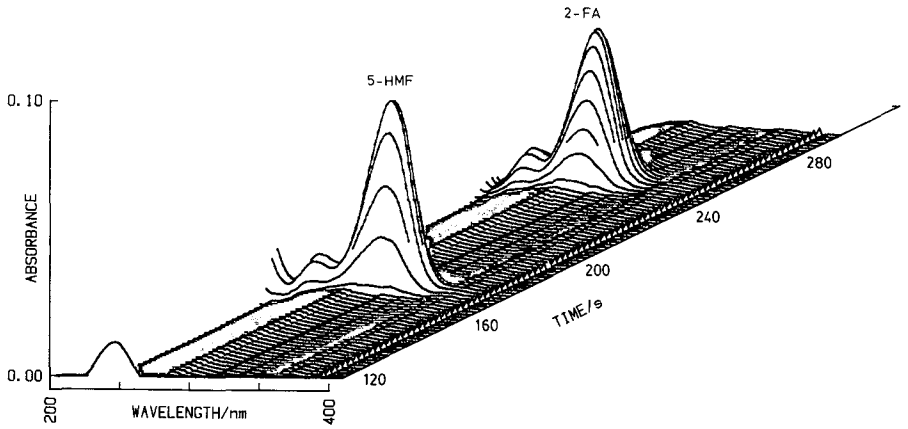

Fig. 3. Three-dimensional plot of a degraded glucose sample with internal standard.

Benzophenone, benzaldehyde, vanillin and benzoic acid were all examined, but apart from their structural dissimilarity to 5-HMF, their phase capacity ratios were too large to be of use. 2-FA was chosen as the internal standard [$k' = 3.18$; relative standard deviation (R.S.D.) = 0.96, $n = 5$] since it was well resolved from 5-HMF in the system as finally optimised ($k' = 2.05$; R.S.D. = 1.0, $n = 5$) and was chemically similar to 5-HMF (Fig. 1). In addition there have been reports of the simultaneous determination of 5-HMF and 2-FA by HPLC[16] and by fluorimetry[17].

Diode array detection

A diode array detector was used to assess the methodology qualitatively. The rapid acquisition of spectral data at wavelengths from 200 to 400 nm allowed spectra to be displayed at any time segment (*i.e.* for any part of the chromatographic peak). Spectra from the leading and trailing edges and the apex of the peak were normalised for ease of comparison to assess peak purity, thus ensuring that the degradation product being detected at that retention time was 5-HMF by comparison with standards. The resolution of the two peaks was readily viewed by plotting the data matrix as a contour or cartographic plot (Fig. 2), using software developed at The University of Bradford. A more commonly seen display of the data is shown in Fig. 3, which is a three-dimensional or pseudoisometric plot.

RESULTS AND DISCUSSION

Eluent optimisation

Inspection of Fig. 4 indicates that at pH 5.5 with an organic modifier concentration of 15% (v/v), a satisfactory k' for 5-HMF is observed (2.05; R.S.D. = 1.0, $n = 5$) with good column performance ($N = 30\,000$ plates/m). Resolution from the internal standard is excellent (Fig. 5). The effect of pH on separation was studied, and it was found that the k' values for 5-HMF and 2-FA were constant and that high column performances were maintained (Fig. 6). The optimum flow-rate for high sample

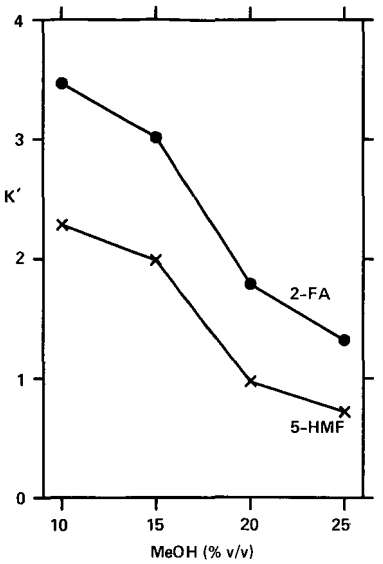

Fig. 4. Plot of k' against methanol concentration in mobile phase at pH 5.5 and a flow-rate of 2.0 ml/min.

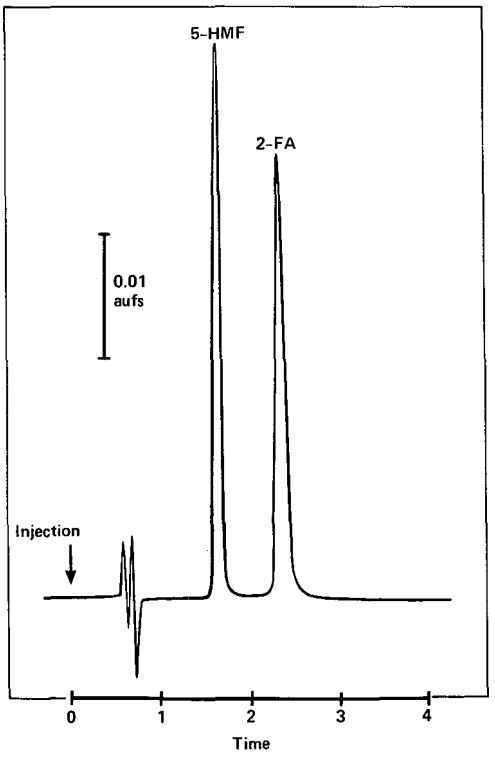

Fig. 5. Chromatogram of 5 μg/ml 5-hydroxymethylfurfural (5-HMF) and 2-furaldehyde (2-FA) under optimised conditions (see text).

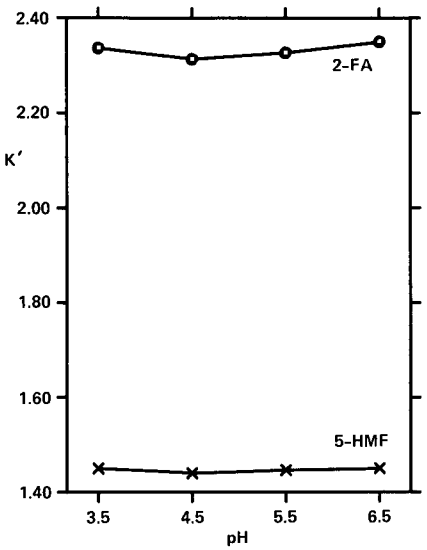

Fig. 6. Plot of k' against pH of buffer portion of mobile phase.

throughput coupled with good resolution of 5-HMF and 2-FA was found to be 2.0 ml/min.

Quantitative comparison of external and internal standard methods

External standard calibration gave a linear response for peak-area ratio against 5-HMF concentration at 0.05 a.u.f.s. over the range 1 – 5 μg/ml, the parameters derived from least-squares regression being $y = 35\,500x - 1540$; $n = 6$; $r = 0.993$. Internal standard calibration displayed a linear regression for peak-area ratio against 5-HMF concentration over the same concentration range at 0.05 a.u.f.s.: $y = 1.90x + 0.024$; $n = 6$; $r = 0.998$.

The R.S.D. of replicate injections for the external standard method at 1 μg/ml was 4.32% ($n=5$) and for the internal standard method at this concentration was 1.30% ($n=5$). The limit of detection of the internal standard method at a signal-to-noise ratio of 2 was 3.2 ng on-column of 5-HMF (R.S.D. = 7.8%; $n=5$). Linearity of the two methods was comparable, but the internal standard method gave superior reproducibility and was therefore the method of choice.

Although there have been some reports that 2-FA may be a degradation product[6,18], these have not been confirmed in the present work. No interference with the internal standard was found in heated glucose solutions under the pharmaceutical sterilisation conditions employed. The method outlined has been found to be suitable for quantitative analysis of 5-HMF produced during heat sterilisation of glucose parenterals.

REFERENCES

1 D. G. Durham, C. T. Hung and R. B. Taylor, *Int. J. Pharm.*, 12 (1982) 31–40.
2 K. R. Heimlich and A. N. Martin, *J. Am. Pharm. Assoc.*, 49 (1960) 592–597.

3 C. T. Hung, A. B. Selkirk and R. B. Taylor, *J. Clin. Hosp. Pharm.*, 7 (1982) 17–23.
4 R. J. Sturgeon, N. K. Athanikar, J. A. Harbison, R. Scott Henry, R. W. Jurgens and A. D. Welco, *J. Parenter. Drug Assoc.*, 34 (1980) 175–182.
5 R. B. Taylor, B. M. Jappy and J. M. Neil, *J. Pharm. Pharmacol.*, 24 (1972) 121–124.
6 R. B. Taylor and V. C. Sood, *J. Pharm. Pharmacol.*, 30 (1978) 510–511.
7 I. Hesson and M. Bojsen-Møller, *Eur. J. Intensive Care Med.*, 2 (1976) 97–101.
8 D. W. Vere, C. H. Sykes and P. Armitage, *Lancet ii*, September, 17 (1960) 627–630.
9 W. Anderson and J. Harthill, *J. Pharm. Pharmacol.*, 34 (1982) 90–96.
10 B. Mielke, *Krankenhauserpharmazie*, 2 (1981) 121–123.
11 F. C. Alfonso, G. E. Martin and R. H. Dyer, *J. Assoc. Off. Anal. Chem.*, 63 (1980) 1310–1313.
12 E. Burtscher, O. Bobleter, W. Schwald, R. Concin and H. Binder, *J. Chromatogr.*, 390 (1987) 401–412.
13 S. W. Hong, H. E. Han and K. S. Chae, *J. Liq. Chromatogr.*, 4 (1981) 285–292.
14 A. F. Fell and B. J. Clark, *Eur. Chromatogr. News*, 1 (1987) 16–22.
15 S. Van der Wal and L. Snyder, *Clin. Chem.*, 27 (1981) 1233–1240.
16 H. J. Jeuring and F. J. E. M. Kuppers, *J. Assoc. Off. Anal. Chem.*, 63 (1980) 1215–1218.
17 T. A. Walmsley and M. Lever, *Anal. Biochem.*, 124 (1982) 446–451.
18 H. Ogata, S. Toshio, E. Akira, M. Toshio and S. Eumiko, *J. Pharm. Pharmacol.*, 30 (1978) 668.

Journal of Chromatography, 467 (1989) 402–405
Elsevier Science Publishers B.V., Amsterdam — Printed in The Netherlands

CHROM. 21 330

Note

Gas–liquid chromatographic resolution of some racemic synthons for lamtidine analogous histamine H_2-receptor antagonists via diastereomeric amides of (1*S*)-(–)-camphanic acid

NADIR BÜYÜKTIMKIN*
Faculty of Pharmacy, University of Istanbul, Beyazit, 34452 Istanbul (Turkey)
and
FRANK KELLER and WALTER SCHUNACK
Institut für Pharmazie, Freie Universität Berlin, Königin-Luise-Strasse 2+4, 1000 Berlin (West) 33 (F.R.G.)
(First received September 5th, 1988; revised manuscript received January 13th, 1989)

The piperidinomethylphenoxy group as a structural feature of lamtidine[1] (Fig. 1) and several other potent long-acting histamine H_2-antagonists[2,3] shows a high affinity for the histamine H_2-receptor[4]. For investigations of structure–activity relationships, the piperidino group of this moiety was replaced with racemic or enantiomeric 3-ethyl-, 3-methyl- or 2-methylpiperidines and 3-methyl- or 2-methylpyrrolidines, respectively. As a result, the enantiomeric compounds derived from these amines showed significantly different histamine H_2-antagonistic activities[5]. The cyclic secondary amines used were resolved according to known methods[6–8]. In a second approach, these amines were obtained by cleavage of the corresponding enantiomeric aminomethylphenols[9]. This paper reports the determination of the optical purity by gas chromatographic (GC) resolution after derivation of these secondary amines using (1*S*)-(–)-camphanoyl chloride[10–12].

EXPERIMENTAL

All chemicals were of analytical-reagent grade. Cyclic amines were purchased from Aldrich (Steinheim, F.R.G.) and Fluka (Buchs, Switzerland) and (1*S*)-(–)-camphanoyl chloride from Aldrich. Optically pure amines were obtained by resolution via diastereomeric salts with tartaric acid and mandelic acid[6–8]. Resolution of a cyclic aminomethylphenol intermediate with di-O-(*p*-toluoyl)tartaric acid followed by

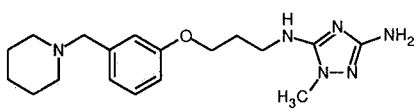

Lamtidine

Fig. 1. Structure of lamtidine.

0021-9673/89/$03.50

cleavage of the so-obtained optically pure aminomethylphenols with hydrogen over palladium yielded optically active secondary amines[9]. The optical rotations of the isolated free amines were measured with a Perkin-Elmer 241 MC polarimeter. A Perkin-Elmer F-22 gas chromatograph equipped with a flame ionization detector was fitted with either a 25 m × 0.33 mm O.D. × 0.25 mm I.D. FS-SE-54-CB-coated fused-silica capillary column having a film thickness of 0.35 μm (Macherey, Nagel & Co., Düren, F.R.G.) or with a 25 m × 0.25 mm I.D. Chirasil-Val-coated glass column (Alltech, Belgium). The injector and detector temperatures were 280°C. The carrier gas was nitrogen at a flow-rate of 1 ml/min in both instances. Temperature programmes from 160 to 240°C at 1°C/min for the first column and from 120 to 170°C at 1°C/min for the second column were applied.

The cyclic secondary amines (0.01 m*M*) and (1*S*)-(–)-camphanoyl chloride (0.02 m*M*) were dissolved in 5 ml of dichloromethane and 0.1 ml of dry pyridine was added. After 4 h the solution was evaporated *in vacuo* and the residue was taken up in 5 ml of dichloromethane. The organic phase was washed successively with 10% aqueous $NaHCO_3$ (10 ml), 1 *M* HCl (10 ml) and twice with water (10 ml), followed by drying over anhydrous Na_2SO_4. The solution was made up to 10 ml and 1 μl of it was injected into the gas chromatograph.

RESULTS AND DISCUSSION

The resolution of racemic amines by GC can be achieved in two ways[13]: either by conversion to diastereomers with a suitable optically active reagent followed by GC under achiral conditions, or by use of a chiral stationary phase. Most popular of the chiral derivatizing reagents for amines are perfluoroacylamino acid chlorides, but they have a tendency to racemize in a short period of time or may show a high racemization rate under the reaction conditions[14,15]. Therefore, in this investigation (1*S*)-(–)-camphanoyl chloride was selected as a reagent of high optical purity and stability[10–12,16,17]. The reaction with cyclic amines proceeded smoothly and quickly

TABLE I

RESOLUTION CONDITIONS FOR DIASTEREOMERIC AMIDES OF (1*S*)-(–)-CAMPHANIC ACID ON AN SE-54-CB-COATED FUSED-SILICA CAPILLARY COLUMN AND A CHIRASIL-VAL-COATED GLASS COLUMN

Amide derived from (according to elution sequence)	*Separation factor*	
	SE-54-CB	*Chirasil-Val*
R-(–)-2-Methylpyrrolidine *S*-(+)-2-Methylpyrrolidine	1.013	1.040
R-(+)-3-Methylpyrrolidine *S*-(–)-3-Methylpyrrolidine	1.0	1.0
R-(–)-2-Methylpiperidine *S*-(+)-2-Methylpiperidine	1.016	1.033
S-(+)-3-Ethylpiperidine *R*-(–)-3-Ethylpiperidine	1.005	1.030
R-(–)-3-Methylpiperidine *S*-(+)-3-Methylpiperidine	1.013	1.033

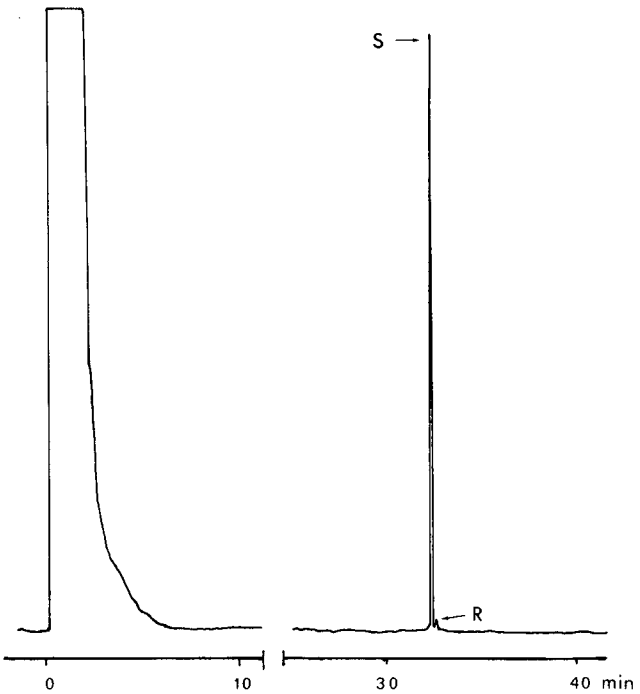

Fig. 2. Chromatogram of (*S*)-(+)-3-ethylpiperidine derivative containing 1% of the (*R*)-(−)-enantiomer on a Chirasil-Val-coated glass column.

within 4 h under ambient conditions. Byproducts did not occur. The addition of pyridine was necessary to shorten the reaction time, as without it more than 36 h were needed to complete the reaction. Heating, although it reduces the reaction time, should be avoided because of the formation of byproducts. During the derivation of the racemic amines, no kinetic or thermodynamic differentiation was observed, as the peak areas of the corresponding diastereomeric amides were equal. The optical impurities of all resolved amines listed in Table I were less than 1%. The solutions in dichloromethane were stable at room temperature for at least 48 h. The separation factors of the diastereomeric amides after chromatography on SE-54-CB-coated fused-silica capillary columns and Chirasil-Val-coated glass columns are listed in Table I.

With an SE-54-CB-coated fused-silica capillary column shorter retention times and good separations down to the baseline were obtained. As expected, the separation factors were better (with slightly longer retention times) for all amides, except the 3-methylpyrrolidine derivative, when the Chirasil-Val-coated column was used[18–21]. For both columns the retention sequence was the same. It was not possible to resolve racemic 3-methylpyrrolidine by this method, as in all instances only a single, sharp peak was observed. For this substance the use of N-trifluoroacetyl-(*S*)-prolyl chloride under the same chromatographic conditions gave clearly separated peaks[22,23]. With the described method an optical impurity of 1% can be determined easily (see Fig. 2).

ACKNOWLEDGEMENTS

We thank the Fonds der Chemischen Industrie and the Deutsche Forschungsgemeinschaft, who supported this work by grants.

REFERENCES

1 R. T. Brittain, M. J. Daly, J. M. Humphray and R. Stables, *Br. J. Pharmacol.*, 76 (1982) 195.
2 M. Tsuritani, *57th Annual Meeting of the Japan Pharmacological Society, Kyoto, 1984*, abstract 0-92.
3 M. Tarutani, H. Sakuma, K. Shiratsuchi and M. Mieda, *Drug Res.*, 35 (1985) 703.
4 J. P. Buyniski, R. L. Cavanagh, A. W. Pircio, A. A. Algieri and R. R. Crenshaw, in C. Melchiorre and M. Gianella (Editors), *Highlights in Receptor Chemistry*, Elsevier, Amsterdam, New York, Oxford, 1984, pp. 195–215.
5 F. Keller, A. Buschauer and W. Schunack, *10th International Symposium on Medicinal Chemistry, Budapest, 1988*, abstract P-109.
6 H.-R. Slivka and H.-J. Hansen, *Helv. Chim. Acta*, 67 (1984) 434.
7 J. W. Sloan, W. R. Martin, R. Hook, M. Bostwick, A. Howell and W. T. Smith, *Life Sci.*, 37 (1985) 1367.
8 B. Ringdahl and R. Dahlbom, *Acta Pharm. Suec.*, 15 (1978) 255.
9 F. Keller, *Dissertation*, Freie Universität Berlin, Berlin, in preparation.
10 H. Gerlach, *Helv. Chim. Acta*, 51 (1968) 1587.
11 H. Gerlach, K. Oertle and K. Thalmann, *Helv. Chim. Acta*, 59 (1976) 755.
12 H. Gerlach, *Helv. Chim. Acta*, 61 (1978) 2773.
13 R. W. Souter, *Chromatographic Separation of Stereoisomers*, CRC Press, Boca Raton, FL, 1985; and references cited therein.
14 J. Hermansson and C. von Bahr, *J. Chromatogr.*, 221 (1980) 109.
15 H. Spahn, H. Weber, E. Mutschler and W. Möhrke, *J. Chromatogr.*, 307 (1984) 145.
16 K. Selvig, M. Ruud-Christensen and A. J. Aasen, *J. Med. Chem.*, 26 (1983) 1514.
17 N. Büyüktimkin, S. Büyüktimkin, S. Elz and W. Schunack, *Sci. Pharm.*, in press.
18 H. Frank, G. J. Nicholson and E. Bayer, *J. Chromatogr.*, 146 (1978) 197.
19 G. J. Nicholson, H. Frank, E. Bayer, *J. High Resolut. Chromatogr. Chromatogr. Commun.*, 2 (1979) 411.
20 H. Frank, A. Rettenmaier, H. Weicher, G. J. Nicholson, E. Bayer, *Anal. Chem.*, 54 (1982) 715.
21 B. Koppenhoefer, H. Allmendinger, G. J. Nicholson, E. Bayer, *J. Chromatogr.*, 260 (1983) 63.
22 N. Büyüktimkin, unpublished results.
23 B. L. Karger, R. L. Stern, W. Keane, B. Halpern and J. W. Westley, *Anal. Chem.*, 39 (1967) 228.

Journal of Chromatography, 467 (1989) 406–413
Elsevier Science Publishers B.V., Amsterdam — Printed in The Netherlands

CHROM. 21 325

Note

Direct enantiomeric separation of anticholinergic drugs derived from (±)-cyclohexyl(3-thienyl)glycolic acid on a novel α_1-acid glycoprotein-bonded chiral stationary phase (Chiral-AGP)

M. LIENNE, M. CAUDE* and R. ROSSET

Laboratoire de Chimie Analytique de l'École Supérieure de Physique et Chimie Industrielles de Paris, 75231 Paris Cedex 05 (France)

and

A. TAMBUTÉ

Direction de Recherches et Études Techniques, Centre d'Études du Bouchet, BP No. 3, Le Bouchet, 91710 Vert-le-Petit (France)

(First received December 6th, 1988; revised manuscript received January 17th, 1989)

In the pharmaceutical and agrochemical areas there is growing interest in studies of the relationship between molecular stereochemistry and pharmaceutical activity, potency and plasma disposition[1]. Differences in the pharmacokinetic and pharmacodynamic behaviours of drug enantiomers have been found for various families of biologically active molecules, including the important class of anticholinergic agents[2] such as atropine[3]. A recent study[4] of compared antimuscarinic effects of (*R*)- and (*S*)-oxyphencyclimine hydrochloride indicated that the (*R*)-(+)- enantiomer inhibited the binding to cholinergic receptor 39 times more potently than the (*S*)-(−)-enantiomer, and this is a general trend observed[5] for heterocyclic amino alcohol esters derived from (−)-glycolic acids compared with those derived from (+)-glycolic acids [*e.g.*, from (*R*)-(−)- or (*S*)-(+)-cyclohexylphenylglycolic acid[6] (CHPGA)]. The glycolic esters of dialkylamino alcohols considered in this paper (Table I, racemates **1**, **4**, **7** and **10**) also proved to exhibit anticholinergic activity; the influence of molecular stereochemistry is now under investigation.

Accordingly, pharmacologists and clinicians now need reliable and accurate analytical methods to carry out enantiomeric assays in biological samples in order to evaluate the magnitude and consequences of stereochemistry in biological processes. The direct resolution of enantiomers by high-performance liquid chromatography (HPLC) on chiral stationary phases (CSPs)[7,8] is such a method. Among various commercially available CSPs, α_1-acid glycoprotein (α_1-AGP) immobilized on silica gel[9] (Enantiopac; LKB, Stockholm, Sweden) appeared particularly suitable for the resolution of cationic drugs, including anticholinergic agents such as atropine[10,11], tropicamide[12], cyclopentolate[10,11], homatropine[10], methylhomatropine[10,11], oxyphencyclimine[10,13] and mepenzolate bromide[10–13]. These amino alcohol esters (except for mepenzolate bromide) are characterized by the presence of a tertiary amino group and an asymmetric carbon located at either the α- (homatropine, methylhomatropine and oxyphencyclimine) or β-position (atropine, cyclopentolate and

0021-9673/89/$03.50

tropicamide) with respect to the hydroxy group. Mepenzolate bromide differs completely, as the chiral carbon belongs to the cyclic amino moiety. The compounds considered here, derived from (±)-cyclohexyl(3-thienyl)glycolic acid (CHTGA), possess structures closely related to homatropine, methylhomatropine and oxyphencyclimine and were therefore expected to be resolved on the α_1-AGP CSP.

This paper reports the direct LC enantiomeric resolution of this new series of anticholinergic drugs on the commercially available protein CSP, Chiral-AGP (ChromTech, Stockholm, Sweden) developed by Hermansson and co-workers[14,15] and for which plasma α_1-AGP is immobilized according to a novel technique on spherical porous silica particles ($d_p = 5$ μm).

EXPERIMENTAL

Apparatus

Analytical chromatography was performed with a modular liquid chromatograph (Gilson, Villiers-le-Bel, France) equipped with a Model 802C manometric module, a Gilson 811 (1.5-ml) dynamic mixer and a Model 116 variable-wavelength UV detector. The column and solvent were thermostated with a Haake Model D8-V circulator bath (−5 to 150°C) (Roucaire, Vélizy-Villacoublay, France) and a water cooling-jacket. All tubing connections were heat-insulated. UV detection was carried out at 230 nm.

Chiral stationary phases

The 100 × 4.6 mm I.D. Chiral-AGP column was purchased from ChromTech.

Syntheses of anticholinergic compounds ***1–12***

Caution. These compounds display potent anticholinergic activity and it is advisable to handle them carefully. The glassware was washed thoroughly and residues were disposed of by steeping in 6 M hydrochloric acid.

The preparation of compounds **1–12** (Table I), either as enantiomers or racemates, was carried out by refluxing in a molar ratio of 2-(3-thienyl)-2-cyclohexyl-2-hydroxyacetic acid[16] with the corresponding β- or γ-dialkylaminoalkyl halogenated derivative [purchased as hydrochlorides from Aldrich (Milwaukee, WI, U.S.A.)] in 2-propanol as follows.

In a round-bottomed flask were placed 4.8 g (20 mmol) of 2-(3-thienyl)-2-cyclohexyl-2-hydroxyacetic acid, 20 mmol of the corresponding halogenated derivative (freshly prepared)[17] and 60 ml of 2-propanol. The mixture was refluxed with magnetic stirring under a nitrogen atmosphere for 2 h (**1–6**) or 8 h (**7–12**). The solid which appeared after cooling to room temperature was collected by filtration under suction and washed with 10 ml of cold 2-propanol. Crystallization from ethanol afforded pure **1–12** as hydrochlorides. Physical data are listed in Table I and ^{1}H NMR data in Table II.

Solvents

Aqueous buffer solutions were prepared either directly[18] from mixtures of 0.2 *M* solutions of $NaH_2PO_4 \cdot 2H_2O$ and $Na_2HPO_4 \cdot 2H_2O$ (extra-pure grade, Merck, Darmstadt, F.R.G.), or from a commercially available sodium phosphate buffer (25

TABLE I

PHYSICAL DATA REFERRING TO THE SYNTHESIS OF COMPOUNDS **1–12**

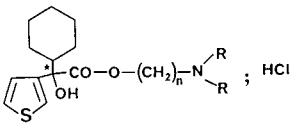

1-12

No.	*n*	*R*	*Configuration*	$[\alpha]_{365}^{25}$ (°) (*water, c = 1*)	*Melting point (°C)*	*Yield (%)*
1	2	CH_3	Racemate		186–188	43
2			*R*	−16.8	208–210	36
3			*S*	+16.1	208–210	35
4	2	C_2H_5	Racemate		205–207	96
5			*R*	−17.6	212–214	92
6			*S*	+18.0	212–214	93
7	3	CH_3	Racemate		168–169	65
8			*R*	−17.7	194–196	55
9			*S*	+18.4	194–196	36
10	3	C_2H_5	Racemate		169–170	75
11			*R*	−10.7	152–154	62
12			*S*	+10.5	151–153	67

TABLE II

200 MHz ^{1}H NMR SPECTRA OF RACEMIC COMPOUNDS **1**, **4**, **7** AND **10**

Chemical shifts in ppm from internal standard [2,2,3,3-$^2H_4$]3-(trimethylsilyl)propionic acid (sodium salt) (TSP-d_4) in ^2H_2O (c = 20 mg ml^{-1}) at 295 K. Racemates and enantiomers showed identical spectra.

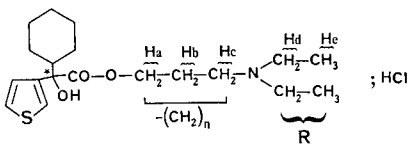

Compound	*3H (aromatic)*	*11H (cyclohexyl)*		*2Ha*	*2Hb*	*2Hc*	*4Hd*	*6He*
		$-(CH_2)_5-$	$-CH-$					
(±)-**1**: n=2, R=CH_3	7.28 (m) 7.50 (m)	0.9–1.9 (m)	2.39 (m)	4.52 (t)	–	3,52 (t)	–	2.87 (s)
(±)-**4**: n=2, R=C_2H_5	7.26 (m) 7.48 (m)	0.9–1.9 (m)	2.35 (m)	4.52 (t)	–	3.52 (t)	3.18 (q)	1.27 (t)
(±)-**7**: n=3, R=CH_3	7.27 (m) 7.48 (m)	0.9–1.85 (m)	2.35 (m)	4.28 (m)	2.09 (m)	3.01 (d.d)	–	2.82 (s)
(±)-**10**: n=3, R=C_2H_5	7.24 (m) 7.49 (m)	0.9–1.9 (m)	2.36 (m)	4.30 (m)	2.07 (m)	3.01 (d.d)	3.17 (q)	1.24 (t)

m*M*, pH 6.88) (Merck) (in both instances diluted to afford 8 m*M* buffers). Deionized water was doubly distilled on a Buchi-Fontavapor 285 apparatus (Roucaire). The pH of the aqueous buffer eluent was controlled with a Model Minisis 8000 pH/millivoltmeter (Tacussel, Villeurbanne, France) and Tacussel glass TB/HS and Tacussel C8 calomel reference electrodes. Aqueous solvents were filtered through 0.65-μm DAWP Millipore membrane filters (Touzart et Matignon, Vitry-sur-Seine, France) and then degassed with helium.

2-Propanol was of LiChrosolv grade purchased from Merck. Solutes were dissolved, in an ultrasonic bath, in the 8 m*M* sodium phosphate buffer (pH 7.0). The concentrations of the solutes were around $4 \cdot 10^{-2}$ mg ml^{-1}, corresponding to an amount injected of about 2 nmol (20 μl).

RESULTS AND DISCUSSION

Enantiomeric resolution of (±)-CHTGA by crystallization of diastereomeric salts with either (−)- or (+)-ephedrine and assignment of absolute configuration by circular dichroism measurements have been reported previously[16]. The control of optical purity was carried out by HPLC using a β-cyclodextrin-bonded CSP[19] (Cyclobond-I; Astec, Whippany, NJ, U.S.A.); this CSP is able to resolve a series of aromatic carboxylic acids[19], including (±)-CHPGA[20,21] (precursor of the anticholinergic ester oxyphenonium bromide), but not the ester derivatives.

Investigations carried out on the Chiral-AGP column (Table III) showed that a baseline resolution could be achieved, depending on the mobile phase composition and solute structure (Fig. 1). Several observations can be made from Table III: (a) whatever the *n* value, N-diethylamino substitution leads to both higher retention (for both enantiomers) and selectivity than N-dimethyl substitution; (b) whatever the N-dialkylamino substitution, the retention and selectivity decrease with lengthening of the alkyl "joining block" (as termed in ref. 2) from $n=2$ to $n=3$; (c) the general trend with increasing pH is a concomitant higher retention and selectivity gain, however, for (±)-**1** and (±)-**10** the selectivity is altered to a limited extent compared with the retention.

Enhancement of retention and selectivity with increasing steric bulkiness at the basic nitrogen atom seems to be a general trend with the α_1-AGP CSP[9], already emphasized by Schill *et al.*[10] for a series of compounds related to metoprolol and by Hermansson and co-workers[15,22] for a series of N-dialkyl-substituted succinimides. The latter compounds have some structural similarities with the glycolates in this paper (Fig. 2), but for N-dialkylsuccinimides an increase in *n* from 2 to 3 resulted in a decrease in selectivity, unlike the aforementioned results for thienylglycolates. Such discrepancies can be attributed to other specific structural features of these two series of compounds (cyclic structure for succinimides, etc.) and to the replacement of an ester group for an amide group at the asymmetric centre (Fig. 2).

The increase in retention observed for both enantiomers on changing R can be ascribed mainly to stronger hydrophobic interactions with the protein. For the solute (±)-**10** the selectivity variations on decreasing the 2-propanol content in the mobile phase, are slight; this means that enantiomers are affected to a similar extent by addition of 2-propanol (k' represents the ratio of the sum of the solute–CSP interactions to the sum of solute–mobile phase interactions); accordingly, 2-propanol, which

TABLE III

INFLUENCE OF THE MOBILE PHASE pH ON THE RESOLUTION OF RACEMIC ANTICHOLINERGIC AGENTS **1**, **4**, **7** AND **10**

Column, Chiral-AGP; mobile phase, 8 m*M* sodium phosphate buffer with 2-propanol added;flow-rate, 0.9 ml min^{-1}; t_0 = 1 min; temperature, 20°C; UV detection at 230 nm.

Solute	*2-Propanol (%, v/v)*	*Elution order*	*pH 6.61*			*pH 6.80*			*pH 7.00*			*pH 7.20*			*pH 7.43*		
			k_2' [a]	α [b]	R_s [c]	k_2'	α	R_s	k_2'	α	R_s	k_2'	α	R_s	k_2'	α	R_s
(±)-**1**: n=2, R=CH_3	10	(*R,S*)	10.6	1.48	2.7	13.4	1.58	3.0	13.3	1.54	2.6	21.1	1.57	2.7	26.7	1.55	1.5
(±)-**4**: n=2, R=C_2H_5	10	(*R,S*)	17.6	2.00	3.7	22.9	2.11	4.0	24.2	2.27	4.5	31.2	2.24	3.6	49.5	2.33	2.0
(±)-**7**: n=3, R=CH_3	6	(*S,R*)	13.6	>1.0*	–	17.8	1.18	0.6	19.5	1.17	0.9	31.8	1.16	0.8	46.0	1.29	1.2
(±)-**10**: n=3, R=C_2H_5	6	(*R,S*)	17.7	1.21	1.2	24.2	1.23	1.2	23.2	1.25	1.2	38.1	1.24	1.2	49.1	1.24	1.0
	10	(*R,S*)	7.8	1.18	1.0	9.6	1.19	1.1	9.1	1.23	1.1	14.4	1.21	1.1	24.8	1.20	0.8

[a] Capacity factor of the second eluted enantiomer was calculated from dead retention time t_0 (t_0 = 1 min) as follows: $k' = (t_r - t_0)/t_0$.

[b] Selectivity $\alpha = k_2'/k_1'$.

[c] R_s (resolution factor) = 2 (distance of the two enantiomer peak positions / sum of the band widths of the two peaks at their bases) : $R_s = 2(t_{r2} - t_{r1}) / (w_1 + w_2)$.

The asterix indicates the beginning of separation.

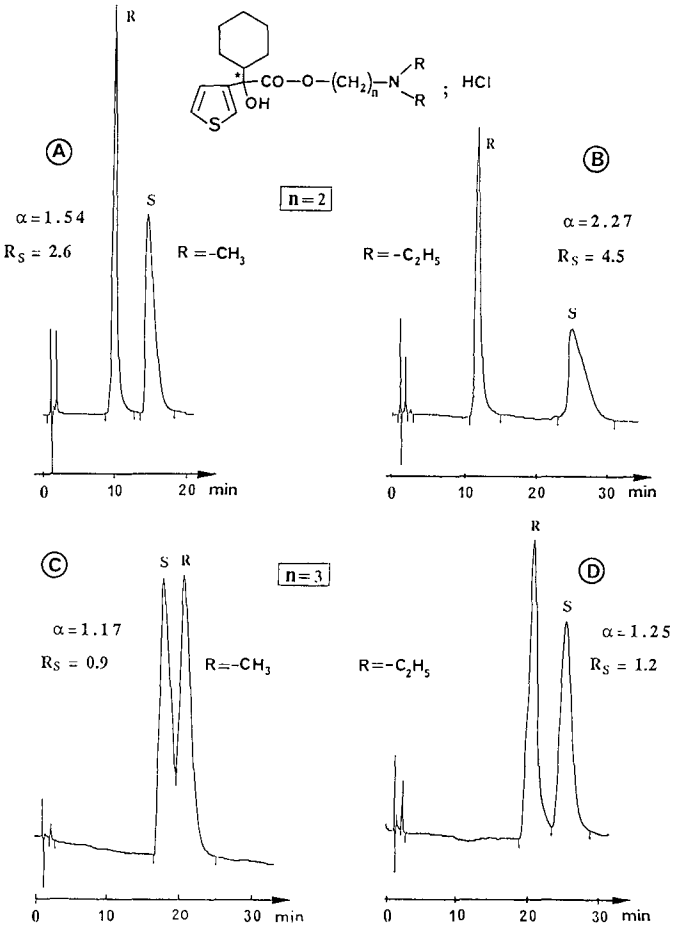

Fig. 1. Influences of the distance between the asymmetric carbon and the nitrogen atom and the N-diaminoalkyl substitution on the resolution of amino alcohols glycolic esters. Column: Chiral-AGP. (A) (±)-**1**; (B) (±)-**4**; (C) (±)-**7**; (D) (±)-**10**. Mobile phase: 8 m*M* sodium phosphate buffer (pH 7.0) + (A) and (B) 10% and (C) and (D) 6% (v/v) 2-propanol. Other conditions as in Table III.

can compete with the solute on the protein binding sites through hydrophobic and/or hydrogen bonding interactions, regulates the retention and to a minor extent the enantiorecognition process for such cationic drugs.

Small variations in the mobile phase pH may be responsible for a significant improvement in selectivity [*e.g.*, for solutes (±)-**4** and (±)-**7**]. The influence of pH on stereoselectivity may result from conformational modifications of the protein involving its ionic binding sites (protein secondary or tertiary structure).

Moreover, regarding the solute structure, the selectivity is markedly affected by the *n* value, *i.e.*, the distance between the cationic ammonium site and the α-hydroxy

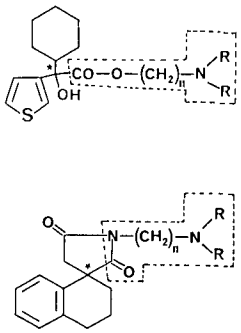

Fig. 2. Structures of (A) N-dialkylamino alcohol glycolic esters (this work) and (B) N-dialkylaminosuccinimides studied by Hermansson *et al.*[22]. Dotted regions mark similar chemical moieties. A possesses an ester function and B an amide function.

group (on the asymmetric carbon), which is probably engaged in hydrogen bonding formation with the protein. This finding suggests that a specific spatial fitting of solute structure with the protein is required for enantiorecognition. Further, different protein binding sites or functional groups of the same binding sites may be involved in the chiral recognition mechanism, depending on the nearest functional environment at the asymmetric centre (*e.g.*, the relative positions of the α-hydroxy group and the basic nitrogen atom), thus leading to differences in the enantiorecognition ability of the CSPs. Accessibility to the protein binding sites is governed by the conformational state: modifications of intramolecular hydrogen bonding and/or electrostatic interactions due to addition of 2-propanol or mainly to pH changes will alter the type and the shape of the binding sites and thus affect its enantiorecognition ability.

Compound (±)-**7** with $n=3$ and R = methyl was expected to be the worst resolved [assumptions (a) and (b) on p. 409]; nevertheless, the observed inversion of elution order, compared with other solutes, was not predictable (Table III).

CONCLUSION

The use of an aqueous buffered mobile phase with α_1-AGP protein-derived CSP is advantageous for the analysis of biological samples and the good resolutions obtained on the Chiral-AGP column make it suitable for the enantiomeric purity control of thienylglycolates **1–12**. Considering such cationic drugs, ionic binding to the protein and additional hydrogen bond formation and hydrophobic interactions are suggested to account for chiral recognition mechanisms.

ACKNOWLEDGEMENT

The authors express their thanks to Arlette Bégos (Centre d'Etudes du Bouchet) for the synthesis of the anticholinergic drugs studied in this paper.

REFERENCES

1 I. W. Wainer and D. E. Drayer (Editors), *Drug Stereochemistry: Analytical Methods and Pharmacology*, Marcel Dekker, New York, 1988.
2 G. Ssasz and Zs. Budvari-Barany in G. Ssasz (Editor) *Pharmaceutical Chemistry of Adrenergic and Anticholinergic Drugs*, CRC Press, Boca Raton, FL, 1985, pp. 103–133.
3 R. B. Barlow, F. M. Franks and J. D. M. Pearson. *J. Med. Chem.*, 16 (1973) 439.
4 L. Schjelderup, M. R. Kozlowski, A. Weissman and A. J. Aasen, *J. Pharm. Res.*, 5 (1988) 236.
5 E. R. Atkinson, D. D. McRitchie, L. F. Shoer, L. S. Harris, S. Archer, M. D. Aceto, J. Pearl and F. P. Luduena, *J. Med. Chem.*, 20 (1977) 1613.
6 R. W. Brimblecombe, D. M. Green, T. D. Inch and P. B. J. Thompson, *J. Pharm. Pharmacol.*, 23 (1971) 745.
7 M. Lienne, M. Caude, A. Tambuté and R. Rosset, *Analusis*, 15 (1987) 431.
8 M. Zief and L. Crane (Editors), *Chromatographic Chiral Separations* (*Chromatographic Science Series*, Vol. 40), Marcel Dekker, New York, 1987.
9 J. Hermansson and G. Schill, in M. Zief and L. Crane (Editors), *Chromatographic Chiral Separations*, Marcel Dekker, New York, 1987, p. 245.
10 G. Schill, I. W. Wainer and S. A. Barkan, *J. Liq. Chromatogr.*, 9 (1986) 641.
11 G. Schill, I. W. Wainer and S. A. Barkan, *J. Chromatogr.*, 365 (1986) 73.
12 J. Hermansson, *J. Chromatogr.*, 298 (1984) 67.
13 J. Hermansson, *J. Chromatogr.*, 269 (1983) 71.
14 J. Hermansson, paper presented at the *1st International Symposium on Separation of Chiral Molecules, Paris, May 31 – June 2, 1988.*
15 M. Enquist (Eriksson) and J. Hermansson, paper presented at the *12th International Symposium on Column Liquid Chromatography, Washington, DC, June 19–24, 1988.*
16 A. Tambuté and A. Collet, *Bull. Soc. Chim. Fr.*, 1–2 (1984) II-77.
17 R. R. Burtner. *J. Am. Chem. Soc.*, 71 (1949) 2578.
18 D. D. Perrin and B. Dempsey, *Buffers for pH and Metal Ion Control*, Chapman & Hall, London, 1979, p. 138.
19 P. Macaudière, M. Caude, R. Rosset and A. Tambuté, *J. Chromatogr.*, 450 (1988) 255.
20 K. G. Feitsma, J. Bosman, B. F. H. Drenth and R. A. de Zeeuw, *J. Chromatogr.*, 333 (1985) 59.
21 K. G. Feitsma, B. F. H. Drenth and R. A. de Zeeuw, *J. Chromatogr.*, 387 (1987) 447.
22 J. Hermansson, K. Ström and R. Sandberg, *Chromatographia*, 24 (1987) 520.

Journal of Chromatography, 467 (1989) 414–422
Elsevier Science Publishers B.V., Amsterdam — Printed in The Netherlands

CHROM. 21 391

Note

Normal-phase and reversed-phase liquid chromatographic techniques for the determination of dithranol and its degradation products

IRENE C. L. CHEAH, BALVANT R. SITARAM*, ARTHUR PAPPAS, NGUYEN L. THI, BARRIE C. FINNIN and BARRY L. REED

School of Pharmaceutics, Victorian College of Pharmacy, 381 Royal Parade, Parkville, Victoria 3052 (Australia)

(First received December 23rd, 1988; revised manuscript received February 6th, 1989)

Dithranol is an effective anti-psoriatic agent when applied topically to psoriatic lesions[1]. A number of analytical procedures including thin-layer chromatographic techniques[2], fluorescence spectroscopy[3–6], direct ultraviolet spectroscopy[7,8] and gas chromatographic–mass spectrometric techniques[9] have been described for the assay of dithranol as a raw material, in complex pharmaceutical formulations, and during the study of its degradation under various experimental conditions. Major inadequacies in methodologies for extraction and subsequent separation and detection of dithranol and its degradation products, however, remain.

More recently, a number of liquid chromatographic (LC) methods employing ultraviolet detection for the analysis of dithranol and its degradation products have been described. Caron and Shroot[10] reported the application of both reversed-phase and normal-phase chromatography to the analysis of these compounds in creams and ointments containing dithranol. However, only limited resolution of dithranol and danthron was achieved on either system under the conditions described. Schaltegger *et al.*[11] have also described a reversed-phase chromatographic system which permits the baseline resolution of dithranol and danthron but does not include the simultaneous analysis of dianthrone. The method of Burton and Gadde[12], while allowing the simultaneous assay of dithranol, danthron and dianthrone is characterised by limited resolution of dithranol and danthron and a prolonged analysis time. An improved separation of dithranol and its degradation products was achieved by Newcombe[13] using normal-phase chromatography. However, the assay was characterised by a prolonged analysis time and poor peak shape for dianthrone. While Whitefield *et al.*[14] have also recently described a normal-phase LC method, no chromatograms illustrating the separation achieved or accompanying validation data were presented.

In addition, few studies have addressed the constraints that the marked instability of dithranol places on methodologies for the extraction of these compounds. Despite the potential for artifact the majority of investigators[12–14] have failed to provide adequate documentation of extraction efficiences. In the present study we describe selective normal-phase and reversed-phase LC techniques which permit the baseline resolution of dithranol, danthron and dianthrone and their simultaneous

0021-9673/89/$03.50

detection at the nanogram level. A validation of methods for the extraction and analysis of dithranol and its degradation products is also presented.

EXPERIMENTAL

Materials

Anthracene, chrysophanic acid (1,8-dihydroxy-3-methyl-anthraquinone), danthron (1,8-dihydroxyanthraquinone) and dithranol (1,8-dihydroxy-9-anthrone) were purchased from Aldrich (Milwaukee, WI, U.S.A.). 1,4-Naphthoquinone came from Fluka (Buchs, Switzerland). Dianthrone (1,8,1′,8′-tetrahydroxy-10,10′-dianthrone) was kindly donated by Dr. Braham Shroot (Centre International de Recherches Dermatologiques, Sophia Antipolis, Valbonne, France). All solvents used were of analytical grade or LC standard. Water was glass distilled prior to use.

Commercial samples of dithranol marketed for the preparation of pharmaceutical products were obtained from Bleakley (Brooklyn, Australia), Hartington (Chesterfield, U.K.), Hilditch-Vine (Sydney, Australia) and Prosana (Sydney, Australia). Proprietary pharmaceutical products containing dithranol were obtained from the following sources; Psorin® ointment (0.16%) was purchased from Cambden Pharmaceuticals (Melbourne, Australia), Dithrocream® (0.1%) from Dermal Labs. (Gosmore, U.K.) and Psoridrate® cream (0.1 and 0.2%) from Norwich Eaton (Newcastle upon Tyne, U.K.). The U.S.P. Reference Standard of dithranol was obtained from U.S.P. Pharmacopeia (Rockville, MD, U.S.A.).

Instrumentation

Chromatography was performed using an LDC Constametric liquid chromatograph (Model III). All samples were introduced into the column by means of a Rheodyne 7125 injector fitted with a 100-μl loop. The spectroscopic detector used was a Perkin Elmer LC-75 spectrophotometer. Chromatographic data were recorded using a Perkin Elmer M-2 calculating integrator linked to a BBC Goerz Metrawatt SE-120 chart recorder.

Liquid chromatography

Reversed-phase chromatography. Separation of dithranol, danthron and dianthrone was achieved on an ODS column (DuPont Zorbax, 25 cm × 4.6 mm I.D., 6 μm) protected by an RP-18 Newguard pre-column cartridge (Brownlee Labs., Santa Clara, CA, U.S.A.). The mobile phase consisted of acetonitrile–glacial acetic acid–distilled water (68.5:1.5:30, v/v/v) and was maintained at a flow-rate of 2.00 ml/min.

Normal-phase chromatography. Separation of dithranol, danthron and dianthrone was also achieved on a silica column (DuPont Sil, 25 cm × 4.6 mm I.D., 6 μm) protected by a silica Newguard pre-column cartridge (Brownlee Labs, Santa Clara, CA, U.S.A.). The mobile phase consisted of 2,2,4-trimethylpentane–1,2-dichloroethane–glacial acetic acid (91:6:3, v/v/v) and was maintained at a flow-rate of 2.00 ml/min. Anhydrous conditions were maintained by connecting the mobile phase reservoir to a glass cylinder containing silica gel dessicant. Detection was routinely performed by ultraviolet absorption spectrometry at 354 nm. All separations were performed using a column temperature of 22°C.

Stop-flow spectroscopic analysis. Ultraviolet spectroscopy was performed by halting the flow of the mobile phase as each analyte entered the detector flow cell. Spectra were then recorded.

Extraction procedures

Preparation of standard extracts. Standard solutions of dithranol of known concentrations were prepared in dichloroethane. To 4 ml of this solution was added 1 ml of internal standard solution (1 mg/ml in dichloroethane). The solution was filtered through a glass microfibre filter (Whatman GF/B, 1.0 μm, 2.5 cm) held in a stainless-steel filter holder (Millipore, Milford, MA, U.S.A.) using a gas tight glass syringe (Hamilton, Reno, NV, U.S.A.) fitted with an PTFE plunger. The first 2 ml of filtrate were discarded. Aliquots (10 μl) were taken from the remaining filtrate for LC analysis.

Preparation of ointment extracts. Dichloroethane (4 ml) and 1 ml of internal standard solution (1 mg/ml in dichloroethane) were added to dithranol ointment in a 10-ml glass vial. The sample was sonicated for 5 min to completely disperse the ointment in the extraction solvent. The suspension was then filtered as described above and aliquots of the filtrate (10 μl) were assayed as described in the Experimental section.

Preparation of cream extracts. Dichloroethane (4 ml) and 1 ml of internal standard solution (1 mg/ml in dichloroethane) were added to 125 mg of dithranol cream in a 10-ml glass vial. The sample was homogenised using a Polytron (Kinematica, Littau-Luzern, Switzerland) for 20 s to disperse the cream in the extraction solvent. The suspension was then filtered and aliquots of the filtrate (10 μl) were assayed as described in the Experimental section.

Determination of recoveries. Known amounts of dithranol, danthron or dianthrone in dichloroethane were spiked into 125 mg of ointment or cream base. The sample was then extracted into dichloroethane as described above. The percentage recovery was determined by a comparison of peak areas obtained to appropriate standards.

RESULTS

Reversed-phase chromatography

The use of reversed-phase chromatography performed on a Zorbax ODS column as described above permitted the complete separation of dithranol, danthron and dianthrone and the proposed internal standard chrysophanic acid (Fig. 1a) with an overall analysis time of less than 15 min. To achieve optimum sensitivity and selectivity for dithranol, detection was routinely performed by ultraviolet absorption at 354 nm. Neither of the alternative columns tested (Phase-Sep Spherisorb ODS, Waters μBondapak C_{18}) were able to adequately separate dithranol and danthron despite modifications to the mobile phase.

Normal-phase chromatography

The normal-phase assay described by Newcombe[13] was evaluated for its suitability for the separation of dithranol, danthron and dianthrone. Although complete separation of the compounds was achieved, the assay required an overall

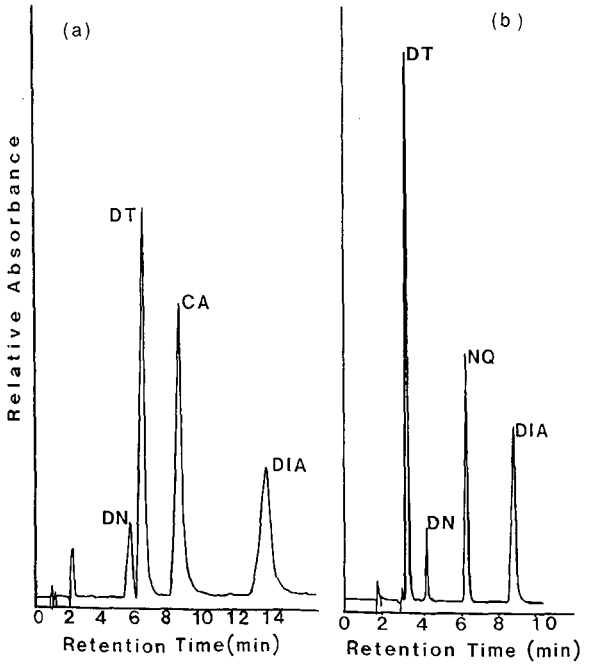

Fig. 1. Chromatograms illustrating the separation of dithranol (DT), danthron (DN), dianthrone (DIA), 1,4-naphthoquinone (NQ) and chrysophanic acid (CA), achieved (a) on a DuPont Zorbax ODS column and (b) on a DuPont Zorbax Sil column. A 10-μl aliquot mixture containing each compound (40 μg/ml in dichloroethane) was introduced onto the ODS column. LC was performed as described in the Experimental section.

analysis time of greater than 25 min. In addition, a marked instability of retention times was apparent. Modifications to the mobile phase used by Newcombe[13] resulted in an improved separation with a reduction in overall analysis time to less than 10 min (Fig. 1b). Alternative columns studied (Waters μPorasil, Brownlee Labs. Silica Spheri-5, and Phase-Sep Spherisorb silica S5) resulted in an inferior separation of dithranol and danthron due to peak tailing.

The spectral characteristics of dithranol, danthron and dianthrone were recorded on-line following separation by both normal- and reversed-phase chromatography. Absorption maxima for dithranol, dianthrone and danthron were observed at 354, 360 and 425 nm, respectively.

Internal standardisation

1,4-Naphthoquinone was routinely used as an internal standard during normal-phase chromatography. The 1,4-naphthoquinone peak was completely resolved from dithranol and its degradation products (Fig. 1b). 1,4-Naphthoquinone, however, was unsuitable as an internal standard for the reversed-phase assay as it was inadequately retained on the ODS column (retention time 2 min). The internal standard (1,8-dihydroxy-9-anthron-10-yl maleic acid dimethyl ester) successfully used by Caron and Shroot[10] was not available commercially. Of a number of anthrones examined both anthracene (retention time 9.5 min) and chrysophanic acid (retention

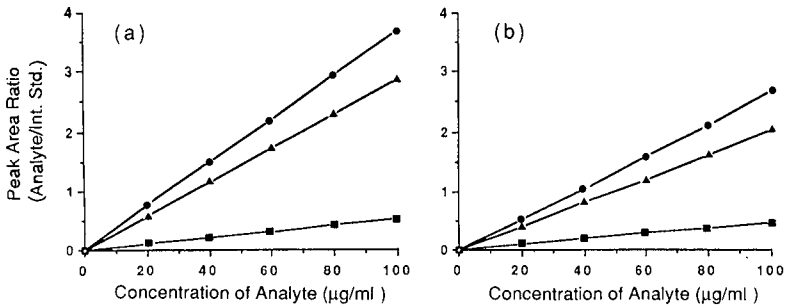

Fig. 2. Standard curves of peak area ratio (analyte/internal standard) *versus* concentration of analyte obtained following (a) reversed-phase and (b) normal-phase chromatography. Aliquots of standard solutions (0–100 μg/ml) containing dithranol (●), danthron (■) or dianthrone (▲) with chrysophanic acid (200 μg/ml) or 1,4-naphthoquinone (200 μg/ml) as internal standard were analysed as described in the Experimental section.

time 8.7 min) had retention times intermediate between dithranol and dianthrone and were completely resolved from dithranol and its degradation products. Anthracene was unsuitable as an internal standard for the analysis of dithranol ointment samples which also contained coal tar as a therapeutic ingredient, due to its presence as a constituent of tar. As a consequence, chrysophanic acid was routinely used in all subsequent studies.

Validation of the reversed- and normal-phase analyses

Sequential analyses of a 10-μl aliquot of a standard solution of dithranol 40 μg/ml in dichloroethane (400 ng on column) performed by either reversed- or normal-phase chromatography yielded coefficients of variation (C.V.) for the determinations of less than 1.2%.

Linear relationships were observed between relative absorbance (peak area ratio of standard/internal standard) and the concentration of dithranol, danthron and dianthrone following chromatography on the Zorbax ODS and Zorbax silica columns within the range of concentrations examined (0–100 μg/ml) (Fig. 2).

The minimum detectable limits at the absorption maxima for dithranol (4.8 and 1.5 ng), danthron (4.8 and 2.1 ng) and dianthrone (10.0 and 3.26 ng) were determined (reversed-phase and normal-phase chromatography, respectively). The minimum detectable limits were two to three fold lower for all compounds for the normal than for the reversed-phase assay. At the wavelength routinely employed for the analysis of dithranol (354 nm), the sensitivity of danthron detection was reduced by a factor of five. The minimum detectable limit for danthron at 354 nm was 10.4 ng for normal-phase chromatography and 23.8 ng for reversed-phase chromatography.

Extraction of dithranol from ointment samples

It is essential that dithranol remains stable in the extraction solvent and also that the solvent be able to dissipate the ointment base and provide an efficient recovery of dithranol. The chlorinated hydrocarbons were found to be suitable in this regard. A chromatogram illustrating the analysis of dithranol and its degradation products in an extract of Psorin ointment using normal-phase chromatography is illustrated in Fig. 3.

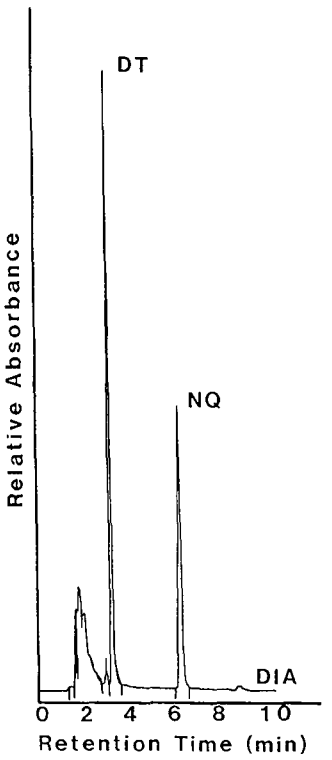

Fig. 3. Chromatogram illustrating the analysis of dithranol (DT) and its degradation product dianthrone (DIA) in Psorin ointment. The internal standard is 1,4-naphthoquinone (NQ). Ointment extracts were prepared and analyses performed by normal-phase chromatography as described in the Experimental section.

Dithranol was found to be stable in the solvents chloroform, dichloromethane and dichloroethane for at least 48 h at 20°C in the absence of light. Of these solvents dichloroethane was the preferred solvent because of its higher boiling point (83–84°C) and the efficiency with which it dispersed the ointment base. Dithranol, danthron and dianthrone were all shown to be stable in dichloroethane for at least 30 h.

Determination of recoveries

Psorin ointment base (125 mg) spiked with 200 μg of dithranol, danthron or dianthrone (in 1 ml of dichloroethane) was extracted and analysed using normal-phase LC as described above. The recovery for each compound from the ointment base was greater than 92% with C.V. values of less than 3.5% (Table I). Recoveries from ointment base triturated with dithranol (0.16%, w/w) immediately before extraction and analysis were identical to those determined by exogenous spiking (Table I).

Since all of the cream-based products studied were of commercial origin, no drug-free bases were available. Recoveries were therefore determined by a subtraction of dithranol content obtained prior to the addition of exogenous dithranol from that obtained following the addition. The recoveries of dithranol from two commercially

TABLE I

RECOVERIES OF DITHRANOL, DANTHRON AND DIANTHRONE FROM PSORIN OINTMENT BASE

Ointment samples were spiked, extracts were prepared and analyses performed by normal-phase chromatography as described in the Experimental section. Results are presented as mean ± standard error of the mean (S.E.M.) for the number of determinations in parenthesis.

Compound	*Recovery (%)*
Dithranol	98.1 ± 0.4 (5)
	99.3 ± 2.0[a] (5)
Danthron	101.0 ± 0.3 (5)
Dianthrone	92.5 ± 0.3 (4)

[a] Dithranol incorporated into Psorin ointment base by trituration immediately before extraction.

available creams were determined. The recoveries from Dithrocream 0.1%, and Psoridrate cream 0.1% were 103.6 ± 1.8% and 95.6 ± 1.4% respectively (five determinations).

Applications of the LC analysis methods

Analysis of commercial samples of dithranol. A number of commercial samples were analysed to determine the amount of dithranol present. Of the samples examined only the sample marketed by Bleakley had degraded to a significant degree ($p < 0.01$) at the time of analysis. A significant proportion of the dithranol lost (7.1%) could be accounted for in the form of dianthrone (Table II). The dithranol content of the other samples did not differ significantly from the U.S.P. reference standard. No danthron was detected in any of the samples tested.

Analysis of commercially available dithranol products. A number of commercially available dithranol-containing pharmaceutical products were also analysed to deter-

TABLE II

ANALYSIS OF COMMERCIAL SAMPLES OF DITHRANOL

Solutions prepared for analysis contained 100 μg/ml of dithranol in dichloroethane. Results are presented as mean ± S.E.M. of 3 determinations based on peak areas, and were referenced to the U.S.P. reference standard. Analysis were performed by normal-phase chromatography as described in the Experimental section. ND = Not detected.

Supplier	*Dithranol content (%)*	*Dianthrone content (as %dithranol)*
U.S.P. reference standard	100.0 ± 3.1	ND
Bleakley	84.4 ± 1.1[a]	7.1 ± 0.2
Hartington	101.1 ± 5.2	ND
Hilditch-Vine	96.6 ± 1.7	ND
Prosana	97.3 ± 3.9	ND

[a] $p < 0.01$:significantly different from the U.S.P. reference standard using the two-tailed Student *t*-test.

TABLE III

ANALYSIS OF COMMERCIAL DITHRANOL PRODUCTS

Cream and ointment samples were extracted as described in the Experimental section (*Extraction procedures*). Analyses were performed by reversed-phase LC. The results are expressed as mean ± S.E.M. for 5 determinations. ND = Not detected.

Product and batch No.	*Labelled dithranol (%, w/w)*	*Dithranol recovered (%)*	*Dianthrone recovered (as %dithranol)*	*Total recovery (%)*
Dithrocream B. CHK 84	0.1	98.0 ± 1.1	5.0 ± 0.7	103.0 ± 1.8
Dithrocream B. DHG 84	0.25	104.0 ± 0.7	1.9 ± 0.1	105.9 ± 0.8
Psoradrate cream B. EB 4032	0.1	92.0 ± 0.4	ND	92.0 ± 0.4
Psoradrate cream B. EA 4014	0.2	86.8 ± 1.5	17.0 ± 2.3	103.8 ± 3.8

mine their dithranol content (Table III). The quantities of degradation products were also determined. While no danthron could be detected in any of the products, varying amounts of dianthrone were observed in all products with the exception of Psoridrate (0.1%) cream. Apart from Psoridrate (0.1%) cream, the amounts of dianthrone present in the products could account for the apparent loss of dithranol. In most cases the total recovery (in the form of either dithranol or its degradation products) exceeded 100% of the specified amount of dithranol. This may be indicative of the presence of an undeclared overage of dithranol.

DISCUSSION

The reversed-phase and normal-phase LC assays developed in this study enabled the complete separation of dithranol and its degradation products danthron and dianthrone at ambient temperatures. The maintenance of anhydrous conditions during normal-phase chromatography ensured that retention times remained reproducible. Superior resolution of dithranol and danthron and lower minimum detectable limits were achieved with the normal-phase system than attained using the reversed-phase assay. Despite the obvious advantages associated with the normal-phase LC techniques, reversed-phase chromatography remains not only an invaluable confirmatory assay but also an essential method for the analysis of samples with an aqueous content.

The extraction of dithranol (and its degradation products) from pharmaceutical cream and ointment samples was achieved using dichloroethane. Prior stability studies indicated that in the absence of light, dithranol, dianthrone and danthron were stable for at least 30 h at room temperature. Although dichloroethane provided an efficient extraction medium for the complete dispersion of ointment samples (oleaginous systems) by simple sonication, cream bases could not be effectively dispersed by this method. Consequently, high-speed homogenisation was used to achieve satisfactory

dissipation of cream-based formulations. Using the extraction methods described, the overall recoveries of dithranol achieved from all commercial preparations examined in our studies exceeded 95%. Detailed studies on Psorin® ointment also indicated highly efficient recoveries for the degradation products danthron (100%) and dianthrone (93%). A critical comparison of these extraction efficiencies with those of previously reported methodologies[10–12,14] is difficult as recoveries have not been adequately documented. In contrast to the method of Caron and Shroot[10] the chromatographic systems developed in our study allow direct analysis of the undiluted dichloroethane extracts.

The analysis of several commercial dithranol samples which serve as starting materials for the manufacture of topical dithranol-containing pharmaceutical products indicated that the level of purity of the compound obtained from different sources may vary. While the majority of sources were found to supply high-purity dithranol, the material obtained from Bleakley contained less than 85% dithranol. The fact that the sample also contained substantial amounts of dianthrone (7%) indicated that degradation of dithranol had occurred either during synthesis or subsequent storage of the compound.

Analyses performed on a number of commercial dithranol-containing pharmaceutical products indicated that in most of these products dithranol had undergone degradation with the formation of significant amounts of dianthrone. Danthron was not detected in any of the products analysed. The LC techniques described in the present study have provided the basis for the development of assays for dithranol and its degradation products both in the raw material state and in complex formulations.

REFERENCES

1 D. C. Gorsulowski, J. J. Voorhees and C. N. Ellis, *Arch. Dermatol.*, 121 (1985) 1509.
2 H. M. Elsabbagh, C. W. Whitworth and I. C. Schramm, *J. Pharm. Sci.*, 68 (1979) 338.
3 A. Segal, C. Katz and B. L. Van Duuren, *J. Med. Chem.*, 14 (1971) 1152.
4 T. Melo E Sa, L. Dubertret, P. Prognon, A. Gond, G. Mahuzier and K. Santus, *J. Invest. Dermatol.*, 80 (1983) 1.
5 K. K. Mustakallio and U. Lamminsivu, *Br. J. Dermatol.*, 105 (Suppl. 20) (1981) 54.
6 L. Juhlin and B. Shroot, *Acta. Derm. Venereol.*, (Suppl. 120) (1985) 27.
7 *British Pharmacopoeia*, University Press, Cambridge, 1980.
8 *United States Pharmacopeia*, Mack Publishing, Easton, PA, XXth revision, 1980.
9 P. Prognon, A. Gond, L. Dubertret and G. Mahuzier, *Ann. Pharm. Fr.*, 40 (1982) 329.
10 J. C. Caron and B. Shroot, *J. Pharm. Sci.*, 70 (1981) 1205.
11 A. Schaltegger, U. Bloch and A. Krebs, *Dermatologica*, 165 (1982) 363.
12 F. W. Burton and R. R. Gadde, *J. Chromatogr.*, 328 (1985) 317.
13 D. W. Newcombe, *Pharm. J.*, 233 (1984) 800.
14 M. Whitefield, G. M. A. Leeder and A. R. Mosedale, *Pharm. J.*, 234 (1985) 223.

Journal of Chromatography, 467 (1989) 423–429
Elsevier Science Publishers B.V., Amsterdam — Printed in The Netherlands

CHROM. 21 377

Note

Packed-column supercritical fluid chromatographic separation of highly explosive compounds

W. H. GRIEST*, C. GUZMAN[a] and M. DEKKER[b]

Analytical Chemistry Division, Oak Ridge National Laboratory, P.O. Box 2008, Bldg. 4500-S, MS-6120, Oak Ridge, TN 37831-6120 (U.S.A.)

(Received December 12th, 1988)

Supercritical fluid chromatography (SFC) is complementary to gas chromatography (GC) and high-performance liquid chromatography (HPLC) because of its ability to mobilize compounds not readily chromatographed by GC and the greater ease by which it can be interfaced with GC-like ionization detectors and mass spectroscopy[1,2] than can HPLC. A case in point is highly explosive compounds, including nitrosubstituted aromatic hydrocarbons, nitramines, and nitroesters. The thermal lability of these compounds limits the applicability of GC and they are traditionally analyzed using reversed-phase HPLC[3]. The feasibility of applying SFC to high explosives is suggested by the work of West and Lee[4] in the separation of nitro-substituted polycyclic aromatic hydrocarbons and the separation of high molecular weight, nitro-substituted dyes by Jackson and Later[5] using capillary column SFC with carbon dioxide and nitrogen-selective thermionic detectors or pentane and UV absorbance detection, respectively. Chromatograms showing the SFC of several high explosives have been published in a book of chromatograms[6] from the 1988 Workshop on Supercritical Fluid Chromatography. As far as we can determine, this paper is the first report of a packed-column SFC separation of highly explosive compounds and their manufacturing byproducts, and the first report of the SFC of N-methyl-N,2,4,6-tetranitroaniline and pentaerytheritoltetranitrate. The results indicate that SFC can supplant HPLC as an analytical tool for high explosives.

EXPERIMENTAL

Equipment

The SFC system was a Suprex (Pittsburgh, PA, U.S.A.) Model SFC 200A equipped with an electrically actuated 1-μl Valco injection valve, a 250 mm × 1 mm I.D. Deltabond Cyano column with 5-μm particles (Keystone Scientific, State College, PA, U.S.A.), a Kratos Model 757 variable-wavelength UV absorbance detector with a 12-μl flowcell, and a flame ionization detector arranged in series. A 150-mm column of Deltabond Cyano phase also was used in some experiments. The injection valve was

[a] Historically Black College or University Program student participant, Catholic University of Puerto Rico.

[b] Grant Lakes Collegiate Association student participant, Earlham College, Richmond, IN.

0021-9673/89/$03.50

maintained at room temperature by pumping water through the cooling jacket with a laboratory pump. A tapered restrictor was drawn at the tip of the 25 μm I.D. fused-silica flame ionization detector interface tubing to achieve a gaseous flow-rate of *ca.* 30 ml/min, and a breakthrough time of 1.12 min with carbon dioxide at 162 atm and 100°C. The flame ionization detector was held at 350°C. SFC was performed using carbon dioxide at a column oven temperature of 100°C and a pressure program of 162 atm (0.607 g/cm^3) held for 1 min, programmed to 250 atm (0.822 g/cm^3) over 13 min (6.77 atm/min), held at 250 atm for 1 min, and programmed to 350 atm (0.906 g/cm^3) over 15 min (6.67 atm/min). Only the UV absorbance detector was used in this work. The 1-V signal of the UV detector output was collected with an IBM XT personal computer equipped with a Cyborg (Newton, MA, U.S.A.) 411 interface and an I150 16-bit board, and was processed using Maxima 2.0 software (Dynamic Solutions, Ventura, CA, U.S.A.). The data collection rate was 3 points/s.

Materials

The SFC-grade carbon dioxide was purchased from Scott Specialty Gases (Plumstead, PA, U.S.A.) in an aluminum cylinder with a helium-pressurized headspace, and was used as received. All highly explosive compounds and byproducts were obtained from the Picatinny Arsenal (Dover, NJ, U.S.A.) in their Standard Analytical Reference Material grade. The compounds and their abbreviations are 2,6-dinitrotoluene (2,6-DNT), 2,4-dinitrotoluene (2,4-DNT), 2,4,6-trinitrotoluene (TNT), trinitroglycerin (NG), pentaerytheritoltetranitrate (PETN), N-methyl-N-2,4,6-tetranitroaniline (TETYRYL), hexahydro-1,3,5-trinitro-1,3,5-triazine (RDX), and octahydro-1,3,5,7-tetranitro-1,3,5,7-tetrazocine (HMX). TNT, 2,6-DNT, 2,4-DNT, TETRYL, and RDX were used without further purification to prepare stock solutions of *ca.* 1 mg/ml in acetonitrile, and dilutions in the range 0.5–20 μg/ml in methylene chloride. The NG and PETN were prepared from older stock solutions in ethanol, and their concentrations were approximately 4 and 8 times (respectively) those of the other explosives. The standards were stored in the dark at 1°C. All solvents were distilled in glass grade from Burdick and Jackson (Muskegon, MI, U.S.A.).

RESULTS AND DISCUSSION

Fig. 1 demonstrates that different chemical classes of highly explosive compounds and their manufacturing byproducts (*i.e.*, nitrosubstituted aromatics, nitroesters, and nitramines) can be successfully chromatographed and separated using packed-column SFC with a carbon dioxide mobile phase. With the exception of the latest-eluting compound, RDX, the peak shapes are reasonably symmetrical and the resolution is good. Retention times, capacity factors, selectivity, and peak resolution are listed in Table I. To our knowledge, this is the first report on the SFC of TETRYL and PETN, and the first report of packed-column SFC for any high explosives.

The elution order 2,6-DNT < 2,4-DNT < NG < TNT < PETN < TETRYL < RDX < HMX is generally in increasing polarity and molecular weight, as might be expected for a mobile phase with no dipole moment[2]. The 2,4-DNT is retained more than the 2,6-isomer, probably reflecting the steric hindrance of the methyl group upon the interaction of the two neighboring nitro groups in the latter with the stationary phase. NG and TNT, with three nitro-groups, are retained further. PETN and

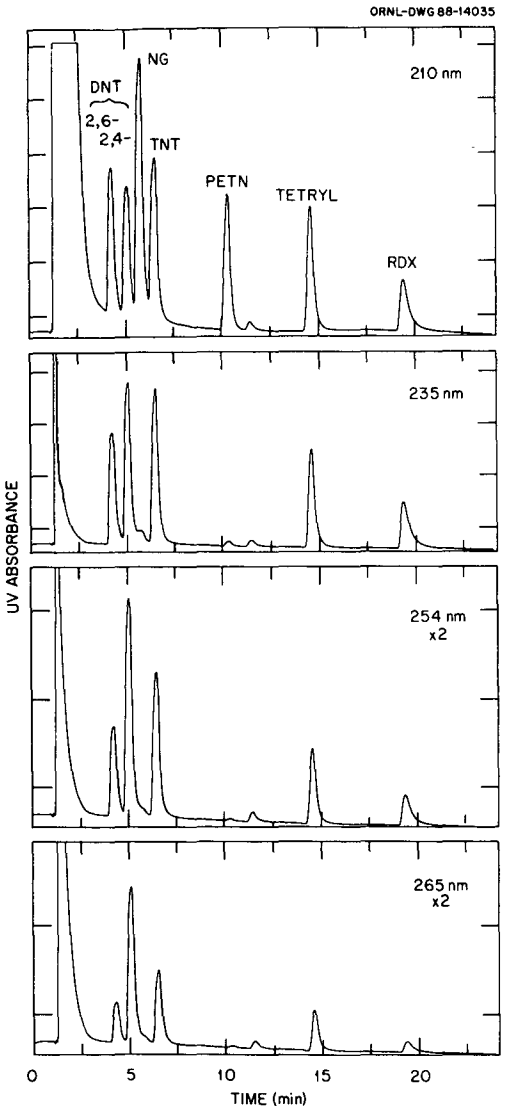

Fig. 1. Packed-column SFC of highly explosive compounds with UV absorbance detection at 210, 235, 254 and 265 nm. Vertical scale expanded two-fold at 254 and 265 nm. Abbreviations listed in Experimental.

TETRYL each have four nitro-groups and elute even later. RDX elutes after TETRYL, yet it contains only three nitro-groups. Its strong retention perhaps is conferred by the polarity from the heterocyclic nitrogen. Under the conditions used for these experiments, HMX, which contains an additional nitro-group and in-ring nitrogen and methylene, would not elute from the 250-mm column. In earlier work, a non-reproducible, tailing chromatographic peak for HMX eluted after RDX on the 150-mm column. These observations suggest that carbon dioxide is not sufficiently

TABLE I
CHROMATOGRAPHIC DATA FOR HIGH EXPLOSIVES AND BYPRODUCTS

Compound	*Retention time (min)*	*Capacity factor*[a], *k'*	*Selectivity*[b], *α*	*Resolution*[c], *R*
2,6-DNT	4.32	2.86		
2,4-DNT	5.12	3.57	1.28	1.33
NG	5.81	4.19	1.17	1.06
TNT	6.54	4.84	1.16	1.12
PETN	10.33	8.22	1.70	6.32
TETRYL	14.61	12.04	1.46	6.58
RDX	19.43	16.35	1.36	5.67

[a] $k' = (t_R - t_0)/t_0$, where t_R = retention time of the compound and t_0 = retention time of the leading edge of the solvent peak.
[b] $\alpha = (t_{R2} - t_0)/(t_{R1} - t_0)$, where t_{R2} = retention time of the later-eluting compound.
[c] $R = (t_{R2} - t_{R1})/(w_2 + w_1)$ (0.5), where w = peak width at the baseline.

polar to efficiently mobilize HMX in packed columns, which are recognized[7] to be more active than capillary columns. Experiments are under way with polar modifiers such as hexanol which have been found[8,9] to mask the activity of the silica surface and improve the solubilizing characteristics of carbon dioxide. The success of capillary columns in eluting HMX with carbon dioxide at lower densities[6] indicates that the former is probably the predominant factor limiting the packed column. Although the Deltabond cyano phase has been shown[10] to be far superior to conventional, non-crosslinked cyano phases for the SFC of basic nitrogen-containing compounds, there appears to be a residual silanol activity for nitramines.

It is significant that the elution order of the explosives by SFC on the Deltabond cyano phase is similar to that reported[3] for HPLC on a cyanopropyl stationary phase using a reversed-phase eluent of water–methanol (50:50, v/v), which is considerably more polar than carbon dioxide. The elution order in HPLC is almost reversed when an octadecylsilane phase is used[3]. This suggests that interactions with the cyano groups in the stationary phase are quite selective among the chemical types represented in these classes of explosive compounds, regardless of the physical state of the mobile phase. The strong retention of TETRYL, RDX, and HMX both in SFC and HPLC on the cyano phase is consistent with unpublished data from D. C. Leggett (noted by Jenkins and Walsh[3]) showing that the solubilities of nitramines are increased 20- to 30-fold in acetonitrile *versus* methanol.

It is evident that the SFC separation is less rapid but more selective than the HPLC separation. The capacity factors of the explosives range from 2.86 to 16.4 for SFC *versus* from 1.37 to 2.28 for HPLC[3]. The SFC separation is *ca.* two-fold longer than the HPLC separation under these conditions. However, SFC is more selective. For example, the selectivity for the pair 2,6-DNT/2,4-DNT is 1.28 for SFC *versus* 1.08 for HPLC[3] and for 2,4-DNT/TNT the corresponding selectivities are 1.51 *versus* 1.05 for SFC and HPLC, respectively. The greater retention and selectivity of the SFC probably reflects the lesser polarity of carbon dioxide *versus* methanol–water. Use of a binary mobile phase in SFC would be expected to decrease the capacity factor and the selectivity, and facilitate the efficient elution of the HMX.

The reproducibility of the packed-column SFC separation is quite good considering the critical requirement for precise pressure/density control over hundreds of atm of programmed mobile phase density. The retention time reproducibility was determined for ten analyses employing six concentration levels of the seven high explosives at 210 nm. The reproducibility, as expressed by the relative standard deviation of the retention times for each compound, was only 0.2–0.3%. This level of precision was readily repeatable on a daily basis. This is equivalent to that reported by other workers[10] using packed-column SFC. Over longer periods of time, however, there is a gradual drift of retention times. The retention time of TNT increased 1.2% over a period of five days of heavy instrument use, and over nineteen days, the retention time increased by 3.3%. This increase in retention is attributed to a slow accumulation of material in the tapered restrictor opening. The net effect would be to decrease the mobile phase flow-rate under pressure-controlled conditions. Increasing the temperature of the restrictor might reduce this effect. The peak area reproducibility was investigated only briefly. The relative standard deviations of the peak areas for the compounds in the 20 μg/ml standard run three times at 210 nm ranged from 0.18% for 2,6-DNT to 2.8% for TETRYL. Inclusion of a greater number of runs probably would decrease the relative standard deviations, but this degree of precision appears to be typical[10].

The UV absorbance detector is well suited for determination of the highly explosive compounds. Fig. 1 shows the separations recorded at 210, 235, 254, 265, 280, and 290 nm. At 210 nm, all seven compounds are detected, but the tail of the solvent peak intrudes into the chromatogram to a much greater extent than at the other wavelengths. This causes a serious downward baseline drift at high sensitivites. At 235 nm, the solvent peak tail is greatly diminished and the nitroesters are barely detectable because they lack the strong UV chromophore of the aromatic group in the nitrotoluenes. However, the nitrotoluenes, nitroaniline, and nitramines are detected with nearly the same sensitivity as at 210 nm, as demonstrated by the peak area ratios plotted in Fig. 2. In fact, for 2,4-DNT, the sensitivity at 235 nm is greater than that at 210 nm. At 254 nm, the NG and PETN are relatively undetectable. The optimum

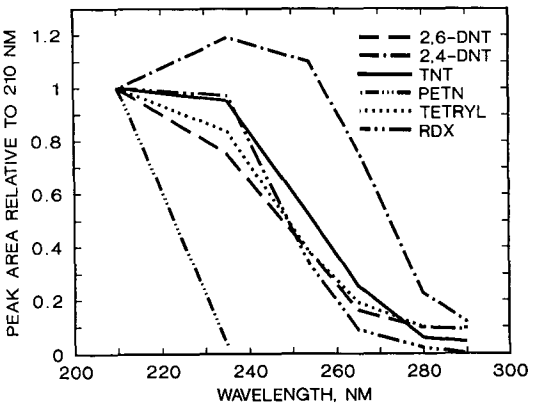

Fig. 2. Sensitivities of UV absorbance detection relative to 210 nm for highly explosive compounds at 210, 235, 254, 265, 280 and 290 nm.

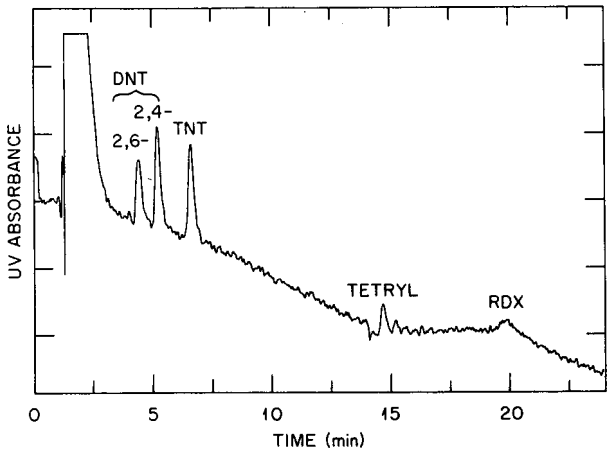

Fig. 3. SFC of lowest concentration standard (0.5 μg/ml, except for *ca.* 2 μg/ml of NG and *ca.* 4 μg/ml of PETN) with UV absorbance detection at 235 nm.

wavelength for detection would depend upon a number of sample- and analyte-specific factors, but 235 nm appears to offer good sensitivity and greater selectivity if NG and PETN are not sought. A chromatogram of the lowest concentration standard [0.5 μg/ml of all compounds except NG (*ca.* 2 μg/ml) and PETN (*ca.* 4 μg/ml)] recorded at 235 nm is shown in Fig. 3. The limits of detection estimated for a signal-to-noise ratio of 4 are 0.33 μg/ml for 2,6-DNT, 0.21 μg/ml for 2,4-DNT, 0.22 μg/ml for TNT, and 0.9 μg/ml for TETRYL. These are *ca.* 10-fold higher than the lowest reported[3] concentrations detected by HPLC with UV detection at 254 nm using a fixed-wavelength detector and a 100-μl injection volume. The much greater injection volume and probably greater source intensity of the fixed-wavelength detector may account for this difference in sensitivities.

Applications of the SFC technique to real-world samples have only been briefly tested. A 5-g soil sample known to be contaminated with explosives was extracted ultrasonically for 18 h in 40 ml of acetonitrile[3], and a portion of the extract, solvent-exchanged into methylene chloride, was injected into the SFC. No chromatographic peaks corresponding to explosive compounds were detected, and when an explosives standard was injected immediately afterward, the peak shapes and responses were badly degraded. Washing the column with carbon dioxide for several hours failed to regenerate the separation. This observation suggests that the soil sample extract contaminated the column and that carbon dioxide alone was insufficiently polar to clean out the contaminants. More polar mobile phases or sample pretreatments may be required to make packed column SFC more useful for the analysis of complex samples which contain polar, high molecular weight extraneous matter.

CONCLUSIONS

SFC can achieve good separations of explosive compounds and their by-products. Further work must focus on the selection of mobile phase modifiers to

extend the range of compounds (*e.g.*, HMX) which can be readily eluted from packed columns and to alleviate the effects of extraneous sample matrix components. More inert capillary columns may extend the elution range with carbon dioxide without modifiers. Sample pretreatments or chemical class isolations also may be necessary for analysis of complex environmental sample matrices.

ACKNOWLEDGEMENT

Oak Ridge National Laboratory is operated by Martin Marietta Energy Systems, Inc., under contract DE-AC05-840R21400 with the U.S. Department of Energy.

REFERENCES

1 M. L. Lee and K. E. Markides, *Science*, 235 (1987) 1342–1347.
2 *Supercritical Fluid Chromatography (SFC): Bridging the Gap Between GC and HPLC*, Technical Notes 925, Brownlee Labs, Inc., Santa Clara, CA, November, 1986.
3 T. F. Jenkins and M. E. Walsh, *"Development of an Analytical Method for Explosive Residues in Soil"*, *CRREL Report 87-7*, U.S. Army Gold Regions Research & Engineering Laboratory, Hanover, NH, June, 1987.
4 W. R. West and M. L. Lee, *J. High Resolut. Chromatogr. Chromatogr. Commun.*, 9 (1986) 161–167.
5 W. P. Jackson and D. W. Later, *J. High Resolut. Chromatogr. Chromatogr. Commun.*, 9 (1986) 175–177.
6 K. Markides and M. L. Lee (Compilers), *SFC Applications*, Brigham Young University Press, Provo, UT, 1988, pp. 175–177.
7 S. K. Yarbro and D. R. Gere, *Chromatography*, April (1987) 49–55.
8 J. M. Levy and W. M. Ritchey, *J. Chromatogr. Sci.*, 24 (1986) 242–248.
9 A. L. Blilie and T. Greibrokk, *Anal. Chem.*, 57 (1985) 2239–2242.
10 M. Ashraf-Khorassani, L. T. Tayor and R. A. Henry, *Anal. Chem.*, 60 (1988) 1529–1533.

Journal of Chromatography, 467 (1989) 430–435
Elsevier Science Publishers B.V., Amsterdam — Printed in The Netherlands

CHROM. 21 360

Note

High-performance liquid chromatography as an alternative to microbiological measurements in the assay of tetracyclines

AVA RAY* and ROY HARRIS

Department of Chemistry, National Institute for Biological Standards and Control, Blanche Lane, South Mimms, Potters Bar, Hertfordshire EN6 3QG (U.K.)

(First received November 7th, 1988; revised manuscript received January 30th, 1989)

There has recently been a move to replace expensive biological assays by chemical assays, *e.g.* high-performance liquid chromatography (HPLC). This is the case for some antibiotics such as the tetracyclines[1]. It has already been shown that comparable results can be obtained by HPLC and bioassay for the measurement of oxytetracycline from various sources[2]. Having shown that this HPLC method[2] is acceptable for straightforward assays it is important to see if it is robust enough for assaying samples kept under extreme conditions. Degradation in the samples should be equally reflected by bioassay and HPLC.

This report describes the adaptations of the previous HPLC method mentioned above, *e.g.*, flow-rate, temperature and column packing, to look at tetracyclines kept at elevated temperatures as part of an accelerated degradation experiment[3,4] and assayed by HPLC and bioassay. The reliability of the HPLC assay was also tested by the comparison of data for the same samples assayed after a three year shorter storage period.

EXPERIMENTAL

The compounds assayed were seven different tetracycline standards stored in ampoules under nitrogen at +20°C, +37°C or +56°C: chlortetracycline, 2nd International Standard (IS) (CTC); oxytetracycline, 1st IS (OTC); tetracycline, 2nd IS (TC); demeclocycline, 1st International Reference Preparation (IRP) (DEM); methacycline, 1st IRP (MET); minocycline, 1st IRP (MIN) and doxycycline, 1st IRP (DOX).

Stock solutions of tetracyclines, with the exception of OTC, were prepared in HPLC-grade water (250 μg ml^{-1}) and were either used directly for HPLC analysis or diluted in phosphate buffer (pH 6.0) for use in the biological assays. OTC was made up in 5 ml of 0.1 *M* hydrochloric acid and diluted to 100 ml with HPLC-grade water.

Biological assays were carried out using *B. pumilis* NCTC 8241, following the method recommended by the British Pharmacopoeia[5].

Samples were assayed chemically using an adaptation of a previously reported HPLC method[2] adapted in our laboratory. The HPLC system consisted of a Spectra-Physics SP8100 liquid chromatograph equipped with an SP8110 autosampler and an

0021-9673/89/$03.50

SP8440 variable-wavelength detector. An SP 4200 computing integrator was used to calculate peak areas and heights. Samples (2.5 μg in 10 μl) were chromatographed on a Spherisorb ODS-2 (5 μm) column (250 × 4.6 mm I.D.) (Phase Separations, Gwent, U.K.) maintained at 40°C and detected at 280 nm. The solvent system, 0.2 *M* ammonium oxalate–0.1 *M* NaEDTA–dimethylformamide (55:20:25, v/v/v) was degassed with helium and pumped at a flow-rate of 1 ml min^{-1} except in the cases of CTC and MIN where flow-rates of 1.2 ml min^{-1} and 1.5 ml min^{-1} respectively were used in order to reduce retention times. Each sample was chromatographed six times. Results from HPLC data were calculated as follows: (area of tetracycline peak in the sample/area of tetracycline peak in the standard) · labelled potency of standard and will be referred to hereafter as "potency" of sample notionally as IU mg^{-1}. Ratios were calculated for both types of assay relative to standard preparations stored continuously at −20°C.

RESULTS AND DISCUSSION

For most of the samples the HPLC and microbiological assay results were in good agreement. "Potency" values calculated for chemical and biological assays are shown in Table I. Since a linear relationship exists between tetracycline content measured by either area or height of the HPLC peak (see Fig. 1, correlation coefficient = 0.99), only integration values for areas were used in Table I. The relationship between HPLC and bioassay results are shown graphically in Fig. 2 which shows a correlation between the methods within acceptable limits (correlation coefficient = 0.96). The HPLC data were compared with HPLC results obtained for the same samples 3 years previously. When there was no degradation, the results are reproducible (Table II); where samples

TABLE I
COMPARISON OF "POTENCY" VALUES OBTAINED BY BIOASSAY AND HPLC
Average storage period = 20 years.

Compound (potency of standard IU mg^{-1})	*Storage temperature (°C)*	*"Potency" mean as calculated by HPLC peak area (IU mg^{-1})*	*Bioassay (IU mg^{-1}) Mean (with fiducial limits)*
CTC (1000)	20	1011.5	1022 (899.2–1164.2)
	37	943.8	889 (778.1–1009.8)
OTC (900)	20	880.9	828 (791.0–866.9)
	37	679.5	638 (607.3–670.1)
TC (982)	37	988.8	1007 (958.2–1058.5)
	56	990.3	983 (935.0–1032.9)
DEM (1000)	20	996.2	978 (939.8–1017.9)
	37	1016.5	1020 (980.0–1061.7)
MET (924)	37	928.0	952 (922.9–992.6)
	56	942.3	925 (892.1–959.3)
MIN (863)	37	797.2	868 (843.0–894.8)
	56	536.2	593 (579–608.7)
DOX (870)	37	854.5	856 (833.7–878.2)
	56	848.3	831 (809.6–853.0)

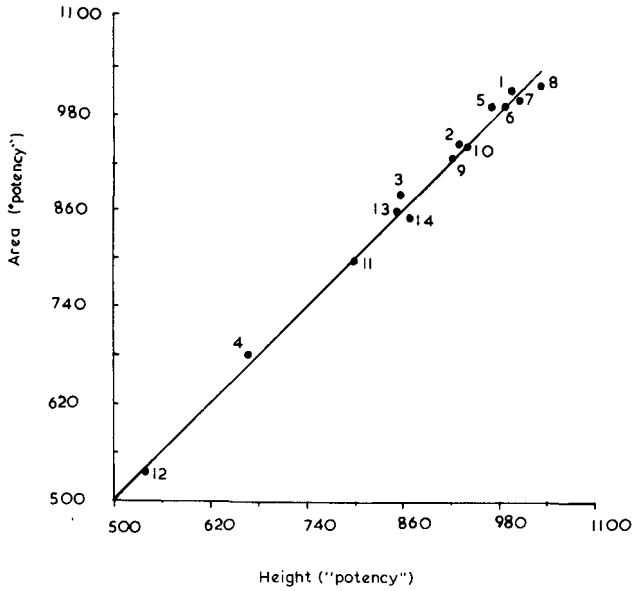

Fig. 1. Graph to show the linear relationship between "potency" means calculated by HPLC peak areas and peak heights for seven tetracyclines stored at elevated temperatures. CTC: 20°C(1), 37°C(2). OTC: 20°C(3), 37°C(4). TC: 37°C(5), 56°C(6). DEM: 20°C(7), 37°C(8). MET: 37°C(9), 56°C(10). MIN: 37°C(11), 56°C(12). DOX: 37°C(13), 56°C(14).

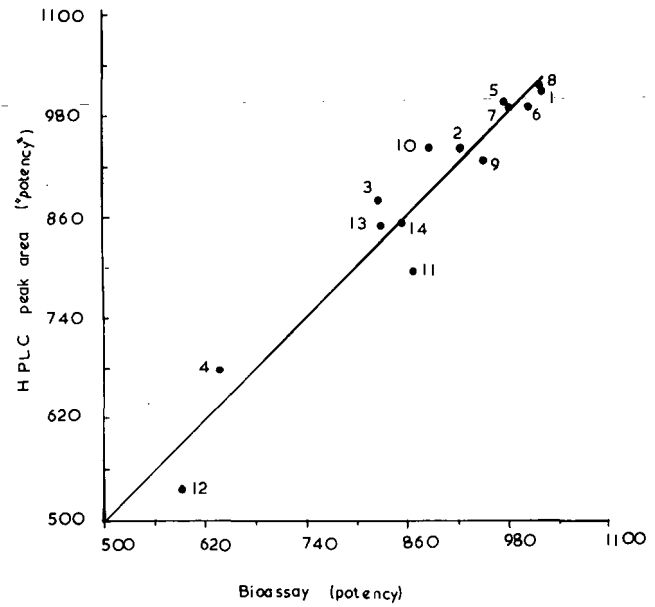

Fig. 2. Graph to show the comparison of "potency" values obtained by bioassay and those calculated from HPLC peak areas (see Table I). CTC: 20°C(1), 37°C(2). OTC: 20°C(3), 37°C(4). TC: 37°C(5), 56°C(6). DEM: 20°C(7), 37°C(8). MET: 37°C(9), 56°C(10). MIN: 37°C(11), 56°C(12). DOX: 37°C(13), 56°C(14).

TABLE II

COMPARISON OF "POTENCY" VALUES CALCULATED FROM HPLC DATA OBTAINED FROM THE PRESENT EXPERIMENT AND FROM HPLC ANALYSIS CARRIED OUT IN 1985 USING THE SAME SAMPLES

Sample (potency of standard IU mg^{-1})	*Storage temperature (°C)*	*Present experiments (calculated from peak area)*	*1985 experiments (calculated from peak area)*
CTC (1000)	20	1011.5	1001.0
	37	943.8	938.0
OTC (900)	20	880.9	873.9
	37	679.5	784.8[a]
TC (982)	37	998.8	986.9
	56	990.3	968.2
DEM (1000)	20	996.2	1014.0
	37	1016.5	1013.0
MET (924)	37	928.0	926.7
	56	942.3	899.0
MIN (863)	37	797.0	839.8[a]
	56	536.0	633.4[a]

[a] In these cases degradation has obviously occurred. For all other experiments the coefficients of variation between the mean of the two values are within 2%.

had degraded over the 3-year period, for example OTC and MIN, this was obvious from the peak area values.

The main advantage of a chemical assay is that results can be obtained rapidly. The retention times of the tetracycline samples on the column were short with a maximum run time of 17 min (flow-rate, 1.5 ml min^{-1}) being required in the case of MIN. Replicates of samples and standards could be run in a few hours. This compares favourably with the overnight incubation required with the microbiological assay. With the HPLC assay the degree of degradation can be calculated immediately by comparison of the integration values of the standard material and the test. Establishing degradation with the bioassay is more complicated. A degraded sample compared to the standard will give a potency ratio of less than 1 by bioassay, which will make the assay statistically unacceptable. To check the robustness of the assay, the procedure can then be repeated using an adjusted assumed potency value for the degraded sample. If this gives a potency ratio close to 1, it can be assumed that the decreased potency of the test sample is due to degradation and not to errors in the assay system. This was exemplified in the case of MIN. A further problem which may arise when using bioassay to measure degradation is that the degradation product(s) may also have antimicrobial properties and the results of the bioassay will not be a true representation of the antimicrobial potency of the original material. Degradation products are less likely to confuse the results of the HPLC analysis. The degradation products were not observed by HPLC analysis either because they might be absorbed on the column and not eluted or because breakdown may affect the UV absorbing properties of the resulting products. Degradation is thus most clearly observed through lower integration values for peak areas and peak heights and smaller peaks on a chromatogram (Fig. 3). Therefore the complex adjustments to the bioassay

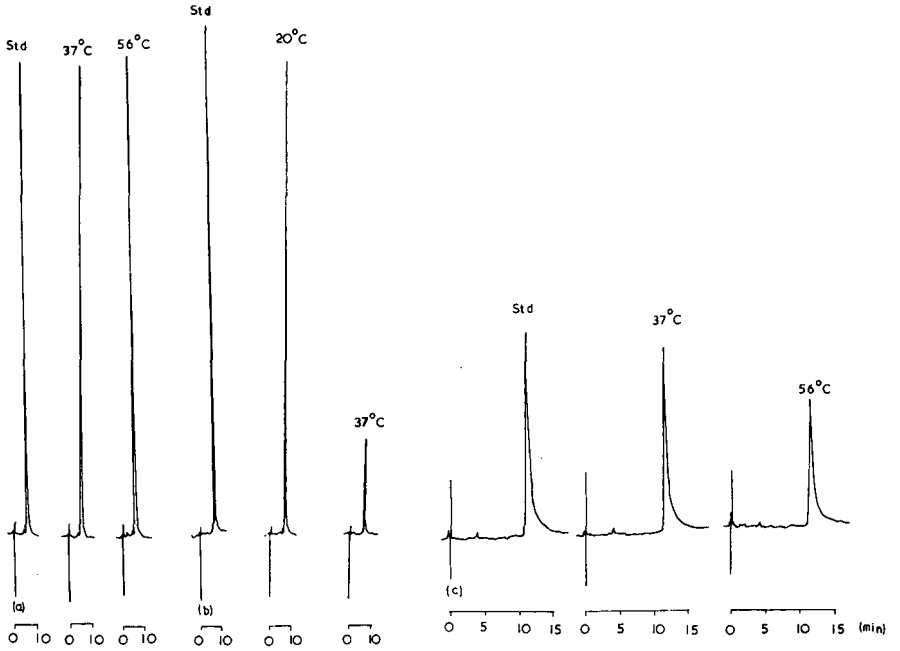

Fig. 3. Chromatograms of (a) TC showing no degradation, (b) OTC and (c) MIN both showing increased degradation at elevated temperatures. Std = standard stored at −20°C; wavelength = 280 nm; a.u.f.s. = 0.16.

procedure required for degraded compounds are not needed for HPLC assay, making the latter a more rapid and cost-effective method.

From Table I it can be seen that with the exception of OTC (stored at 37°C) and MIN, the tetracycline preparations show little significant degradation at elevated storage temperatures. The table shows however, that the agreement between potency values calculated by HPLC and bioassay for MIN is not as good as that for other preparations. MIN samples stored at 37°C and 56°C had a carbonised appearance and were brown and black respectively as compared with the yellow colour of the standard. The samples were prepared by dissolution in water followed by repeated sonication in order to ensure maximum solubilisation.

From the chromatograms shown in Fig. 3, the decrease in peak height with increase in storage temperature in the cases of OTC and MIN can be seen. The six replicate values for each sample were reproducible with coefficients of variation less than 4%, with the exception of CTC (coefficient of variation, C.V. = 7%). Since no degradation product of MIN was detected by HPLC, a spectrophotometric scan from 190 to 700 nm was carried out and showed no difference in absorption maxima (344, 277 and 247 nm) between the standard and both samples stored at 37°C and 56°C. Thus it seems that at least in the case of MIN, degradation did not lead to any compounds resolved in this HPLC system.

The column is maintained at 40°C during HPLC analysis to prevent the oxalate buffer from precipitating and to improve resolution of the peaks, although analyses can be performed at room temperature provided that the column is thoroughly washed

to prevent blockage with ammonium oxalate and thus reducing unnecessary wear on the pump seals.

The results reported here are in accordance with other comparative studies of HPLC and microbiological assays of tetracycline[6] and other antibiotics[7]. There are many examples in the literature of the use of HPLC for the assay of tetracyclines in animal tissue[6,8] and foodstuffs such as honey[9]. It has been reported[6] that the HPLC assay of CTC in pig tissues proved to be more reliable and offered greater sensitivity than three bioassay techniques. However it should be pointed out that the three microbiological assays: swab-on-premises, microbial inhibitor test and thin-layer chromatography–bioautography, reported by Korsund and MacNeil[6] are not of the same precision as the British Pharmacopoeia recommended bioassay[5] used here and would not therefore be expected to compare favourably with an HPLC assay.

CONCLUSION

The comparative study presented here shows that the chemical assay of members of the tetracycline group has several practical advantages over the bioassay and that the results of both methods are in good agreement (Fig. 2). The HPLC method can be easily adapted for use with several commercial columns by minor adjustments to running conditions such as flow-rate and temperature.

ACKNOWLEDGEMENT

We would like to thank Dr. R.E.G. Das for constructive comments on the manuscript.

REFERENCES

1 *British Pharmacopoeia 1980, Addendum 1982*, HMSO, London, 1982, p. 85, Appendix A, p. A4.
2 W. N. Barnes, A. Ray and L. J. Bates, *J. Chromatogr.*, 347 (1985) 173.
3 M. S. Tydeman and T. B. L. Kirkwood, *J. Biol. Stand.*, 12 (1984) 195.
4 T. B. L. Kirkwood and M. S. Tydeman, *J. Biol. Stand.*, 12 (1984) 207.
5 *British Pharmacopoeia 1988*, Vol. II. HMSO, London, 1988, Appendix XIVA, p. A147.
6 G. O. Korsund and J. D. MacNeil, *Food Addit. Contam.*, 5 (1987) 149.
7 J. Marincel, N. Bosnjak and M. Lamut, *Acta Pharm. Jugosl.*, 38 (1988) 35.
8 R. B. Ashworth, *J. Assoc. Off. Anal. Chem.*, 16 (1985) 1013.
9 H. Oka, Y. Ikai, N. Kawamura, K. Uno, M. Yamada, K.-I. Harada and M. Suzuki, *J. Chromatogr.*, 400 (1987) 253.

Journal of Chromatography, 467 (1989) 436–440
Elsevier Science Publishers B.V., Amsterdam — Printed in The Netherlands

CHROM. 21 338

Note

Separation of intravenous IgG containing albumin by high-performance size-exclusion chromatography on TSKgel G3000SWXL

YOSUKE YAMASAKI* and YOSHIO KATO
TOSOH Corporation, Central Research Laboratory, Tonda, Shinnanyo, Yamaguchi 746 (Japan)
(Received December 19th, 1988)

Intravenous IgG has been widely applied for clinical purposes such as hypo-and agammaglobulinaemia, antibiotic therapy and thrombocytopenia[1–4]. Some of these intravenous IgG contain albumin as a stabilizer and it is therefore important to determine both IgG and albumin for quality control. There have been many reports of the separation of monoclonal IgG and albumin by high-performance liquid chromatography (HPLC), ion-exchange chromatography (IEC)[5–14], hydroxyapatite chromatography (HAC)[15,16], hydrophobic interaction chromatography (HIC)[9] and affinity chromatography (AFC)[17–20]. None of these methods, however, is satisfactory for quality control owing to the long analysis time and complex elution as in the gradient method. On the other hand, size-exclusion chromatography (SEC) has been widely used for quality control purposes owing to its simple operation, in spite of the lower resolution, and it has been employed for the separation of monoclonal antibodies[5,6,21] and immunoglobulin in serum[22]. Although chromatographic variables for protein separation have been extensively studied[23–29], there are no reports of the study of the separation of IgG and albumin by SEC. Lee *et al.*[30] reported the separation of intravenous IgG containing albumin by SEC. However, they removed albumin from the sample by IEC prior to the SEC analysis.

Recently, a new SEC column, TSKgel G3000SWXL, has become commercially available[31]. According to the manufacturer, this column has twice the number of theoretical plates as the conventional G3000SW, and IgG could be separated quantitatively within 15 min. We examined the elution conditions for the separation of IgG and albumin in intravenous IgG by SEC on TSKgel G3000SWXL and the results are reported in this paper.

EXPERIMENTAL

Human IgG was purchased from Miles Labs. (Kankakee, IL, U.S.A.) and human albumin from Sigma (St. Louis, MO, U.S.A.). The intravenous IgG sample Gammagard was obtained from Baxter (Tokyo, Japan), Venilon from Fujisawa Pharm. (Osaka, Japan) and Venoglobulin-I from Green Cross (Osaka, Japan). According to the manufacturers, the ratios of IgG to albumin in the samples were 50:1, 20:1 and 5:1, respectively.

All chromatographic procedures were performed with an HPLC system con-

0021-9673/89/$03.50

sisting of a CCPM pump (TOSOH, Tokyo, Japan), a Model 7125 sample injector (Rheodyne, Cotati, CA, U.S.A.) with a 100-μl sample loop and a UV-8000 detector (TOSOH). UV detection was applied at 280 nm (0.64 a.u.f.s.). The samples were separated on a TSKgel G3000SWXL column (300 × 7.8 mm I.D.) at a flow-rate of 1.0 ml/min; 50 mM sodium phosphate of various pH values containing 0.1 M Na_2SO_4, and the same buffer containing 0.3 M NaCl or 0.3 M $NaClO_4$, were used for the evaluation of the elution conditions. Amounts of 100 μg of IgG and albumin in 100 μl of buffer were separated on the column for evaluation of the elution conditions, and 250 μg of an intravenous IgG sample in 5 μl of solution were separated. The total recoveries were calculated from the peak areas on the chromatograms.

The resolution (R_s) between IgG and albumin was determined using the equation

$$R_s = 2(V_2 - V_1)/[(W_1 + W_2)(\log M_1 - \log M_2)]$$

where V_1 is the elution volume of IgG monomer (ml), V_2 the elution volume of albumin monomer (ml), W_1 the peak width of IgG monomer (ml), W_2 the peak width of albumin monomer (ml), M_1 the molecular mass of IgG monomer (155 000) and M_2 the molecular mass of albumin monomer (67 000).

RESULTS AND DISCUSSION

Fig. 1 shows the dependence of the difference in the elution volumes of IgG and albumin on the pH of the buffer containing three kinds of salts. The ionic strengths of the salts in buffer were adjusted to be the same (*ca.* 0.3), as ionic interactions between the sample and the packing materials were presumed to occur. The difference in the elution volumes of the two proteins was small and was slightly dependent on the pH of the buffer containing 0.3 M NaCl or $NaClO_4$. On the other hand, when 0.1 M Na_2SO_4 was used, the difference in elution volumes was fairly large and was also slightly dependent on the pH of the buffer. The difference in elution volumes increased with decreasing of pH of the buffer from neutral to 5.0, as elution of albumin was delayed. At pH 4.0, however, IgG was eluted as a broad peak and the resolution

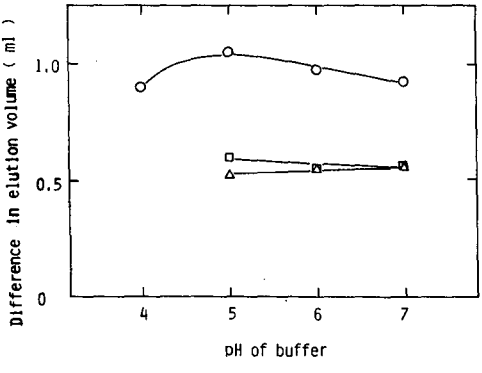

Fig. 1. Dependence of difference in elution volumes of IgG and albumin on pH of buffer on TSKgel G3000SWXL. IgG and albumin were separated with 50 mM sodium phosphate at various pH containing (○) 0.1 M Na_2SO_4, (□) 0.3 M NaCl or (△) 0.3 M $NaClO_4$.

of the two proteins became worse. The change in elution volume suggests that a change in the steric conformation of the proteins or some interaction with the packing materials occurs, depending on the pH of the buffer. It was found that 50 m*M* sodium phosphate (pH 5.0) containing Na_2SO_4 was the optimum elution buffer for the separation of the two proteins. We also examined acetate and citrate buffers containing Na_2SO_4 but a better resolution could not be obtained.

Fig. 2 shows the dependence of the resolution between IgG and albumin on the concentration of Na_2SO_4 in the buffer. Although a buffer of pH 6.8 was also examined, the R_s value could not be determined as it was too low. Fig. 2 indicates that the two proteins could be separated with higher resolution in pH 5.0 than pH 6.0 buffer. The dependence of resolution on the salt concentration in buffer was greater at pH 6.0 than pH 5.0. Accordingly, the optimum concentration of Na_2SO_4 was found to be 0.1 *M* in both buffers, where the ionic interaction of the sample with the packing materials would be negligible. At a 0.2 *M* concentration of Na_2SO_4 the R_s value was lower, which suggests a hydrophobic interaction of the sample with the packing material. Above 0.5 *M* Na_2SO_4, IgG showed a broad peak and the R_s value could not be determined. The resolution also decreased with salt concentrations below 0.1 *M*, which suggests an ionic interaction between the proteins and the packing material. Accordingly, the optimum separation buffer for the two proteins was found to be 50 m*M* sodium phosphate (pH 5.0) containing 0.1 *M* Na_2SO_4.

Figs. 3–5 show comparisons of the separation of intravenous IgG with conventional and optimum elution conditions. The sample in Fig. 3 contains a trace amount of albumin (IgG: albumin = 50:1). Albumin in the sample was recognized as a small peak under the optimum conditions, in spite of a shoulder obtained with conventional eluents. The separation was completed within 15 min. The recovery was 96% under the optimum conditions.

Fig. 4 shows the separation of intravenous IgG containing albumin (IgG: albumin = 20:1). The albumin peak appeared clearly under the optimum conditions and the peak was also recognized with the conventional eluents. The recovery was 92% under the optimum conditions.

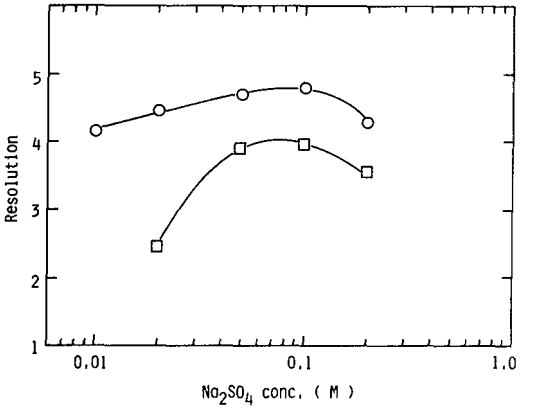

Fig. 2. Dependence of resolution between IgG and albumin on concentration of Na_2SO_4 in buffer on TSKgel G3000SWXL. IgG and albumin were separated with 50 m*M* sodium phosphate at (○) pH 5.0 or (□) pH 6.0 containing various concentrations of Na_2SO_4.

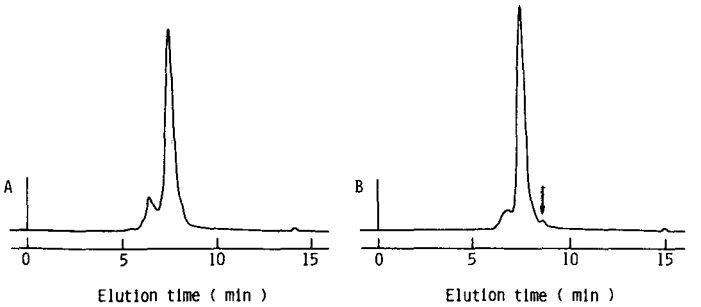

Fig. 3. Separation of intravenous IgG containing albumin by high-performance SEC on TSKgel G3000SWXL: 5 μl (250 μg) of Gammagard were separated with (A) 50 m*M* sodium phosphate (pH 6.7) containing 0.3 *M* NaCl or (B) 50 m*M* sodium phosphate (pH 5.0) containing 0.1 *M* Na_2SO_4 at a flow-rate of 1.0 ml/min at 25°C. UV detection at 280 nm. Total recoveries were (A) 102% and (B) 96%.

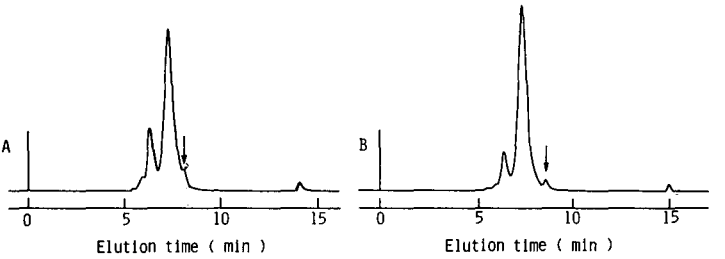

Fig. 4. Separation of intravenous IgG containing albumin by high-performance SEC on TSKgel G3000SWXL: 5 μl (250 μg) of Venilon were separated. Conditions as in Fig. 3. Total recoveries were (A) 94% and (B) 92%.

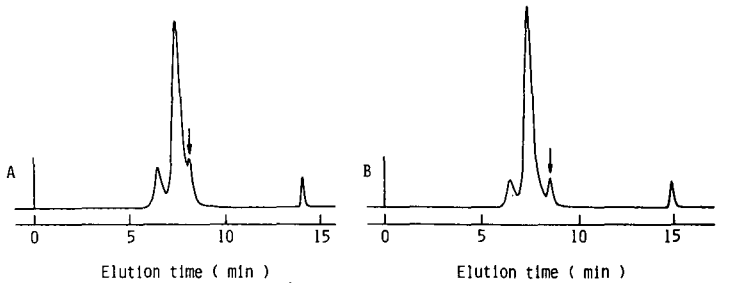

Fig. 5. Separation of intravenous IgG containing albumin by high-performance SEC on TSKgel G3000SWXL: 5 μl (250 μg) of Venoglobulin-I were separated. Conditions as in Fig. 3. Total recoveries were (A) 100% and (B) 101%.

In Fig. 5, intravenous IgG (IgG: albumin = 5:1) occurs as a sharp albumin peak under the optimum conditions. The recovery was quantitative. In addition, IgG monomer and dimer were also separated well in all the chromatograms. The compositions of the dimer and monomer, however, differed slightly with the two elution conditions. An intermolecular change in IgG might occur, depending on the pH of the eluent.

In conclusion, the separation of albumin from IgG in intravenous IgG was achieved by SEC on TSKgel G3000SWXL with 50 m*M* sodium phosphate (pH 5.0) containing 0.1 *M* Na_2SO_4. The separation was completed within 15 min with high resolution and the recovery was more than 92%. Accordingly, TSKgel G3000SWXL would be very useful not only for determining the composition of IgG components and albumin in intravenous IgG, but also for separating IgG such as monoclonal antibodies from albumin in ascites fluid or supernatants.

REFERENCES

1 Y. Masuho, K. Tomibe, K. Matsuzawa and A. Ohtsu, *Vox Sang.*, 32 (1977) 175.
2 Y. Masuho, K. Tomibe, T. Watanabe and Y. Fukumoto, *Vox Sang.*, 32 (1977) 290.
3 T. Doi, T. Nakajima, M. Nishida and T. Suyama, *Chem. Pharm. Bull.*, 26 (1978) 3492.
4 M. Kato, K. Kadota and T. Okuda, *Jpn. J. Antibiot.*, 38 (1985) 2688.
5 S. W. Burchiel, J. R. Billman and T. R. Alber, *J. Immunol. Methods*, 69 (1984) 33.
6 P. Clezardin, J. L. McGregor, M. Manach, H. Boukerche and M. Dechavanne, *J. Chromatogr.*, 319 (1985) 67.
7 J. R. Deschamps, J. E. K. Hildreth, D. Derr and J. T. August, *Anal. Biochem.*, 147 (1985) 451.
8 M.-J. Gemski, B. P. Doctor, M. K. Gentry, M. G. Pluskal and M. P. Strickler, *BioTechniques*, 3 (1985) 378.
9 P. Clezardin, G. Bougro and J. L. McGregor, *J. Chromatogr.*, 354 (1986) 425.
10 P. Clezardin, N. R. Hunter, I. R. MacGregor, J. L. MacGregor, D. S. Pepper and J. Dawes, *J. Chromatogr.*, 358 (1986) 209.
11 B. Pavlu, U. Johansson, C. Nyhlén and A. Wichman, *J. Chromatogr.*, 359 (1986) 449.
12 D. R. Nau, *BioChromatography*, 1 (1986) 82.
13 A. Jungbauer, F. Unerluggauer, F. Steindl, F. Rüker and H. Katinger, *J. Chromatogr.*, 397 (1987) 313.
14 P. Gallo, A. Siden and B. Tavolato, *J. Chromatogr.*, 416 (1987) 53.
15 T. L. Brooks and A. Stevens, *Int. Lab.*, Nov./Dec. (1985) 72.
16 Y. Yamakawa and J. Chiba, *J. Liq. Chromatogr.*, 11 (1988) 665.
17 T. M. Phillips, N. S. More, W. D. Queen, T. V. Holohan, N. C. Kramer and A. M. Thompson, *J. Chromatogr.*, 317 (1984) 173.
18 P. Formstecher, H. Hammadi, N. Bouzerna and M. Dautrevaux, *J. Chromatogr.*, 369 (1986) 379.
19 M. E. Goldman, R. J. Weber, A. H. Newman, K. C. Rice, P. Skolnick and S. M. Paul, *J. Chromatogr.*, 382 (1986) 264.
20 D. S. Hage and R. R. Walters, *J. Chromatogr.*, 386 (1987) 37.
21 P. Parham, M. J. Androlewicz, F. M. Brodsky, N. J. Holes and J. P. Ways, *J. Immunol. Methods*, 53 (1982) 133.
22 G. San, G. Schneider, S. Loeke and H. W. Doerr, *J. Immunol. Methods*, 59 (1983) 121.
23 D. E. Schmidt, Jr., R. W. Giese, D. Conron and B. L. Karger, *Anal. Chem.*, 52 (1980) 177.
24 E. Pfannkoch, K. C. Lu, F. E. Regnier and H. G. Barth, *J. Chromatogr. Sci.*, 18 (1980) 430.
25 H. Engelhardt and D. Mathes, *Chromatographia*, 14 (1981) 325.
26 W. Kopaciewicz and F. E. Regnier, *Anal. Biochem.*, 126 (1982) 8.
27 D. Ratge and H. Wisser, *J. Chromatogr.*, 230 (1982) 47.
28 Y. Kato and T. Hashimoto, *J. High Resolut. Chromatogr. Chromatogr. Commun.*, 6 (1983) 45.
29 Y. Kato and T. Hashimoto, *J. High Resolut. Chromatogr. Chromatogr. Commun.*, 6 (1983) 325.
30 J. K. Lee, F. J. Deluccia, E. L. Kelly, C. Davidson and F. R. Borger, *J. Chromatogr.*, 444 (1988) 141.
31 Y. Kato, Y. Yamasaki, H. Moriyama, K. Tokunaga and T. Hashimoto, *J. Chromatogr.*, 404 (1987) 333.

Journal of Chromatography, 467 (1989) 441–446
Elsevier Science Publishers B.V., Amsterdam — Printed in The Netherlands

CHROM. 21 389

Note

Analysis of phenols from lignin depolymerization by capillary gas chromatography

R. W. THRING and E. CHORNET*
Department of Chemical Engineering, University of Sherbrooke, Sherbrooke, Quebec J1K 2R1 (Canada)
and
R. P. OVEREND
National Research Council of Canada, Ottawa K1A 0R6 (Canada)
(First received November 7th, 1988; revised manuscript received February 6th, 1989)

Lignin degradation by hydrogenation/hydrogenolysis in the absence and presence of catalysts as well as alkaline hydrolysis yields a wide variety of monomeric products. Among these are phenols, guaiacol, syringol, catechol, their respective methyl, ethyl, and propyl derivatives, as well as vanillin and syringaldehyde. The number and abundance of these compounds depend primarily on the severity of conditions of depolymerization utilized, especially the catalyst, but more importantly, the temperature and time of reaction.

The complexity of the product mixtures has been a significant problem, particularly in what concerns the separation and quantification of the monomers. Analysis of the monomeric mixtures by gas chromatography has received wide attention with varying degrees of success.

Clark[1] used paper chromatography to separate phenolic mixtures from lignin degradation. However, the inherent loss of some compounds, especially guaiacol, suggested that this technique is poor for quantitative analysis. Schweers[2] analysed phenolic monomers from hydrogenated lignin by gas chromatography using an SE-30 column, Difficulty was reported with both poor resolution and thermal decomposition of a few products. Scaringelli *et al.*[3] separated phenolic compounds on a Tenax column. High column temperatures (150°C initial oven temperature) were utilized, with the column requiring conditioning at 375°C. Good separation and precision were, however, reported by the authors.

Most of the difficulties encountered in the analysis of phenolic mixtures from lignin depolymerization are due to the presence of compounds containing polar functional groups. These have long been known to be either thermally labile at the temperatures required for separation, or to interact with the column high-boiling liquid phases and inert supports usually available. The interactions, caused by the polar nature and hydrogen-bonding ability of these compounds, lead to their adsorption onto the columns and hence incomplete detection and quantification.

To eluviate these restrictions, derivatization, which is essentially a microchemical synthesis, is carried out to convert the protonic functional groups of such com-

0021-9673/89/$03.50

pounds into non-polar and thermally stable derivatives. The most widely used derivatization methods are silylation and acetylation.

Silylation converts the polar hydroxyl groups in phenolics to their alkylsilyl ethers. The reaction is usually carried out by using the reagent trimethylsilylimidazole at elevated temperatures in the presence of trimethylchlorosilane as catalyst. Clark[4] separated phenolic and catechol compounds after converting them to their trimethylsilylated (TMS) derivatives. Due to steric hindrance, a heating time of 2 h at 150°C was found to be necessary for complete derivatization.

Acetylation introduces the acetyl group by replacing the hydrogen atom(s) of the hydroxyl group(s) attached to the aromatic ring. Treatment with acetic anhydride in the presence of catalytic amounts of pyridine at elevated temperatures leads to a rapid derivatization. However, use of the anhydride can lead to undesirable side reactions with sensitive compounds due to the strong acidity of the medium. Schultz *et al.*[5] hydrogenated HCl lignin and separated the acetylated phenolic products on an OV-17 column. Acetylation was achieved by heating the mixture for 2 h at 60°C. The authors identified fifteen compounds and found that these comprised the majority of the peaks in their chromatograms.

The application of capillary columns to the analysis of phenolic compounds from lignin degradation has not been widely exploited. In the separation of complex fuel-related mixtures, such as gasolines and naphthas, as well as in the separation of essential oils in the flavors and fragrances industries, capillary columns have demonstrated one distinct advantage over the more conventional packed columns, namely, their much higher resolution in shorter analysis times.

In this paper a simple gas chromatographic method for the separation and quantification of phenolic compounds from lignin is described which employs a capillary column. Analytical conditions are reported, which enables the analysis of blends having low as well as high concentrations of phenolic compounds. The method is rapid and offers high precision and accuracy and may be recommended for routine analysis of these compounds from various lignin depolymerization procedures.

EXPERIMENTAL

Materials

The following phenolic compounds were obtained from commercial sources: phenol, *o*-cresol, *p*-cresol, 4-ethylphenol, 4-propylphenol, guaiacol, 4-methyl-, 4-ethyl-, 4-*n*-propylguaiacol, catechol, 4-methyl-, 4-ethylcatechol, syringol, *p*-hydroxybenzaldehyde, vanillin, acetovanillone, syringaldehyde, acetosyringone, and 4-ethylresorcinol (standard). Purified diethyl ether, acetic anhydride and pyridine were purchased from Aldrich.

Preparation and treatment of lignin

Glycol lignin was obtained by thermo-mechano-solvolytic treatment of aspen (*Populus deltoides*) wood using ethylene glycol at 220°C for 4–6 min, followed by dilute acidulation of the spent black liquor. The precipitated lignin was air dried at room temperature and used thereafter.

Alkaline hydrolysis was accomplished in a 500-ml magnetically stirred autoclave. About 5 g of lignin, 2 g of sodium hydroxide and 100 ml of distilled water were

added to the reactor. After testing for leaks by purging with nitrogen, the reactor was brought to 300°C in 7 min by immersing in a preheated salt bath. After treatment for 10 min, the reactor was rapidly cooled by immersing in a cold water bath. The products were separated according to the scheme described in one of our papers[6]. The ether-soluble fraction was analysed for phenols by gas chromatography.

Apparatus

All the data were obtained with a Hewlett-Packard Model 5890 gas chromatography unit equipped with a flame ionization detector. The capillary column, 60 m × 0.25 mm I.D., was a bonded polydimethylsiloxane phase DB-5 (J&W Scientific) purchased from Chromatographic Specialties (Brockville, Canada). The split-injector mode had a split ratio of 120:1 and was maintained at 240°C. The detector temperature was also held at 240°C. High-purity helium, at a constant flow-rate of 1.2 ml/min, was the carrier gas. The recorder connected was a Hewlett-Packard Model 3392 A integrator. A Hamilton 7000 series No. 7001 (Hamilton, Reno, NV, U.S.A.) 1.0-μl syringe was employed for sample injection.

Preparation of sample blends

Phenolic compounds and standard were weighed into a 2.5-ml opaque-colored reaction vial. Derivatization consisted of the following steps: (1) addition of 1.5 ml of acetic anhydride and 1–2 drops of pyridine; (2) sealing the vial and shaking vigorously; (3) heating at 70°C for 1 h in a stirred water bath. The mixture was then cooled to room temperature and directly injected into the gas chromatograph.

Adequacy of the method was verified by the absence of extraneous peaks other than those attributed to the acetylated products in the chromatogram.

Chromatographic procedures

Before injecting a sample, the column was pre-equilibrated with acetic anhydride for 1 h (blank run). After pre-equilibrium, an aliquot of 0.3 μl of the solute mixture was injected into the system thus ensuring that there was no saturation of the column and detector due to large concentrations of phenols which may be present.

The initial column temperature was set at 65°C with no initial temperature hold. The oven temperature programme was as follows: heating rate 6°C/min, hold at 140°C for 10 min, then heated at 4°C/min to 240°C, hold for 10 min, and cooled to 65°C. Duplicate analyses were carried out for each sample.

RESULTS AND DISCUSSION

Qualitative analysis

The acetate derivatives of the phenolic compounds were chromatographed by using several different analysis conditions. A chromatogram of 18 acetylated compounds and the standard obtained under the conditions described is shown in Fig. 1A. These conditions were found to effect the best separation for the compounds considered. Fig. 1B shows the chromatogram of acetylated products obtained from the alkaline hydrolysis of glycol lignin. All the acetylating reagents eluted within 7.8 min.

No peak tailing was evident for all the compounds. However, the peaks corre-

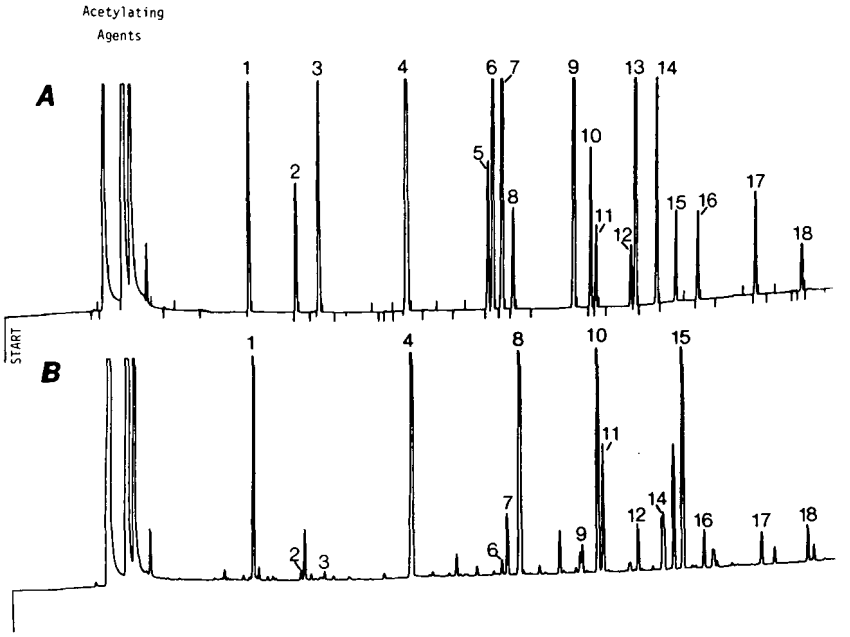

Fig. 1. Chromatograms of (A) standard mixture, and (B) acetylated phenolic products obtained from the hydrolysis of glycol lignin at 300°C, 10 min reaction time in 2% sodium hydroxide solution. Peaks (acetates): 1 = Phenol; 2 = *o*-cresol; 3 = *p*-cresol; 4 = 4-ethylphenol and/or guaiacol; 5 = *p*-hydroxybenzaldehyde; 6 = 4-*n*-propylphenol; 7 = 4-methylguaiacol; 8 = catechol; 9 = 4-ethylguaiacol; 10 = syringol; 11 = 4-methylcatechol; 12 = vanillin; 13 = 4-*n*-propylguaiacol; 14 = 4-ethylcatechol; 15 = 4-ethylresorcinol (standard); 16 = acetovanillone; 17 = syringaldehyde; 18 = acetosyringone.

sponding to the acetates of guaiacol and 4-ethylphenol overlapped. For subsequent quantification of these two compounds, standard blends were separately prepared and chromatographed for each one. Increased resolution may be feasible by adjusting the programmed temperature rate and/or the initial oven temperature. Tests indicated that changing the initial oven temperature is more effective. Due to apparatus limitations, our initial oven temperature could not be adjusted to lower than 65°C.

Quantitative analysis

For quantitative analysis, 4-ethylresorcinol was used as internal standard. The choice of internal standard was primarily based on its absence in products from lignin depolymerization by alkaline hydrolysis (which we verified), as well as from published work on lignin degradation that we have seen to date. Also, for the DB-5 column the peak of the acetate derivative of 4-ethylresorcinol was seen to be well separated from the other peaks with no overlapping, its retention time fairly centered in relation to the other compounds.

Calibration curves were prepared by chromatographing sample mixtures of increasing ratio of phenolic concentration to standard (w/w) and then plotting this ratio *versus* the ratio of the peak areas of phenols to standard. The chromatographing conditions used were the same as those described above. Curves were linear in the concentration range used.

TABLE I

RELATIVE RETENTION TIME (t_R), SLOPE (m), INTERCEPT (c) AND CORRELATION COEFFICIENT (r) OF CALIBRATION CURVE OF ACETYLATED COMPOUNDS ON DB-5 (60 m) CAPILLARY COLUMN

Internal standard used: 4-ethylresorcinol.

Compound	t_R	m	c	r
Phenol	0.358	0.4901	0.8975	0.987
o-Cresol	0.429	1.0586	−0.1766	0.999
p-Cresol	0.463	0.5334	0.6760	0.998
4-Ethylphenol	0.594	1.0177	−0.1468	0.999
4-Propylphenol	0.725	0.5373	1.5716	0.999
Guaiacol	0.594	1.3292	−0.3666	0.999
4-Methylguaiacol	0.738	0.7230	1.5849	0.999
4-Ethylguaiacol	0.846	0.8583	0.9689	0.997
4-*n*-Propylguaiacol	0.940	0.9453	0.4050	0.999
Catechol	0.754	1.2534	−0.4625	0.950
4-Methylcatechol	0.879	1.2820	−0.3780	0.996
4-Ethylcatechol	0.971	0.9840	0.1123	1.000
Syringol	0.871	1.1575	0.2554	1.000
p-Hydroxybenzaldehyde	0.718	0.9797	0.2897	0.999
Vanillin	0.933	1.8553	−0.3680	0.983
Acetovanillone	1.033	1.4751	−0.1090	0.968
Syringaldehyde	1.120	2.6669	−0.6089	0.998
Acetosyringone	1.900	1.3980	0.1711	0.987

TABLE II

ACCURACY OF CAPILLARY GAS CHROMATOGRAPHIC METHOD SHOWN THROUGH OBSERVED VALUES *vs.* ACTUAL VALUES IN CALIBRATION COMPOSITE SAMPLE

Compound	*Actual values(mg)*	*Observed values(mg*	*Relative deviation(%)*
Phenol	7.1	7.2	1.41
o-Cresol	9.4	10.0	6.38
p-Cresol	7.3	7.3	0.00
4-Ethylphenol	6.5	6.4	1.54
4-Propylphenol	12.2	12.3	0.82
Guaiacol	27.8	29.5	6.12
4-Methylguaiacol	14.8	14.8	0.00
4-Ethylguaiacol	14.6	14.7	0.68
4-*n*-Propylguaiacol	12.9	13.4	3.88
Catechol	10.2	10.5	2.94
4-Methylcatechol	8.5	8.6	1.18
4-Ethylcatechol	6.1	6.1	0.00
Syringol	16.3	16.4	0.61
p-Hydroxybenzaldehyde	9.2	9.1	−1.09
Vanillin	14.3	14.9	4.20
Acetovanillone	8.1	8.3	2.47
Syringaldehyde	8.8	9.0	2.27
Acetosyringone	9.7	9.4	−3.09

The appropriate equation $y = mx + c$ was found to be applicable. For each compound, the slope m and intercept c were calculated from duplicate analyses of the reference blends. The calibration curve, relative retention time (t_R) and correlation coefficient (r) are shown in Table I. As seen from the values of the correlation coefficient, all the data closely approximate a straight line.

In order to define the accuracy of the method used, a standard mixture was prepared and analysed. The concentration of phenolic compounds ranged from 6 to 28 mg/ml, representing a typical concentration range of these compounds from conventional lignin degradation processes. The mixture was analysed under the conditions reported previously, and the results are reported in Table II. The data indicate high accuracy, deviating in the range of -1 to 6.4% from the true value, in most cases not exceeding 2%. The precision and accuracy of the data in Table II imply that the method should be applicable in analysing phenolic mixtures containing the compounds considered from lignin degradation.

ACKNOWLEDGEMENTS

The authors are indebted to the National Science and Engineering Research Council (Canada), the National Research Council (Canada) and the Ministere de l'Education Superieure et des Sciences (FCAR program) for financial assistance. Thanks are expressed to Michel Trottier for his technical support.

REFERENCES

1 I. T. Clark, *J. Chromatogr.*, 15 (1964) 65–69.
2 W. Schweers, *Pap. Puu*, 48 (4a) (1966) 161–174.
3 F. P. Scaringelli, T. P. Schultz and I. S. Goldstein, *Anal. Lett.*, 13(A4) (1980) 261–269.
4 I. T. Clark, *J. Gas Chromatogr.*, 6 (1968) 53–55.
5 T. P. Schultz, C. L. Chen, I. S. Goldstein and F. P. Scaringelli, *J. Chromatogr. Sci.*, 19 (1981) 235–237.
6 R. W. Thring, E. Chornet, R. P. Overend and M. H. Heitz, *3rd Chemical Congress of North America, ACS Symposium on Lignin: Properties and Materials, Toronto, Canada, June 5–10, 1988*, in press.

Journal of Chromatography, 467 (1989) 447
Elsevier Science Publishers B.V., Amsterdam — Printed in The Netherlands

CHROM. 21 395

Book Review

Chromatographie mit überkritischen verdichteten Gasen zur Trennung von Oligomeren und Polymeren, by F. P. Schmitz, Profil Verlag, Postfach 22 1330, Munich, 1988, VIII + 235 pp., price DM 59.00, ISBN 3-89019-214-9.

Unfortunately, this small volume has no Preface or Introduction to explain the author's purpose in writing it, although one has the impression that it could well be a "Habilitationsschrift". In any case, the volume starts on page 1 with the following statement:

> 1 Trennverfahren für Oligomere und Polymere
>
> Überführt man eine bifunktionelle Verbinding A in das entsprechende Polymere,
>
> $$n\,A \rightarrow A_n$$
>
> so erhält man —unabhängig vom Reaktionstyp— kein einheitliches Produkt, sondern (im Idealfall) ein Gemisch von Homologen, also ein Gemisch von Verbindungen, die sich lediglich in der Anzahl der miteinander verknüpften Bausteine A und damit in ihrer Kettenlänge unterscheiden.

that is, the book commences with a theoretical treatise of the separation of oligomers and polymers. The author works in a very interesting field, namely supercritical fluid chromatography of polymers from the point of view of the physico-chemical variables.

The chapters deal with chromatographic properties of supercritical fluids, separations of oligomers and polymers, temperature and pressure gradients, solvent composition gradients, multiple gradients and separations of various vinylacryl-oligomers; 269 references are cited. Those workers in the field with some fluency in German will be glad to have this volume, which summarizes and enlarges on a number of papers published by the author and his group.

The book is produced from a camera-ready manuscript, with very good line drawings and figures; no typing errors were noted.

M. LEDERER

Author Index

Appleton, J. D., see Cook, A. P. 395
Aue, W. A., see Sun, X.-Y. 75
Azoulay, M., see Morineau, G. 209
Baczynskyj, W. M., see Richfield-Fratz, N. 167
Baer, J. C.
——, Slack, J. A. and Pettit, G. R.
Stability-indicating high-performance liquid chromatography assay for the anticancer drug bryostatin 1 332
Baeyens, W., see Xianren, Q. 15
Bailey, J. E., Jr., see Richfield-Fratz, N. 167
Barry, E. F., see Costanzo, R. B. 373
Bartle, K. D., see Raynor, M. W. 292
Belenkii, A. B., see Ruban, V. F. 41
Belenkii, B. G., see Ruban, V. F. 41
Betts, T. J.
Use of an inexpensive low-temperature liquid crystal stationary phase for the study of volatile oil constituents with short gas chromatographic retention times 272
Bianchi, A.
——, Varney, M. S. and Phillips, J.
Modified analytical technique for the determination of trace organics in water using dynamic headspace and gas chromatography–mass spectrometry 111
Biondi, P. A.
——, Manca, F., Negri, A., Tedeschi, G. and Secchi, C.
Gas chromatographic determination of glycoprotein amino sugars as O-pentafluorobenzyloxime acetates 315
Bitetto, M. di, see Gobetti, M. 327
Blakemore, W. M., see Thompson, H. C., Jr. 159
Blink, A.
——, Suijkerbuijk, M. L., Ishiwata, T. and Feringa, B. L.
Gas chromatographic method for enantiomeric excess determination of alcohols not requiring chiral auxiliary compounds or chiral stationary phases 285
Block, G. G. A. G., see Delcour, J. A. 149
Böhland, H., see Radicke, J. 304
Boreham, C. J.
—— and Fookes, C. J. R.
Separation of nickel(II) alkylporphyrins by reversed-phase high-performance liquid chromatography. Methodology and application 195
Boter, H. L., see Kientz, Ch. E. 385
Božnar, B., see Žmitek, J. 276
Brinkman, U. A. Th., see Kientz, Ch. E. 385
Büyüktimkin, N.
——, Keller, F. and Schunack, W.
Gas–liquid chromatographic resolution of some racemic synthons for lamtidine analogous histamine H_2-receptor antagonists via diastereomeric amides of (1*S*)-(−)-camphanic acid 402
Caude, M., see Lienne, M. 406
——, see Macaudière, P. 357
——, see Nizery, D. 49
Chan, P. F., see Law, B. 267
Cheah, I. C. L.
——, Sitaram, B. R., Pappas, A., Thi, N. L., Finnin, B. C. and Reed, B. L.
Normal-phase and reversed-phase liquid chromatographic techniques for the determination of dithranol and its degradation products 414
Chornet, E., see Thring, R. W. 441
Cook, A. P.
——, Macleod, T. M., Appleton, J. D. and Fell, A. F.
Reversed-phase high-performance liquid chromatographic method for the quantification of 5-hydroxymethylfurfural as the major degradation product of glucose in infusion fluids 395
Costanzo, R. B.
—— and Barry, E. F.
Gas chromatographic detection of selected organochlorine species using an alternating current plasma detector 373
De Jong, G. J., see Kientz, Ch. E. 385
Dekker, M., see Griest, W. H. 423
Delcour, J. A.
——, Vinkx, C. J. A., Vanhamel, S. and Block, G. G. A. G.
Combined monitoring of UV absorbance and fluorescence intensity as a diagnostic criterion in reversed-phase high-performance liquid chromatographic separation of natural phenolic acids 149
De Pozuelo, M. M., see Reuvers, Th. B. A. 321
Di Bitetto, M., see Gobetti, M. 327
Dreux, M., see Nizery, D. 49
Ellegren, H.
—— and Låås, T.
Size-exclusion chromatography of DNA restriction fragments. Fragment length determinations and a comparison with the behaviour of proteins in size-exclusion chromatography 217

Fell, A. F., see Cook, A. P. 395
Feringa, B. L., see Blink, A. 285
Finnin, B. C., see Cheah, I. C. L. 414
Fookes, C. J. R., see Boreham, C. J. 195
Frappier, F., see Morineau, G. 209
Freeman, J. P., see Thompson, H. C., Jr. 159
Frei, R. W., see Kientz, Ch. E. 385
Games, D. E., see Raynor, M. W. 292
Gendron, A., see Lamarre, C. 249
Giddings, J. C., see Ratanathanawongs, S. K. 341
Gilbert, R., see Lamarre, C. 249
Gobetti, M.
——, Di Bitetto, M. and Rossi, R.
Rapid, sensitive high-performance liquid chromatographic method for the analysis of buflomedil hydrochloride and its potential by-products 327
Griest, W. H.
——, Guzman, C. and Dekker, M.
Packed-column supercritical fluid chromatographic separation of highly explosive compounds 423
Grohmann, K., see Himmel, M. E. 309
Gurevich, A. Ya., see Ruban, V. F. 41
Guzman, C., see Griest, W. H. 423
Harris, R., see Ray, A. 430
Hartung, J., see Radicke, J. 304
Hatano, T., see Yoshida, T. 139
Himmel, M. E.
——, Oh, K. K., Quigley, D. R. and Grohmann, K.
Alkaline size-exclusion chromatography of lignins and coal extracts using cross-linked dextran gels 309
Hurlbut, J. A., see Roybal, J. E. 259
Hynning, P.-Å.
——, Remberger, M. and Neilson, A. H.
Synthesis, gas–liquid chromatographic analysis and gas chromatographic–mass spectrometric identification of nitrovanillins, chloronitrovanillins, nitroguaiacols and chloronitroguaiacols 99
Ishiwate, T., see Blink, A. 285
Jönsson, J. Å., see Mathiasson, L. 61
Johnsen, B. A., see Tørnes, J. Aa. 129
Jong, G. J. de, see Kientz, Ch. E. 385
Karlsson, L., see Mathiasson, L. 61
Kato, Y., see Yamasaki, Y. 299, 436
Keller, F., see Büyüktimkin, N. 402
Kientz, Ch. E.
——, Verweij, A., Boter, H. L., Poppema, A., Frei, R. W., De Jong, G. J. and Brinkman, U. A. Th.
On-line flame photometric detection in microcolumn liquid chromatography 385
Kithinji, J. P., see Raynor, M. W. 292
Kocjan, D., see Žmitek, J. 276
Kraats, C. van de, see Schreuder, R. H. 177
Låås, T., see Ellegren, H. 217
Lafont, R., see Raynor, M. W. 292
Lafosse, M., see Nizery, D. 49
Lamarre, C.
——, Gilbert, R. and Gendron, A.
Liquid chromatographic determination of morpholine and its thermal breakdown products in steam–water cycles at nuclear power plants 249
Law, B.
—— and Chan, P. F.
Stability of silica packing materials towards a mixed aqueous–organic eluent at alkaline pH 267
Lesins, V.
—— and Ruckenstein, E.
Gradient flow programming: a coupling of gradient elution and flow programming 1
Lienne, M.
——, Caude, M., Rosset, R. and Tambuté, A.
Direct enantiomeric separation of anticholinergic drugs derived from (±)-cyclohexyl(3-thienyl)glycolic acid on a novel α_1-acid glycoprotein-bonded chiral stationary phase (Chiral-AGP) 406
——, see Macaudière, P. 357
Macaudière, P.
——, Lienne, M., Caude, M., Rosset, R. and Tambuté, A.
Resolution of π-acid racemates and π-acid chiral stationary phases in normal-phase liquid and subcritical fluid chromatographic modes. A unique reversal of elution order on changing the nature of the achiral modifier 357
Macleod, T. M., see Cook, A. P. 395
Manca, F., see Biondi, P. A. 315
Martijn, A., see Schreuder, R. H. 177
Mathiasson, L.
——, Jönsson, J. Å. and Karlsson, L.
Determination of nitrogen compounds by supercritical fluid chromatography using nitrous oxide as the mobile phase and nitrogen-sensitive detection 61
Matsubara, K.-I., see Yamasaki, Y. 299
Michotte, Y., see Xianren, Q. 15
Miller, D. W., see Thompson, H. C., Jr. 159
Miller, G. C., see Richfield-Fratz, N. 167
Moir, D. L., see Nawrocki, J. 31
Morgan, E. D., see Raynor, M. W. 292
Morineau, G.
——, Azoulay, M. and Frappier, F.
Reaction of *o*-phthalaldehyde with amino acids and glutathione. Application to high-performance liquid chromatography determination 209
Munns, R. K., see Roybal, J. E. 259

Murotsu, T., see Yamasaki, Y. 299
Mylchreest, I. C., see Raynor, M. W. 292
Nakajima, K., see Tsuchihashi, H. 227
Nawrocki, J.
——, Moir, D. L. and Szczepaniak, W.
Investigation of small populations of reactive silanols on silica surfaces 31
Negri, A., see Biondi, P. A. 315
Neilson, A. H., see Hynning, P.-Å. 99
Nestorick, D. M., see Thompson, H. C., Jr. 159
Nishikawa, M., see Tsuchihashi, H. 227
Nizery, D.
——, Thiébaut, D., Caude, M. Rosset, R., Lafosse, M. and Dreux, M.
Improved evaporative light-scattering detection for supercritical fluid chromatography with carbon dioxide–methanol mobile phases 49
Nohta, H.
——, Yamaguchi, E., Ohkura, Y. and Watanabe, H.
Simultaneous high-performance liquid chromatographic determination of catecholamine-related compounds by post-column derivatization involving coulometric oxidation followed by fluorescence reaction 237
Oh, K. K., see Himmel, M. E. 309
Ohkura, Y., see Nohta, H. 237
Ohnaka, A., see Yamasaki, Y. 299
Okuda, T., see Yoshida, T. 139
Olías, J. M.
——, Ríos, J. J. and Valle, M.
Methylation of ω-oxocarboxylic acids with diazomethane: effect of solvent on by-product formation 279
Ortíz, G., see Reuvers, Th. B. A. 321
Overend, R. P., see Thring, R. W. 441
Quigley, D. R., see Himmel, M. E. 309
Pappas, A., see Cheah, I. C. L. 414
Pettit, G. R., see Baer, J. C. 332
Phillips, J., see Bianchi, A. 111
Pommer, U., see Radicke, J. 304
Poppema, A., see Kientz, Ch. E. 385
Pozuelo, M. M. de, see Reuvers, Th. B. A. 321
Radicke, J.
——, Hartung, J., Pommer, U. and Böhland, H.
Einsatz der Hochleistungsflüssigkeitschromatographie bei der Untersuchung der metallionkatalysierten Methanolyse des Phosphorsäurephenylesterdiamids 304
Ramos, M., see Reuvers, Th. B. A. 321
Ratanathanawongs, S. K.
—— and Giddings, J. C.
High-speed size characterization of chromatographic silica gy flow/hyperlayer field-flow fractionation 341
Ray, A.
—— and Harris, R.
High-performance liquid chromatography as an alternative to microbiological measurements in the assay of tetracyclines 430
Raynor, M. W.
——, Kithinji, J. P., Bartle, K. D., Games, D. E., Mylchreest, I. C., Lafont, R., Morgan, E. D. and Wilson, I. D.
Packed column supercritical-fluid chromatography and linked supercritical-fluid chromatography–mass spectrometry for the analysis of phytoecdysteroids from *Silene nutans* and *Silene otites* 292
Reed, B. L., see Cheah, I. C. L. 414
Remberger, M., see Hynning, P.-Å. 99
Reuvers, Th. B. A.
——, Ortíz, G., Ramos, M. and De Pozuelo, M. M.
Rapid high-performance liquid chromatographic method for the determination of bencetonium chloride residues in fish products; confirmation by thin-layer chromatography 321
Richfield-Fratz, N.
——, Baczynskyj, W. M., Miller, G. C. and Bailey, J. E., Jr.
Isolation, characterization and determination of trace organic impurities in FD&C Red No. 40 167
Ríos, J. J., see Olías, J. M. 279
Rosset, R., see Lienne, M. 406
——, see Macaudiére, P. 357
——, see Nizery, D. 49
Rossi, R., see Gobetti, M. 327
Roybal, J. E.
——, Munns, R. K., Hurlbut, J. A. and Shimoda, W.
High-performance liquid chromatography of gentian violet, its demethylated metabolites, leucogentian violet and methylene blue with electrochemical detection 259
Ruban, V. F.
——, Belenkii, A. B., Gurevich, A. Ya. and Belenkii, B. G.
Liquid chromatography on packed fused-silica capillary columns with electrochemical detection 41
Ruckenstein, E., see Lesins, V. 1
Rusjakovski, B., see Žmitek, J. 276
Schreuder, R. H.
——, Martijn, A. and Van de Kraats, C.
Determination of diisobutyl- and diisopropylnaphthalenesulphonates in pesticide wettable powders and dispersible granules by high-performance liquid chromatography 177
Schunack, W., see Büyüktimkin, N. 402

Secchi, C., see Biondi, P. A. 315
Shimoda, W., see Roybal, J. E. 259
Shiomi, K., see Tsuchihashi, H. 227
Sitaram, B. R., see Cheah, I. C. L. 414
Slack, J. A., see Baer, J. C. 332
Stan, H.-J.
Application of capillary gas chromatography with mass selective detection to pesticide residue analysis 85
Štendler, T., see Žmitek, J. 276
Suijkerbuijk, M. L., see Blink, A. 285
Sun, X.-Y.
—— and Aue, W. A.
Selective detection of volatile iron compounds by flame photometry 75
Szczepaniak, W., see Nawrocki, J. 31
Takahashi, S., see Tsuchihashi, H. 227
Tambuté, A., see Lienne, M. 406
——, see Macaudière, P. 357
Tedeschi, G., see Biondi, P. A. 315
Thi, N. L., see Cheah, I. C. L. 414
Thiébaut, D., see Nizery, D. 49
Thompson, H. C., Jr.
——, Blakemore, W. M., Nestorick, D. M., Freeman, J. P. and Miller, D. W.
Analysis, characterization, and purification: Requirements for toxicological evaluation of 1,4-dithiane 159
Thring, R. W.
——, Chornet, E. and Overend, R. P.
Analysis of phenols from lignin depolymerization by capillary gas chromatography 441
Tørnes, J. Aa.
—— and Johnsen, B. A.
Gas chromatographic determination of methylphosphonic acids by methylation with trimethylphenylammonium hydroxide 129
Treutter, D.
Chemical reaction detection of catechins and proanthocyanidins with 4-dimethylaminocinnamaldehyde 185
Tsuchihashi, H.
——, Nakajima, K., Nishikawa, M., Shiomi, K. and Takahashi, S.
Headspace gas chromatography of stimulants in urine by in-column trifluoroacetyl derivatization method 227
Valle, M., see Olías, J. M. 279
Van de Kraats, C., see Schreuder, R. H. 177
Vanhamel, S., see Delcour, J. A. 149
Varney, M. S., see Bianchi, A. 111
Verweij, A., see Kientz, Ch. E. 385
Vinkx, C. J. A., see Delcour, J. A. 149
Watanabe, H., see Nohta, H. 237
Wilson, I. D., see Raynor, M. W. 292
Xianren, Q.
——, Baeyens, W. and Michotte, Y.
Multifactor simultaneous statistical optimization of the mobile phase composition for the separation of inorganic anions in reversed-phase ion-interaction chromatography 15
Yamaguchi, E., see Nohta, H. 237
Yamasaki, Y.
—— and Kato, Y.
Separation of intravenous IgG containing albumin by high-performance size-exclusion chromatography on TSKgel G3000SWXL 436
——, Yokoyama, A., Ohnaka, A., Kato, Y., Murotsu, T. and Matsubara, K.-I.
High-performance hydroxyapatite chromatography of nucleic acids 299
Yokoyama, A., see Yamasaki, Y. 299
Yoshida, T.
——, Hatano, T. and Okuda, T.
Chromatography of tannins. IV. Separation of labile oligomeric hydrolysable tannins and related polyphenols by centrifugal partition chromatography 139
Žmitek, J.
——, Štendler, T., Rusjakovski, B., Kocjan, D. and Božnar, B.
Use of ^{1}H NMR spectroscopy in the selection of the mobile phase for high-performance liquid chromatographic monitoring of the synthesis of ibuproxam 276

Erratum

J. Chromatogr., 459 (1988) 251–260

On page 252, in the section "Urine specimens," the fifth line should read "50 ml of 2 *M* sulphuric acid..." instead of "750 ml of 2 *M* sulphuric acid...".

Vol. 467, No. 2

journal of chromatography news section

CLC '89 STOCKHOLM

THE THIRTEENTH SYMPOSIUM ON COLUMN LIQUID CHROMATOGRAPHY

UNDER THE PATRONAGE OF
HER MAJESTY QUEEN SILVIA

STOCKHOLM, SWEDEN, JUNE 25-30, 1989

SCIENTIFIC PROGRAMME

Introductory Lecture

Prospects in Separation Science and Technology: The Future Role of Chromatography
Csaba Horváth

Review Lectures

Chromatography and Biotechnology
Fred Regnier

Novel Analytical and Preparative Chiral Separations
Wolfgang Lindner

The Role of Microcolumn Separation Methods in the Analysis and Characterization of Femtomole Amounts of Biological Macromolecules
Milos Novotny

Biomedical and Pharmaceutical Applications
Fritz Erni

Progress in Synthesis and Characterization of Stationary Phases for Column Liquid Chromatography
Klaus Unger

Coupled Column Separations by LC-GC
Konrad Grob Jr

Keynote Lectures

Chemometrics and Chromatography
Optimization of Chromatographic Separations Using a Combination of Optimization Software and Expert Systems
Peter Schoenmakers

Biomedical Applications
Approaches to Liquid-Chromatographic Separation in Biomedical Analysis
Bengt-Arne Persson

Progress in Detection Techniques
Progress in Optical Detection Techniques
Edward Yeung

Field Flow Fractionation and Related Techniques
Advances in FFF
J. Calvin Giddings

Hydrodynamic Chromatography on Small Sized Non-Porous Silica Gel Particles
Johan Kraak

Quantitative Structure Retention Relationships
Correlations between Chemical Structure of Noncongeneric Solutes and Their Retention in Liquid Chromatography
Roman Kaliszan

Retention mechanisms
Utilization of Secondary Equilibria in LC
Hans Poppe

LC / MS — NMR — IR
On-Line MS in Chromatography and Electrophoresis
Jack Henion

Hyphenated Techniques in Micro-LC
Kiyokatsu Jinno

Chiral separations
Chiral Recognition in Hydrophobic Monolayer on Silica Gel in Reversed Phase LC
Shoji Hara

Interactions between Macromolecules and Small Molecules — Kinetic Aspects
Bengt Mannervik

Separations of Enantiomers Using Ion-Pair Chromatography
Curt Pettersson

Biopolymer separations
Structure-function Studies on Growth Factors: The Need for High Resolution Separations
E.C. Nice

Computers and Chromatography
Development and Optimisation of HPLC Methods by Computer-Assisted Mobile-Phase Mapping
Lloyd Snyder

Novel Approaches of Solid Phases
NMR-Imaging, a Tool for Optimization of Chromatographic Columns
Ernst Bayer

LC-Techniques in Neurochemistry
Microcolumn Separations in Neurochemistry
James W. Jorgenson

Preparative Chromatography
Theory of Non-Linear Chromatography
Georges Guiochon

Preparative Chromatography of Biopolymers
Csaba Horváth

Capillary Liquid Chromatography and Electrophoresis
High-Performance Electrophoresis in Adsorption- and Electroendosmosis-Free 0.025—0.05 μm Capillaries — A Versatile Analytical and Micropreparative Method with a Resolution Approaching the Theoretical Limit
Stellan Hjérten

Supercritical Fluid Chromatography
Possibilities and Limitations of SFC
Milton Lee

Novel Solid Phases
Polymer Coated Stationary Phases Based on Different Types of Inorganic Support Materials such as SiO_2, Al_2O_3 and ZrO_2.
G. Schomburg

Coupled Column Separations
Improved Selectivity in Precolumn Sample Handling of Biological and Environmental Samples
Udo Brinkman

Closing Lecture

A Detailed Examination of the Kinetic Behavior of Protein Structural Changes in Chromatographic Systems
Barry L. Karger

The scientific programme comprises further about 60 lectures, over 400 posters, as well as discussion sessions.

Social programme

The symposium programme includes a welcome party, a reception in the form of a buffet dinner at the Stockholm City Hall, known all over the world as the setting for the annual Nobel Prize banquet. The symposium banquet will be held at a well-reputed restaurant, with a view of the old Royal Palace, in the city centre.

The traditional Wednesday excursions will, among other alternatives, be made to the old university city of Uppsala, with traditions from the Viking era, or by boat into the Stockholm archipelago, or to the Palace of Drottningholm, present residence of the Swedish Royal Family.

For accompanying persons, a full program will be arranged with visits to places of interest both within and outside Stockholm.

We can promise that it will be possible for you to discover the beauty of Stockholm and its surroundings and to feel the atmosphere of the Nordic light.

Attractive post-symposium tours will be arranged on request: for example to the glassblowers in Småland; to the midnight sun in Lapland; or even to Helsinki and Leningrad.

Invitation to "Last minute poster session".
You are invited to participate in the scientific programme by the registration of a last minute poster with deadline April 30. Please, require the Invitation Programme including abstract forms from the Conference secretariat.

For further information, please contact:

Conference secretariat
Stockholm Convention Bureau
CLC '89
Box 6911
S-102 39 Stockholm, Sweden
Tel. 46-8-23 09 90
Telex: S-11556
Telefax: 46-8-34 84 41

ANNOUNCEMENTS OF MEETINGS

GORDON RESEARCH CONFERENCES, "FRONTIERS OF SCIENCE"

The Gordon Research Conferences for the summer of 1989 will be held in New Hampshire and Rhode Island. The object and exclusive purpose of the Gordon Research Conferences is to foster and promote education and science by organizing and operating meetings of research scientists with common interests in the fields of chemistry or related sciences for the purpose of discussions and the free exchange of ideas, thereby stimulating advanced thinking in research at universities, research foundations, and industrial laboratories. This type of meeting is a valuable means of disseminating information and ideas to an extent that could not be achieved through the usual channels of publication and presentation at scientific meetings. It is hoped that each Conference will extend the Frontiers of Science by fostering a free and informal exchange of ideas among persons actively interested in the subject under discussion.

Some meetings in related areas to this journal are: Reactive Polymers, Ion Exchangers and Adsorbents (Newport, RI, U.S.A., July 31–August 4, 1989); and Analytical Chemistry (New Hampton, NH, U.S.A., August 7–11, 1989).

The complete programme for the 1989 Gordon Research Conferences is published in *Science (Washington, D.C.)*, March 3, 1989. Reprints are available on request.

Requests for applications to the conferences, or for additional information, should be addressed to: Dr. Alexander M. Cruickshank, Gordon Research Conferences, Gordon Research Center, University of Rhode Island, Kingston, RI 02881-0801, U.S.A. Tel.: (401) 783-4011 or (401) 783-3372.

6th (MONTREUX) SYMPOSIUM ON LIQUID CHROMATOGRAPHY–MASS SPECTROMETRY (LC–MS, SFC–MS, CZE–MS) AND SHORT COURSE ON LC–MS, SFC–MS AND CZE–MS, ITHACA, NY, U.S.A., JULY 17–21, 1989

The 6th (Montreux) Symposium on Liquid Chromatography–Mass Spectrometry (July 19–21, 1989), preceded by the Short Course on LC–MS, SFC–MS and CZE–MS (July 17–19, 1989), will be held at Cornell University, Ithaca, NY, U.S.A.

The symposium on LC–MS, SFC–MS, CZE–MS and MS–MS will deal with all areas of this topic including technical development with on-line and off-line aspects, theoretical considerations and applications of the techniques in environmental, clinical and pharmaceutical analysis and other fields. Subtopics will be introduced by plenary lectures and invited research lectures followed by brief research presentations and posters. A major portion of the workshop will be devoted to panel and group discussions on the state-of-the-art of LC–MS, SFC–MS, CZE–MS, and MS–MS.

Until June 1, proposals for brief oral or poster-research presentations can be submitted. The registration fee is US$ 495.00, including luncheons, refreshments, receptions, banquet and proceedings. For further information or questions regarding the presentations, please write to or call: Dr. Jack Henion, Equine Drug Testing and Toxicology Program, New York State College of Veterinary Medicine, Cornell University, 925 Warren Drive, Ithaca, NY 14850, U.S.A., tel.: (607) 255-6556.

An exhibition is planned for instrument manufacturers.

An introductory course in LC–MS, SFC–MS, and CZE–MS will be offered on the two days preceding the symposium.

The topics covered will include: (1) ionization methods; (2) LC–MS interfaces; principles, techniques and applications; belt systems; direct inlet systems; thermospray LC–MS; particle beam interfaces; novel interfaces; (3) LC–MS–MS: principles and applications; (4) SFC–MS; (5) CZE–MS. The instructors are: Jack Henion (Cornell University, Ithaca NY, U.S.A.) and Dai Games (University College, Cardiff, U.K.). The registration fee is US$ 525.00 (US$ 475.00 for symposium attendees). This includes course manual, company folders, refreshments, luncheons, banquet and reception. The deadline for course registration is June 1, 1989.

The registration for the Symposium as well as the Short Course should be mailed to: Department of Conference Services, LC–MS, Box 3, Robert Purcell Union, Cornell University, Ithaca, NY 14853, U.S.A.

103rd AOAC INTERNATIONAL MEETING AND EXPOSITION, ST. LOUIS, MO, U.S.A., SEPTEMBER 25–28, 1989

The Association of Official Analytical Chemists will hold its 103rd International Meeting and Exposition in St. Louis, MO, U.S.A., September 25–28, 1989.

The meeting will be interesting for chemists concerned with food, agriculture, pharmaceuticals, the environment or forensics. Symposia titles are: Laboratory information management systems; Laboratory waste disposal technology; Enantiomeric separations; Risk management in the laboratory; Detection of environmental contaminants and natural toxins in food products of animal origin; and Methods of analysis of drug abuse.

There will also be roundtable discussions, more than 200 poster presentations and an exhibition of the latest chemical equipment.

For further details contact: Marketing Department, AOAC, Suite 400, 2200 Wilson Boulevard, Arlington, VA 22201-9907, U.S.A. Tel.: (703) 522-3032.

FACSS XVI, 16th ANNUAL MEETING OF THE FEDERATION OF ANALYTICAL CHEMISTRY AND SPECTROSCOPY SOCIETIES, CHICAGO, IL, U.S.A., OCTOBER 1–6, 1989

FACSS XVI will be held in the Chicago Hilton, Chicago, IL, U.S.A., from October 1 to 6, 1989. Numerous arranged topical symposia are planned for the meeting in all areas of analytical chemistry, including atomic and molecular spectroscopy, chromatography, electrochemistry, laser spectroscopy and mass spectrometry, nuclear magnetic resonance, process analysis, computers and software, environmental analysis, solid materials characterization (including surface analysis), biotechnology, biomedical, pharmaceutical and clinical analyses.

Several awards symposia will be arranged including symposia for the ANACHEM award, and Society for Applied Spectroscopy awards such as the Meggers and Lester Strock awards. In addition, the FACSS meeting will be the forum for the presentation of other awards such as the Distinguished Service, Honorary Membership and Poehlman SAS Awards.

The FACSS instrument exhibit will be designed to complement the FACSS scientific program. The exhibit area will also be the site of the main social events and the scientific posters sessions.

Workshops and short courses, conducted by leading scientists, will be offered before, during and after the conference. Examples of popular topics that have been offered in the past include ICP–MS, GC–MS, LC–MS, sample preparation, lasers in analytical chemistry and chemometrics. In addition, we propose to assemble our third annual FACSS Scientific Software Fair. The participating firms will have their software on display so that FACSS meeting attendees may obtain a "hands on" experience with a variety of products.

For further details contact: Robert Michel, FACSS XVI Program Chair, Department of Chemistry, University of Connecticut, U-60, Storrs, CT 06268, U.S.A. Tel.: (203) 486-3143.

7th INTERNATIONAL SYMPOSIUM ON PREPARATIVE CHROMATOGRAPHY, GHENT, BELGIUM, APRIL 8–11, 1990

The 7th International Symposium on Preparative Chromatography will be organized in Ghent from April 8 to 11, 1990. This symposium is the continuation of the successful Prep-86 (Paris) and Prep-88 (Baden-Baden) meetings.

If you are interested in entering a poster or an oral presentation, the Scientific Committee would like to hear from you as soon as possible. All aspects of preparative chromatography, LC and GC, are welcome (industrial, laboratory prep, economics, engineering, chemical, biochemical, phases, hardware, etc.). If you would like to attend, start planning accordingly.

The meeting is organized locally by the Contactgroup Chromatography of Belgium under the auspices of the Société Française de Chimie and the Deutsche Chemische Gesellschaft.

For further information contact Professor M. Verzele, RUG-LOS, Krijgslaan 281 (S4), B-9000 Ghent, Belgium. Tel.: (091) 225715; fax: (091) 228321.

27th INTERNATIONAL MEETING OF THE ASSOCIATION OF FORENSIC TOXICOLOGISTS, PERTH, AUSTRALIA, OCTOBER 19–23, 1990

Papers are invited for this meeting on all aspects of forensic and clinical toxicology including analytical techniques with special emphasis on immunoassay procedures, interpretation of results, quality assurance, developments in technology, drugs and driving, doping control in human and animal sports.

The closing date for receival of abstracts will be 19 July, 1990.

The full conference social programme will include the Conference Banquet and Reception with as a special highlight an all day visit to Rottnest Island via the beautiful Swan River on which Perth, the capital city of Western Australia, is situated.

For further information contact: V.J. McLinden, Chemistry Centre (WA), 125 Hay Street, Perth, WA 6000, Australia. Tel.: (09) 325 5544, fax: (09) 325 7767.

NOTICE OF CANCELLATION

2nd INTERNATIONAL SYMPOSIUM OF MICROCOLUMN SEPARATION METHODS, BADEN-BADEN, F.R.G. NOVEMBER 8–10, 1989

The above-mentioned symposium, which was announced earlier in this journal, has been cancelled.

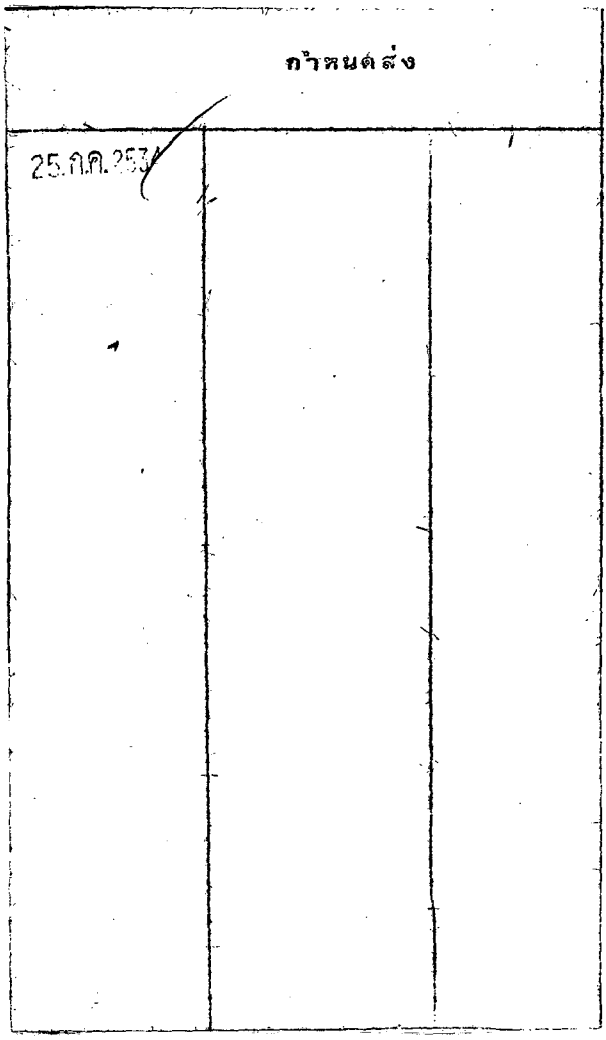
กำหนดส่ง
25 ก.ค. 253

PUBLICATION SCHEDULE FOR 1989

Journal of Chromatography and Journal of Chromatography, Biomedical Applications

MONTH	J	F	M	A	M	J	J	A	S
Journal of Chromatography	461 462 463/1	463/2 464/1	464/2 465/1 465/2	466 467/1 467/2	468 469 470/1 470/2	471 472/1 472/2 473/1	The publication schedule for further issues will be published later		
Bibliography Section		486/1		486/2		486/3		486/4	
Biomedical Applications	487/1	487/2	488/1 488/2	489/1 489/2	490/1 490/2	491/1	491/2	492/1	492/2 493

INFORMATION FOR AUTHORS

(Detailed *Instructions to Authors* were published in Vol. 445, pp. 453–456. A free reprint can be obtained by application to the publisher, Elsevier Science Publishers B.V., P.O. Box 330, 1000 AH Amsterdam, The Netherlands.)

Types of Contributions. The following types of papers are published in the *Journal of Chromatography* and the section on *Biomedical Applications:* Regular research papers (Full-length papers), Notes, Review articles and Letters to the Editor. Notes are usually descriptions of short investigations and reflect the same quality of research as Full-length papers, but should preferably not exceed six printed pages. Letters to the Editor can comment on (parts of) previously published articles, or they can report minor technical improvements of previously published procedures; they should preferably not exceed two printed pages. For review articles, see inside front cover under Submission of Papers.

Submission. Every paper must be accompanied by a letter from the senior author, stating that he is submitting the paper for publication in the *Journal of Chromatography*. Please do not send a letter signed by the director of the institute or the professor unless he is one of the authors.

Manuscripts. Manuscripts should be typed in double spacing on consecutively numbered pages of uniform size. The manuscript should be preceded by a sheet of manuscript paper carrying the title of the paper and the name and full postal address of the person to whom the proofs are to be sent. Authors of papers in French or German are requested to supply an English translation of the title of the paper. As a rule, papers should be divided into sections, headed by a caption (*e.g.*, Summary, Introduction, Experimental, Results, Discussion, etc.). All illustrations, photographs, tables, etc., should be on separate sheets.

Introduction. Every paper must have a concise introduction mentioning what has been done before on the topic described, and stating clearly what is new in the paper now submitted.

Summary. Full-length papers and Review articles should have a summary of 50–100 words which clearly and briefly indicates what is new, different and significant. In the case of French or German articles an additional summary in English, headed by an English translation of the title, should also be provided. (Notes and Letters to the Editor are published without a summary.)

Illustrations. The figures should be submitted in a form suitable for reproduction, drawn in Indian ink on drawing or tracing paper. Each illustration should have a legend, all the *legends* being typed (with double spacing) together on a *separate sheet*. If structures are given in the text, the original drawings should be supplied. Coloured illustrations are reproduced at the author's expense, the cost being determined by the number of pages and by the number of colours needed. The written permission of the author and publisher must be obtained for the use of any figure already published. Its source must be indicated in the legend.

References. References should be numbered in the order in which they are cited in the text, and listed in numerical sequence on a separate sheet at the end of the article. Please check a recent issue for the layout of the reference list. Abbreviations for the titles of journals should follow the system used by *Chemical Abstracts*. Articles not yet published should be given as "in press" (journal should be specified), "submitted for publication" (journal should be specified), "in preparation" or "personal communication".

Dispatch. Before sending the manuscript to the Editor please check that the envelope contains three copies of the paper complete with references, legends and figures. One of the sets of figures must be the originals suitable for direct reproduction. Please also ensure that permission to publish has been obtained from your institute.

Proofs. One set of proofs will be sent to the author to be carefully checked for printer's errors. Corrections must be restricted to instances in which the proof is at variance with the manuscript. "Extra corrections" will be inserted at the author's expense.

Reprints. Fifty reprints of Full-length papers, Notes and Letters to the Editor will be supplied free of charge. Additional reprints can be ordered by the authors. An order form containing price quotations will be sent to the authors together with the proofs of their article.

Advertisements. Advertisement rates are available from the publisher on request. The Editors of the journal accept no responsibility for the contents of the advertisements.

ADVANCED SCIENTIFIC COMPUTING IN BASIC: with applications in chemistry, biology and pharmacology

P. VALKÓ, *Eötvös Loránd University, Budapest, Hungary, and*
S. VAJDA, *Mount Sinai School of Medicine, New York, NY, USA*

Data Handling in Science and Technology Volume 4

Advanced Scientific Computing in BASIC gives a practical introduction to numerical methods and presents BASIC subroutines for real-life computations in the areas of chemistry, biology, and pharmacology. The choice of BASIC as the programming language is motivated by its simplicity, its availability on all personal computers and by its power in data acquisition. While most of the scientific packages currently available in BASIC date back to the period of limited memory and speed, the subroutines presented here can handle a broad range of realistic problems with the power and sophistication needed by professionals and with simple, step-by-step instructions for students and beginners.

The book shows how to extract useful information from measurements via modelling, simulation, and statistical data evaluations. Efficient, robust numerical methods have been chosen to solve related problems in numerical algebra, nonlinear equations and optimization, parameter estimation, signal processing, and differential equations. For each class of routines an introduction to the relevant theory and techniques is given, so that the reader will recognise and use the appropriate method for solving his or her particular problem. Simple examples illustrate the use and applicability of each method.

Contents: 1. Computational linear algebra. 2. Nonlinear equations and extremum problems. 3. Parameter estimation. 4. Signal processing. 5. Dynamical models. Subject index.

1989 xvii + 322 pages; US$ 92.75 / Dfl. 190.00
ISBN 0-444-87270-1
5.25" Diskette: US$ 53.75 / Dfl. 110.00
ISBN 0-444-87271-X

ELSEVIER SCIENCE PUBLISHERS

P.O. Box 211, 1000 AE Amsterdam, The Netherlands
P.O. Box 882, Madison Square Station, New York, NY 10159, USA

Veale 32